

This is to certify that the

dissertation entitled

A. FERROCENYLSULFIDES: PREPARATION AND REACTIVITY  
AS BIDENTATE LIGANDS

B. TRIS(CYCLOPENTADIENYL)ZIROCONIUM DERIVATIVES

presented by

Beth McCulloch

has been accepted towards fulfillment  
of the requirements for

PhD degree in Chemistry

Carl H. Bamkater, Jr.  
Major professor

Date 9-27-83



RETURNING MATERIALS:  
Place in book drop to  
remove this checkout from  
your record. FINES will  
be charged if book is  
returned after the date  
stamped below.

2011	2011	2011
------	------	------

A. FERROCENYLSULFIDES: PREPARATION AND REACTIVITY  
AS BIDENTATE LIGANDS

B. TRIS(CYCLOPENTADIENYL)ZIRCONIUM DERIVATIVES

By

Beth McCulloch

A DISSERTATION

Submitted to  
Michigan State University  
in partial fulfillment of the requirements  
for the degree of

DOCTOR OF PHILOSOPHY

Department of Chemistry

1983



## ABSTRACT

### A. FERROCENYLSULFIDES: PREPARATION AND REACTIVITY AS BIDENTATE LIGANDS

### B. TRIS(CYCLOPENTADIENYL)ZIRCONIUM DERIVATIVES

By

Beth McCulloch

Ferrocenylsulfides,  $\text{Fe}(\text{C}_5\text{H}_4\text{SR})_2$  ( $\text{R} = \text{Me}, \text{iPr}, \text{iBu}, \text{iPent}, \text{Ph}, \text{Bz}$ ) have been prepared by lithiation of ferrocene followed by reaction with the appropriate disulfide. These complexes have been characterized by use of spectroscopic techniques such as proton and carbon NMR, ultraviolet and visible and infrared spectroscopy. The ferrocenylsulfide derivatives readily chelate palladium and platinum halides to form the heterobimetallic complexes,  $\text{Fe}(\text{C}_5\text{H}_4\text{SR})_2\text{MX}_2$  ( $\text{R} = \text{Me}, \text{iPr}, \text{iBu}, \text{Ph}, \text{Bz}; \text{M} = \text{Pd}, \text{Pt}; \text{X} = \text{Cl}, \text{Br}$ ). Proton, carbon and platinum NMR spectra were obtained where possible and infrared, ultraviolet and visible and cyclic voltammetry data of the bimetallic complexes is presented. An X-ray crystal structure of  $\text{Fe}(\text{C}_5\text{H}_4\text{S-iBu})_2\text{-PdCl}_2$  was determined. Dynamic NMR studies suggest that pyramidal sulfur inversion and bridge reversal occur in

solution. Activation parameters for sulfur inversion in  $\text{Fe}(\text{C}_5\text{H}_4\text{S}-i\text{Bu})_2\text{PdX}_2$  ( $\text{X} = \text{Cl}, \text{Br}$ ) were determined as  $13.88 \pm 0.009$  and  $13.42 \pm 0.12$  kcal/mol for the chloride and bromide complexes respectively. Variable temperature Platinum-195 NMR data indicates the presence of two diastereoisomers that increase in relative population as the temperature is lowered.

A chiral ferrocenylsulfide,  $(\text{C}_5\text{H}_5)\text{FeC}_5\text{H}_3[\text{CH}(\text{CH}_3)\text{N}(\text{CH}_3)_2][\text{SCH}_2\text{Ph}]$ , was prepared and its relevance to asymmetric hydrogenation is discussed. A series of dialkyldithiocarbamateferrocene derivatives,  $\text{Fe}(\text{C}_5\text{H}_4\text{SCSNR}_2)_2$  and  $\text{Fe}(\text{C}_5\text{H}_5)(\text{C}_5\text{H}_4\text{SCSNR}_2)$  ( $\text{R} = \text{Me}, \text{Et}, i\text{Pr}$ ) were prepared by reaction of lithioferrocene with tetraalkylthiuram disulfides. Proton and carbon NMR, optical and infrared data were obtained. Dynamic NMR studies indicate that restricted rotation occurs around the carbamate carbon-nitrogen bond in the methyl and ethyl derivatives. Approximate rotational free energy barriers were determined and were correlated with the "thioureide" band in the infrared. Variable temperature NMR spectra of the isopropyldithiocarbamateferrocene derivatives are dominated by restricted rotation of the isopropyl-nitrogen bond and at least two conformers are present at low temperature. The dialkyldithiocarbamate ferrocenes are compared to dithiocarbamate ligands and palladium complexes of the ethyl derivatives were investigated.

The tris(cyclopentadienyl)zirconium complexes,

$(C_5H_5)_3ZrX$  ( $X = Cl, nBu, Me$ ), were prepared. The thermal stability of  $(C_5H_5)_3ZrBu$  was attributed to the three  $\pi$ -bonded cyclopentadienyl rings that block the beta elimination pathway. Reaction of  $(C_5H_5)_3ZrMe$  with carbon monoxide was investigated.

To My Parents and  
My Husband, Ralph

## ACKNOWLEDGMENTS

I would like to express my appreciation to Professor Carl H. Brubaker, Jr. and to the members of the group for their help and friendship.

In addition, I would like to thank Dr. T. J. Pinnavaia for many helpful discussions and Kermit Johnson for technical expertise in obtaining NMR spectra.

## TABLE OF CONTENTS

Chapter	Page
LIST OF TABLES. . . . .	ix
LIST OF FIGURES . . . . .	xii
LIST OF ABBREVIATIONS . . . . .	xvi
A. FERROCENYLSULFIDES: PREPARATION AND REACTIVITY AS BIDENTATE LIGANDS	
I. INTRODUCTION. . . . .	1
II. EXPERIMENTAL. . . . .	14
General Techniques. . . . .	14
1,1'-Bis(methylthio)ferrocene (9) . . . . .	16
1,1'-Bis(isobutylthio)ferrocene (10). . . . .	17
1,1'-Bis(isopropylthio)ferrocene (11) . . . . .	18
1,1'-Bis(phenylthio)ferrocene (12). . . . .	19
1,1'-Bis(benzylthio)ferrocene (13). . . . .	20
1,1'-Bis(isopentylthio)ferrocene (14) . . . . .	21
1,1'-Bis(diphenylphosphino)ferrocene (15) . . . . .	21
Preparation of Metal Complexes. . . . .	22
1,1'-Bis(isobutylthio)ferrocene- palladium dichloride (16) . . . . .	22
1,1'-Bis(isobutylthio)ferrocene- palladium dibromide (17). . . . .	23
1,1'-Bis(isobutylthio)ferrocene- platinum dichloride (18). . . . .	23
1,1'-Bis(isobutylthio)ferrocene- platinum dibromide (19) . . . . .	23

1,1'-Bis(isopropylthio)ferrocene- palladium dichloride (20) . . . . .	24
1,1'-Bis(isopropylthio)ferrocene- palladium dibromide (21). . . . .	24
1,1'-Bis(isopropylthio)ferrocene- platinum dichloride (22). . . . .	24
1,1'-Bis(isopropylthio)ferrocene- platinum dibromide (23) . . . . .	25
1,1'-Bis(methylthio)ferrocenepalladium dichloride (24) . . . . .	25
1,1'-Bis(methylthio)ferrocenepalladium dibromide (25). . . . .	25
1,1'-Bis(methylthio)ferroceneplatinum dichloride (26) . . . . .	25
1,1'-Bis(methylthio)ferroceneplatinum dibromide (27). . . . .	26
1,1'-Bis(benzylthio)ferrocenepalladium dichloride (28) . . . . .	26
1,1'-Bis(benzylthio)ferrocenepalladium dibromide (29). . . . .	26
1,1'-Bis(benzylthio)ferroceneplatinum dichloride (30) . . . . .	26
1,1'-Bis(benzylthio)ferroceneplatinum dibromide (31). . . . .	27
1,1'-Bis(phenylthio)ferrocenepalladium dichloride (32) . . . . .	27
1,1'-Bis(phenylthio)ferrocenepalladium dibromide (33). . . . .	27
1,1'-Bis(phenylthio)ferroceneplatinum dichloride (34) . . . . .	28
1,1'-Bis(phenylthio)ferroceneplatinum dibromide (35). . . . .	28
N,N-dimethyl- $\alpha$ -ferrocenylethylamine (36). . . . .	28

Chapter	Page
(R)- $\alpha$ -[(S)-2-benzylthioferrocenyl]- ethyldimethylamine (37) . . . . .	29
1,1'-Bis(dimethyldithiocarbamate)- ferrocene (38) . . . . .	30
1,1'-Bis(diethyldithiocarbamate)- ferrocene (39) . . . . .	31
1,1'-Bis(diisopropyldithiocarbamate)- ferrocene (40) . . . . .	32
Dimethyldithiocarbamateferrocene (41) . . . . .	33
Diethyldithiocarbamateferrocene (42) . . . . .	34
Diisopropyldithiocarbamateferrocene (43) . . . . .	35
Reaction of $\text{Fe}(\text{C}_5\text{H}_4\text{SCSNET}_2)_2$ (39) with $(\text{PhCN})_2\text{PdCl}_2$ . . . . .	36
Reaction of $\text{FeCp}(\text{C}_5\text{H}_4\text{SCSNET}_2)$ (42) with $(\text{PhCN})_2\text{PdCl}_2$ . . . . .	36
III. RESULTS AND DISCUSSION. . . . .	37
A. $\text{Fe}(\text{C}_5\text{H}_4\text{SR})_2$ (R = Me, iPr, iBu, iPent, Ph, Bz) . . . . .	37
1. Preparation . . . . .	37
2. $^1\text{H}$ NMR. . . . .	39
3. $^{13}\text{C}$ NMR . . . . .	39
4. Infrared Spectra. . . . .	44
B. $\text{C}_5\text{H}_5\text{FeC}_5\text{H}_3[\text{CH}(\text{CH}_3)\text{N}(\text{CH}_3)_2][\text{SCH}_2\text{Ph}]$ . . . . .	46
C. $\text{Fe}(\text{C}_5\text{H}_4\text{SR})_2\text{MX}_2$ (R = Me, iPr, iBu, Ph, Bz; M = Pd, Pt; X = Cl, Br) . . . . .	49
1. Preparation . . . . .	49
2. $^1\text{H}$ NMR. . . . .	50
3. $^{13}\text{C}$ NMR . . . . .	55



Chapter	Page
4. Infrared Spectra. . . . .	56
5. Ultraviolet and Visible Spectra . . . . .	60
6. Structure . . . . .	63
7. Dynamic NMR Studies . . . . .	74
8. $^{195}\text{Pt}$ NMR . . . . .	87
9. Electrochemistry. . . . .	90
D. $\text{Fe}(\text{C}_5\text{H}_4\text{SCSNR}_2)_2$ and $\text{FeCp}(\text{C}_5\text{H}_4\text{SCSNR}_2)$ (R = Me, Et, iPr) . . . . .	96
1. Preparation . . . . .	96
2. $^1\text{H}$ NMR. . . . .	99
3. $^{13}\text{C}$ NMR . . . . .	99
4. Ultraviolet and Visible Spectra . . . . .	104
5. Dynamic NMR Studies . . . . .	108
6. Metal Complexes of $\text{Fe}(\text{C}_5\text{H}_4\text{SCSNet}_2)_2$ and $\text{FeCp}(\text{C}_5\text{H}_4\text{SCSNet}_2)$ . . . . .	116
B. TRIS(CYCLOPENTADIENYL)ZIRCONIUM DERIVATIVES	
I. INTRODUCTION. . . . .	123
II. EXPERIMENTAL. . . . .	125
General Techniques. . . . .	125
Tris(cyclopentadienyl)zirconium- chloride ( $^{48}$ ) . . . . .	125
Attempted Preparation of Tris(cyclo- pentadienyl)zirconiumbutyl ( $^{49}$ ) . . . . .	126
Tris(cyclopentadienyl)zirconiumbutyl ( $^{49}$ ) . . . . .	127
Tris(cyclopentadienyl)zirconium- methyl ( $^{50}$ ) . . . . .	127

Chapter	Page
Photolysis of Tris(cyclopentadienyl)- zirconiummethyl under CO atmosphere. . . .	128
III. RESULTS AND DISCUSSION. . . . .	129
1. $\text{Cp}_3\text{ZrCl}$ . . . . .	129
2. $\text{Cp}_3\text{ZrR}$ (R = nBu, Me). . . . .	131
3. Reaction of $\text{Cp}_3\text{ZrMe}$ with CO . . . . .	135
4. Conclusions . . . . .	136
APPENDIX A - Photolysis of ( $\mu$ -Oxo)Bis(Chloro- zirconocene) . . . . .	138
APPENDIX B. . . . .	142
REFERENCES. . . . .	150

# LIST OF TABLES

Table		Page
1	Metal Complexes Derived from Ferrocenylphosphine and Ferrocenylarsine Ligands . . . . .	6
2	$^1\text{H}$ NMR Data for Ferrocenylsulfide Complexes, $\text{Fe}(\text{C}_5\text{H}_4\text{SR})_2$ R = Me, iPr, iBu, iPent, Ph, Bz. Spectra obtained in $\text{CDCl}_3$ at room temperature . . . . .	40
3	$^{13}\text{C}$ NMR Data for Ferrocenylsulfide Complexes, $\text{Fe}(\text{C}_5\text{H}_4\text{SR})_2$ , R = Me, iPr, iBu, iPent, Ph, Bz. Spectra obtained in $(\text{CH}_2\text{Cl}_2/\text{D}_2\text{O})$ solution at room temperature. . . . .	42
4	Infrared Data for Ferrocenylsulfide Complexes, $\text{Fe}(\text{C}_5\text{H}_4\text{SR})_2$ , R = Me, iPr, iBu, Ph, Bz . . . . .	45
5	$^1\text{H}$ NMR and $^{13}\text{C}$ NMR Data for $\text{Fe}(\text{C}_5\text{H}_4\text{S-iBu})_2$ and Metal Derivatives, $\text{PdCl}_2$ , $\text{PdBr}_2$ , $\text{PtCl}_2$ and $\text{PtBr}_2$ . . . . .	51
6	Infrared Data for $\text{Fe}(\text{C}_5\text{H}_4\text{SR})_2\text{MX}_2$ (R = Me, iPr, iBu, Ph, Bz; M = Pd, Pt; X = Cl, Br) in Region $400\text{--}200\text{ cm}^{-1}$ .	

Table		Page
6 Cont	Measured as Nujol Mulls between CsBr Plates. . . . .	58
7	Electronic Absorption Spectra of Ferrocenylsulfide complexes $\text{Fe}(\text{C}_5\text{H}_4\text{SR})_2$ , $\text{Fe}(\text{C}_5\text{H}_4\text{SR})_2\text{MX}_2$ (R = iBu, Ph, Me; M = Pd, Pt; X = Cl, Br) at 24°C in MeCN solution at approx. conc. $8.0 \times 10^{-5}$ M. . .	61
8	Positional Parameters and Esd's for $\text{Fe}(\text{C}_5\text{H}_4\text{S-iBu})_2\text{PdCl}_2$ . . . . .	66
9A	Anisotropic Thermal Parameters with Esd's for $\text{Fe}(\text{C}_5\text{H}_4\text{S-iBu})_2\text{PdCl}_2$ . . . . .	68
9B	Isotropic Thermal Parameters with Esd's for $\text{Fe}(\text{C}_5\text{H}_4\text{S-iBu})_2\text{PdCl}_2$ . . . . .	69
10	Selected Bond Distances (Å) with Esd's for $\text{Fe}(\text{C}_5\text{H}_4\text{S-iBu})_2\text{PdCl}_2$ . . . . .	71
11	Selected Bond Angles (deg) with Esd's for $\text{Fe}(\text{C}_5\text{H}_4\text{S-iBu})_2\text{PdCl}_2$ . . . . .	72
12	Dihedral Angle and Bridgehead Angle of selected [3]ferrocenophanes. . . . .	74
13	Least-Squares Planes in $\text{Fe}(\text{C}_5\text{H}_4\text{S-iBu})_2\text{PdCl}_2$ . . . . .	75
14	Torsion Angles in $\text{Fe}(\text{C}_5\text{H}_4\text{S-iBu})_2\text{PdCl}_2$ . . .	76
15	$^{195}\text{Pt}$ NMR Data for Ferrocenylsulfide- platinum Complexes, $\text{Fe}(\text{C}_5\text{H}_4\text{SR})\text{PtX}_2$ , R = iBu, iPr, Ph, Bz; X = Cl, Br.	

Table	Page
15 Cont Measurements made in $\text{CDCl}_3$ solution at room temperature . . . . .	88
16 Cyclic Voltammetry Data for Ferro- cenyisulfide Complexes. . . . .	94
17 $^1\text{H}$ NMR Data for $\text{Fe}(\text{C}_5\text{H}_4\text{SCSNR}_2)_2$ and $\text{Fe}(\text{C}_5\text{H}_5)(\text{C}_5\text{H}_4\text{SCSNR}_2)$ Complexes (R = Me, Et, iPr) . . . . .	100
18 $^{13}\text{C}$ NMR Data for $\text{Fe}(\text{C}_5\text{H}_4\text{SCSNR}_2)_2$ and $\text{Fe}(\text{C}_5\text{H}_5)(\text{C}_5\text{H}_4\text{SCSNR}_2)$ (R = Me, Et, iPr). Measured in $\text{CH}_2\text{Cl}_2/\text{D}_2\text{O}$ solution at ambient temperature unless otherwise shown . . . . .	102
19 Electronic Absorption Spectra of $\text{Fe}(\text{C}_5\text{H}_4\text{SCSNR}_2)_2$ and $\text{Fe}(\text{C}_5\text{H}_5)(\text{C}_5\text{H}_4\text{SCSNR}_2)$ (R = Me, Et, iPr) at $24^\circ\text{C}$ in MeCN solution at approx. conc. $8.0 \times 10^{-5} \text{ M}$ . . .	106
20 NMR Parameters, Kinetic and Infrared Data for $\text{Fe}(\text{C}_5\text{H}_4\text{SCSNR}_2)_2$ and $\text{Fe}(\text{C}_5\text{H}_5)-$ $(\text{C}_5\text{H}_4\text{SCSNR}_2)$ where R = Me, Et . . . . .	110
21 $^1\text{H}$ NMR Data for Cyclopentadienyl- zirconium Complexes . . . . .	130

# LIST OF FIGURES

Figure		Page
1	Proton decoupled (above) and gated decoupled (below) $^{13}\text{C}$ NMR Spectra of $\text{Fe}(\text{C}_5\text{H}_4\text{S-iPr})_2$ . . . . .	43
2	$^1\text{H}$ NMR Spectra of $\text{Fe}(\text{C}_5\text{H}_4\text{S-iBu})_2$ and $\text{Fe}(\text{C}_5\text{H}_4\text{S-iBu})_2\text{PdCl}_2$ . . . . .	53
3	$^1\text{H}$ NMR Spectra of $\text{Fe}(\text{C}_5\text{H}_4\text{S-iPr})_2\text{PdCl}_2$ and $\text{Fe}(\text{C}_5\text{H}_4\text{S-iPr})_2\text{PtCl}_2$ . . . . .	54
4	Infrared Spectra of (A) $\text{Fe}(\text{C}_5\text{H}_4\text{SPh})_2$ , (B) $\text{Fe}(\text{C}_5\text{H}_4\text{SPh})_2\text{PtCl}_2$ and (C) $\text{Fe}-$ $(\text{C}_5\text{H}_4\text{SPh})_2\text{PdBr}_2$ . . . . .	57
5	Far Infrared Region for $\text{Fe}(\text{C}_5\text{H}_4\text{S-iBu})_2-$ $\text{PdX}_2$ and $\text{Fe}(\text{C}_5\text{H}_4\text{S-iBu})_2\text{PtX}_2$ where $\text{X} = \text{Cl}$ (above), and $\text{Br}$ (below). . . . .	59
6	Structure and Numbering Scheme for $\text{Fe}(\text{C}_5\text{H}_4\text{S-iBu})_2\text{PdCl}_2$ . . . . .	64
7	Stereoview of $\text{Fe}(\text{C}_5\text{H}_4\text{S-iBu})_2\text{PdCl}_2$ . . . . .	65
8	Variable Temperature $^1\text{H}$ NMR Spectra for $\text{Fe}(\text{C}_5\text{H}_4\text{S-iBu})_2\text{PdCl}_2$ . . . . .	77
9	Variable Temperature $^1\text{H}$ NMR Spectra for $\text{Fe}(\text{C}_5\text{H}_4\text{S-iBu})_2\text{PtCl}_2$ . . . . .	83

Figure		Page
10	Variable Temperature $^{13}\text{C}$ NMR Spectra for $\text{Fe}(\text{C}_5\text{H}_4\text{S-iBu})_2\text{PdCl}_2$ in Region from 70-80 ppm. . . . .	86
11	Variable Temperature $^{195}\text{Pt}$ NMR Spectra for $\text{Fe}(\text{C}_5\text{H}_4\text{S-iBu})_2\text{PtCl}_2$ . . . . .	89
12	Variable Temperature $^{195}\text{Pt}$ NMR Spectra for $\text{Fe}(\text{C}_5\text{H}_4\text{S-iPr})_2\text{PtCl}_2$ . . . . .	91
13	Cyclic Voltammograms of (A) $\text{Fe}(\text{C}_5\text{H}_4\text{S-iBu})_2$ , (B) $\text{Fe}(\text{C}_5\text{H}_4\text{S-iBu})_2\text{PtCl}_2$ and (C) $\text{Fe}(\text{C}_5\text{H}_4\text{S-iBu})_2\text{PdCl}_2$ . . . . .	93
14	$^1\text{H}$ NMR Spectra of $\text{Fe}(\text{C}_5\text{H}_5)(\text{C}_5\text{H}_4\text{SCSNet}_2)$ (above) and $\text{Fe}(\text{C}_5\text{H}_4\text{SCSNet}_2)_2$ (below). . . .	101
15	$^{13}\text{C}$ NMR Spectra of (A) $\text{Fe}(\text{C}_5\text{H}_4\text{S-iPr})_2$ , (B) $\text{Fe}(\text{C}_5\text{H}_4\text{SCSNiPr}_2)_2$ and (C) $\text{Fe}-$ $(\text{C}_5\text{H}_5)(\text{C}_5\text{H}_4\text{SCSNet}_2)$ . . . . .	104
16	$^{13}\text{C}$ NMR Spectra of $\text{Fe}(\text{C}_5\text{H}_5)(\text{C}_5\text{H}_4\text{SCSNMe}_2)$ (above) and $\text{Fe}(\text{C}_5\text{H}_4\text{SCSNet}_2)_2$ (below). . . .	105
17	Ultraviolet-visible Spectra for (A) $\text{Fe}(\text{C}_5\text{H}_4\text{SCSNMe}_2)_2$ and (B) $\text{Fe}(\text{C}_5\text{H}_5)-$ $(\text{C}_5\text{H}_4\text{SCSNMe}_2)$ . . . . .	107
18	Variable Temperature $^1\text{H}$ NMR Spectra of $\text{Fe}(\text{C}_5\text{H}_4\text{SCSNiPr}_2)_2$ . . . . .	111
19	Variable Temperature $^1\text{H}$ NMR Spectra of $\text{Fe}(\text{C}_5\text{H}_5)(\text{C}_5\text{H}_4\text{SCSNiPr}_2)$ . . . . .	112
20	Conformers A and B of $\text{Fe}(\text{C}_5\text{H}_5)-$ $(\text{C}_5\text{H}_4\text{SCSNiPr}_2)$ . . . . .	114

Figure	Page
21	Slow exchange $^1\text{H}$ NMR Spectrum of $\text{Fe}(\text{C}_5\text{H}_5)(\text{C}_5\text{H}_4\text{SCS}\text{Ni-Pr}_2)$ . . . . . 114
22	Resolution Enhanced $^1\text{H}$ NMR Spectrum of $\text{Fe}(\text{C}_5\text{H}_5)(\text{C}_5\text{H}_4\text{SCS}\text{NiPr}_2)$ at Slow Exchange. . . . . 115
23	Infrared Spectra of (A) $\text{Fe}(\text{C}_5\text{H}_5)-$ $(\text{C}_5\text{H}_4\text{SCS}\text{NEt}_2)$ and (B) Pd Complex: (C) $\text{Fe}(\text{C}_5\text{H}_4\text{SCS}\text{NEt}_2)_2$ and (D) Pd Complex . . . . 118
24	Infrared Spectra of $\text{Fe}(\text{C}_5\text{H}_4\text{SCS}\text{NEt}_2)_2$ (above) and $\text{Fe}(\text{C}_5\text{H}_4\text{SCS}\text{NEt}_2)_2\text{PdCl}_2$ (below) . . . . . 121
25	Infrared Spectra of $\text{Fe}(\text{C}_5\text{H}_5)-$ $(\text{C}_5\text{H}_4\text{SCS}\text{NEt}_2)$ (above) and $\text{Fe}(\text{C}_5\text{H}_5)-$ $(\text{C}_5\text{H}_4\text{SCS}\text{NEt}_2)\text{PdCl}_2$ (below). . . . . 122
26	ESR Spectrum obtained from reaction of $\text{Cp}_3\text{ZrCl}$ with $\text{BuLi}$ in THF solution. . . . 133
A1	$^1\text{H}$ NMR Spectra of $(\text{Cp}_2\text{ZrCl})_2\text{O}$ during photolysis at (A) $t = 0$ , (B) $t = 75$ min, (C) $t = 6$ h 35 min and (D) $t = 16$ h. . . . . 140
A2	ESR Signal Obtained from Photolysis of $(\text{Cp}_2\text{ZrCl})_2\text{O}$ . . . . . 141
B1	$^1\text{H}$ NMR Spectra of $\text{Fe}(\text{C}_5\text{H}_4\text{SPh})_2$ (above) and $\text{Fe}(\text{C}_5\text{H}_4\text{SCH}_2\text{Ph})_2$ (below). Inset cyclopentadienyl proton region. . . . 142



Figure	Page
B2	$^1\text{H}$ NMR spectrum of $\text{Fe}(\text{C}_5\text{H}_4\text{S-iPr})_2$ (above) and $^{13}\text{C}$ NMR spectrum of $\text{Fe}-$ $(\text{C}_5\text{H}_4\text{SCNiPr}_2)_2$ in $\text{CDCl}_3$ at $57^\circ\text{C}$ (below) . . . . . 143
B3	$^{13}\text{C}$ NMR Spectra of $\text{Fe}(\text{C}_5\text{H}_4\text{SCH}_2\text{Ph})_2$ proton decoupled (above) and gated decoupled (below) . . . . . 144
B4	$^{13}\text{C}$ NMR Spectra of $\text{Fe}(\text{C}_5\text{H}_4\text{SMe})_2$ proton decoupled (above) and gated decoupled (below) . . . . . 145
B5	$^1\text{H}$ NMR Spectra of $\text{Fe}(\text{C}_5\text{H}_4\text{SPh})_2\text{PtCl}_2$ (above) and $\text{Fe}(\text{C}_5\text{H}_4\text{SPh})_2\text{PtBr}_2$ at $50^\circ\text{C}$ (below). . . . . 146
B6	$^{195}\text{Pt}$ NMR Spectra of $\text{Fe}(\text{C}_5\text{H}_4\text{PPh}_2)_2-$ $\text{PtCl}_2$ (above) and $\text{Fe}(\text{C}_5\text{H}_4\text{S-iBu})_2\text{PtCl}_2$ (below) . . . . . 147
B7	$^1\text{H}$ NMR Spectra of $\text{Fe}(\text{C}_5\text{H}_5)(\text{C}_5\text{H}_4\text{SCSMe}_2)$ (above) and $\text{Fe}(\text{C}_5\text{H}_4\text{SCSMe}_2)_2$ (below). . . . 148
B8	$^1\text{H}$ NMR Spectra of $\text{Fe}(\text{C}_5\text{H}_5)(\text{C}_5\text{H}_4\text{SCSniPr}_2)$ (above) and $\text{Fe}(\text{C}_5\text{H}_4\text{SCSniPr}_2)_2$ (below) . . . 149

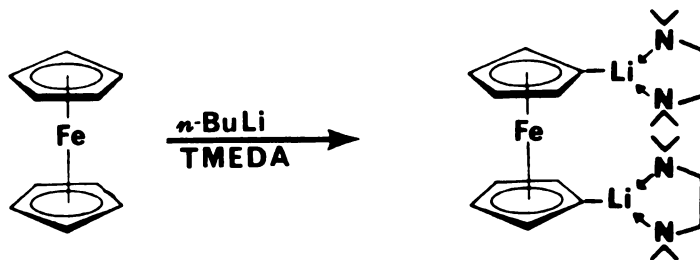
## LIST OF ABBREVIATIONS

Bz	= benzyl
Cp	= cyclopentadienyl
Et	= ethyl
Fc	= ferrocenyl
Fdpp	= 1,1-Bis(diphenylphosphino)ferrocene
iBu	= isobutyl
iPent	= isopentyl
iPr	= isopropyl
Me	= methyl
Ph	= phenyl
CH <sub>2</sub> Cl <sub>2</sub>	= methylene chloride
DMF	= N,N-dimethylformamide
MeCN	= acetonitrile
THF	= tetrahydrofuran
SCE	= standard calomel electrode

## I. INTRODUCTION

Ferrocene, which was discovered in 1951, has proved to be a remarkably stable and unusually reactive organo-iron complex. It readily undergoes a variety of aromatic substitution reactions such as acylation, alkylation, formylation, mercuration and sulfonation<sup>1</sup>. Electrophilic substitution reactions are however limited to electrophiles which do not oxidize the iron atom or destroy the cyclopentadienyl ring-metal bond. The metalation reaction complements electrophilic substitution in that it provides an alternate route to introducing reactive functional groups on to ferrocene.

Metalation may be achieved by reaction of ferrocene with butyllithium, amylsodium or phenylsodium<sup>2</sup>. Ferrocene is dilithiated in over 90% yield by a mixture of butyllithium and tetramethylethylenediamine (TMEDA)<sup>3</sup>.



The dimetalated species may be isolated as a pyrophoric red-orange crystalline solid where TMEDA chelates the dilithium reagent. Use of the lithium reagent isolated as a solid, rather than the in situ slurry, leads to higher yields in the subsequent reaction with electrophiles. The advantage of the butyllithium/TMEDA metalation reagent is that only dilithioferrocene is produced whereas sodium and potassium derivatives of ferrocene result in mixtures of the mono and dimetalated species.

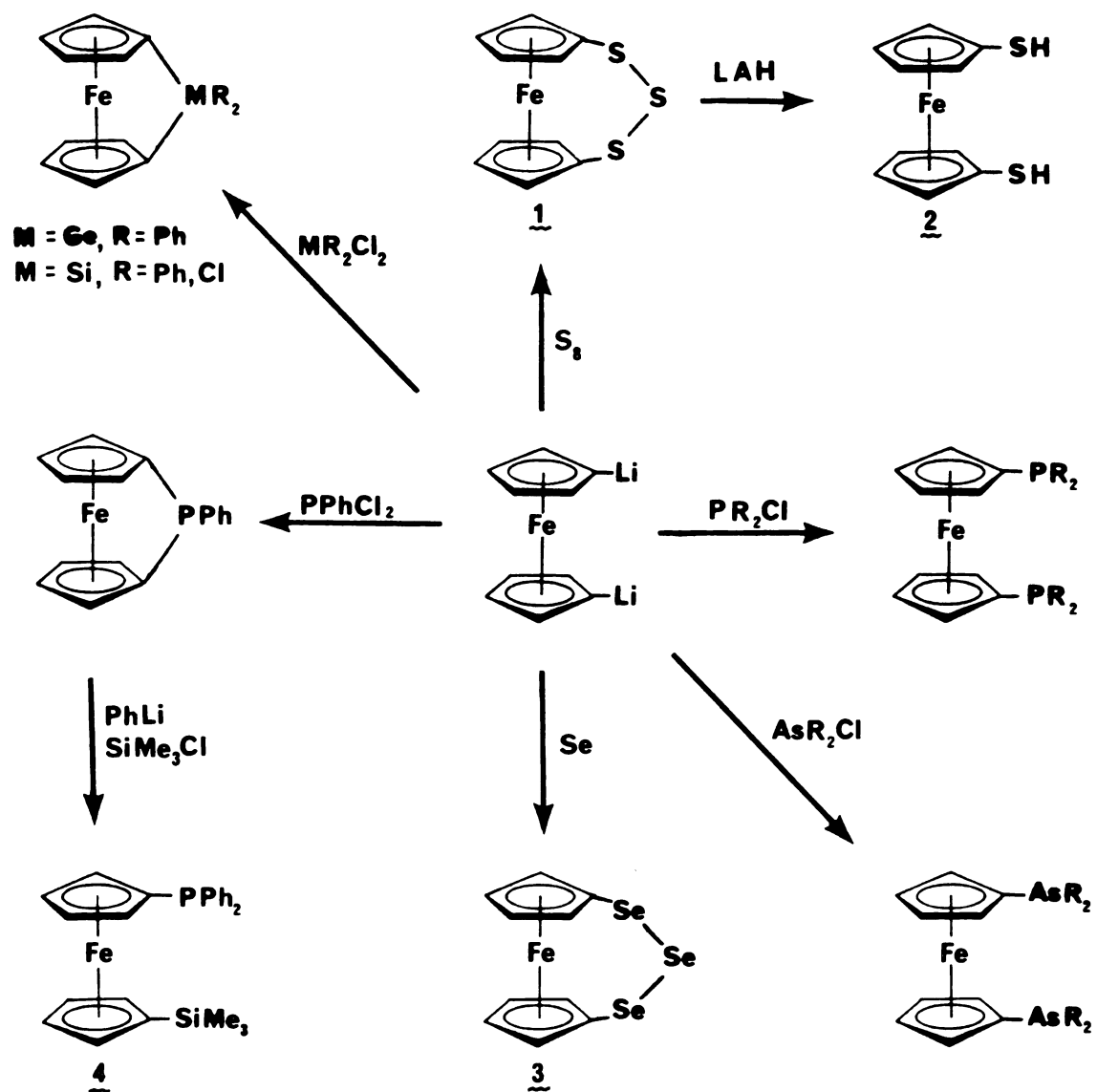
In contrast to dilithioferrocene, preparation of monolithioferrocene by addition of stoichiometric amounts of butyllithium/TMEDA to ferrocene leads to a mixture of the monolithiated and dilithiated species<sup>4</sup>. Another route to lithioferrocene where alkyllithium is added to chloromercuriferrocene produces a reactive dialkylmercury compound that forms undesirable side products<sup>5</sup>. High yields of lithioferrocene, with no concurrent dilithiation, can however be obtained by reaction of butyllithium and bromoferrocene<sup>6</sup>.

The organic chemistry of ferrocene is extensive and literally thousands of derivatives have been prepared. One of the more recent applications of ferrocene is its use as a ligand in transition metal complexes<sup>7</sup>. Metalation has proved to be a useful synthetic method for the introduction of potential donors such as phosphines and arsines on to the cyclopentadienyl ring.

Scheme 1 illustrates the variety of different donor substituents that may be incorporated into ferrocene. In 1970 Davison prepared ferrocenylphosphines and ferrocenylarsines in high yield from 1,1'-dilithioferrocene. In addition reaction of dilithioferrocene with elemental sulfur gave 1,2,3-trithia-[3]ferrocenophane (1) which can be reduced quantitatively to 1,1'-dithiolferrocene (2)<sup>8</sup>. Recently Osborne has prepared the selenium analog (3)<sup>9</sup>.

An interesting class of compounds, the [1]-ferrocenophanes which have phosphorous, arsenic or Gp 6A elements as the bridging atoms, have been obtained from dilithioferrocene and  $\text{RPhCl}_2$ ,  $\text{RAsCl}_2$ <sup>10,11</sup> or  $\text{R}_2\text{MCl}_2$  ( $\text{M} = \text{Ge}$ ,  $\text{R} = \text{Ph}$ ;  $\text{M} = \text{Si}$ ,  $\text{R} = \text{Ph}$ ,  $\text{Cl}$ )<sup>12</sup>, respectively. These compounds exhibit unusual spectroscopic properties as the cyclopentadienyl rings are severely tilted towards the bridge atom. Wrighton and coworkers<sup>13</sup> have used (1,1'-ferrocenediyl)dichlorosilane to derivatize a number of electrode and silica surfaces by opening the highly reactive, strained C-Si-C bond in the ferrocenophane.

The [1]-ferrocenophanes are cleaved by alkylolithium reagents to give a ring opened ferrocenyllithium reagent. Subsequent reaction with electrophiles gives rise to ferrocene derivatives with mixed functionality as in (4). Recently Cullen<sup>11</sup> reported the preparation of ring-substituted ferrocenophanes with phosphorous and arsenic bridges. These are precursors to chiral ferrocenes with mixed functionality



Scheme 1

that have important applications in asymmetric synthesis.

Table 1 contains metal complexes specifically derived from either ferrocenylphosphine or ferrocenylarsine ligands. Davison<sup>14</sup> has prepared a variety of complexes with first row transition metal halides and 1,1'-bis(diphenylphosphino)-ferrocene, (fdpp), and concluded that fdpp is a rigid, sterically demanding ligand that reacts very much like 1,2-bis(diphenylphosphino)ethane, (diphos).

In a study of the reaction of ferrocenylarsines with Gp 6 metal carbonyls and Gp 8 metal halides Davison<sup>15,16</sup> concluded that only 1,1'-bis(dimethylarsino)ferrocene, (fdma), formed bis chelate complexes such as (fdma)<sub>2</sub>Mo(CO)<sub>3</sub> and Pd(fdma)<sub>2</sub>Cl<sup>+</sup> and Pd(fdma)<sub>2</sub><sup>2+</sup>. The authors postulate that the 1,1'-bis(diphenylarsino)ferrocene ligand, (fdpa), forms only mono chelate complexes owing to the steric bulk of the phenyl groups.

Ferrocenylphosphine ligands have recently been employed in catalysis. Workers at Celanese<sup>18</sup> reported that rhodium complexes containing 1,1'-bis(diarylphosphino)ferrocenes induce high rates and high selectivity to linear aldehydes in alpha-olefin hydroformylation. In particular the rhodium complex of 1,1'-bis[bis(alpha,alpha,alpha-trifluoro-p-tolyl)phosphino]-ferrocene was found to catalyze the hydroformylation of 1-hexene to give 100% conversion with 93.2% selectivity to hexanal<sup>19</sup>. A mechanistic study of the highly selective catalyst suggests that three phosphorous atoms are bound to each rhodium atom in a dirhodium complex.

Table 1. Metal Complexes Derived from Ferrocenylphosphine and Ferrocenylarsine Ligands.

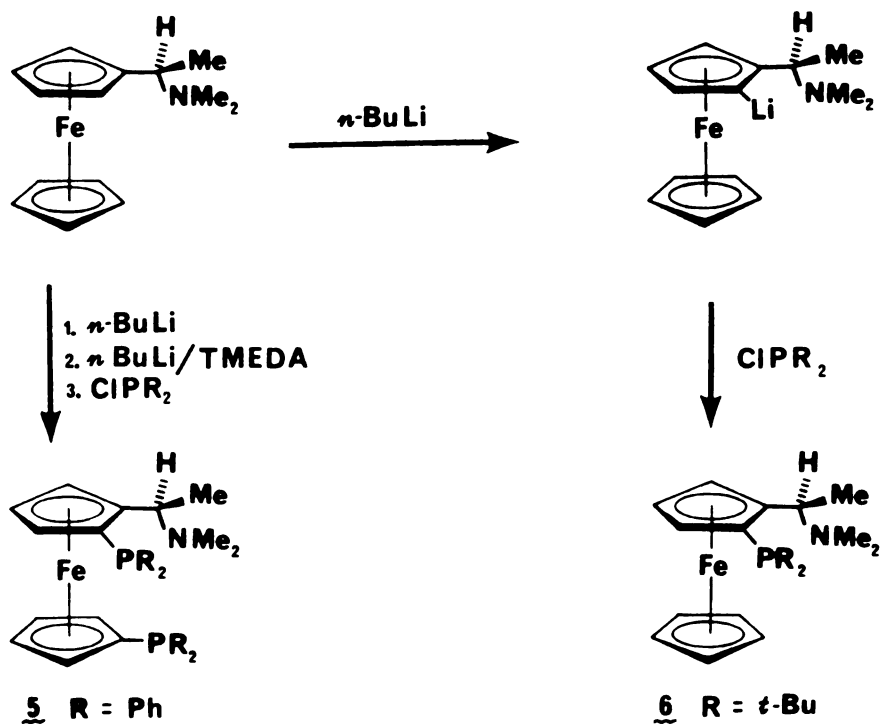
Metal	Complex	Ref.
<u>Fdpp</u>		
$(\text{PhCN})_2\text{MCl}_2$ M = Pd, Pt	$(\text{Fdpp})\text{MCl}_2$	17
$\text{RhH}(\text{CO})(\text{PPh}_3)_3$	$(\text{Fdpp})\text{RhH}(\text{CO})(\text{PPh}_3)_3$	18
CuI	$(\text{Fdpp})\text{CuI}$	14
$\text{M}(\text{CO})_6$ M = Cr, Mo, W	$(\text{Fdpp})\text{M}(\text{CO})_4$	
$\text{V}(\text{CO})_6$	$[(\text{Fdpp})\text{V}(\text{CO})_4](\text{NEt}_4)$	
$\text{Ta}(\text{CO})_6 \text{NEt}_4$	$[(\text{Fdpp})\text{Ta}(\text{CO})_4](\text{NEt}_4)$	
$\text{MX}_2$ M = Co, Ni X = Cl, Br, I	$(\text{Fdpp})\text{MX}_2$	
$\text{HgX}_2$ X = Cl, Br, I, SCN	$(\text{Fdpp}) \cdot n\text{HgX}_2$ n = 1, 2	20
$\text{Hg}(\text{CN})_2$	$[(\text{Fdpp})_2\text{Hg}](\text{BF}_4)_2$	
$\text{SnX}_4$	$(\text{Fdpp}) \cdot n \text{SnX}_4$ n = 1.5	
$(\text{Et}_2\text{S})_2\text{PtCl}_2$	$(\text{Fdpp})\text{PtCl}_2$	21
<u>Fdma, Fdpa</u>		
$\text{M}(\text{CO})_6$ M = Cr, Mo, W	$(\text{Fdpa})\text{M}(\text{CO})_4$ ; $(\text{Fdma})\text{M}(\text{CO})_4$ ; $(\text{Fdma})_2\text{Mo}(\text{CO})_3$ ; $\mu - (\text{Fdma}) - [(\text{Fdma})\text{Mo}(\text{CO})_3]_2$	15
$\text{MX}_2$ M = Pd, Pt X = Cl, Br, I	$(\text{Fdpa})\text{MX}_2$ ; $(\text{Fdma})\text{MX}_2$ $(\text{Fdma})\text{MX}^+$ ; $(\text{Fdma})_2\text{M}^{2+}$	16
$\text{Rh}(\text{C}_8\text{H}_{12})\text{Cl}_2$	$[\text{Rh}(\text{Fdma})_2](\text{PF}_6)$	22



Seyferth has very recently reported the use of 1,1'-ferrocenylenephosphine oligomers in the cobalt catalyzed hydroformylation of 1-hexene<sup>23</sup>. The polymeric ligands chelate to cobalt in a tridentate fashion and give hydroformylation results comparable to triphenylphosphine ligands.

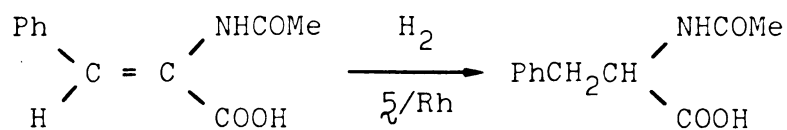
Palladium phosphine complexes are known to catalyze cross-coupling reactions between organometallic compounds and alkyl and aryl halides. Kumada<sup>17</sup> has shown that the ferrocenylphosphine ligand in the complex, (fdpp)PdCl<sub>2</sub>, is superior to diphos for coupling sec-butyilmagnesium-chloride with bromopropene, bromobenzene and bromostyrene.

Another recent development in ferrocene chemistry is the use of chiral ferrocene derivatives as ligands in transition metal catalyzed asymmetric synthesis. Chiral ferrocenylphosphines are prepared by the stereoselective lithiation of  $\alpha$ -ferrocenylethyldimethylamine followed by treatment with chlorophosphines (See Scheme 2). Rhodium complexes with chiral ferrocenylphosphine ligands such as (5) and (6) have been used as catalysts in asymmetric hydrogenation, Grignard cross-coupling and hydrosilylation<sup>24</sup>. In particular, acylaminoacids have been produced in over 90% optical purity by the asymmetric hydrogenation of  $\alpha$ -acetaminocinnamic acids catalyzed by a rhodium complex of (5) as shown below.



Scheme 2

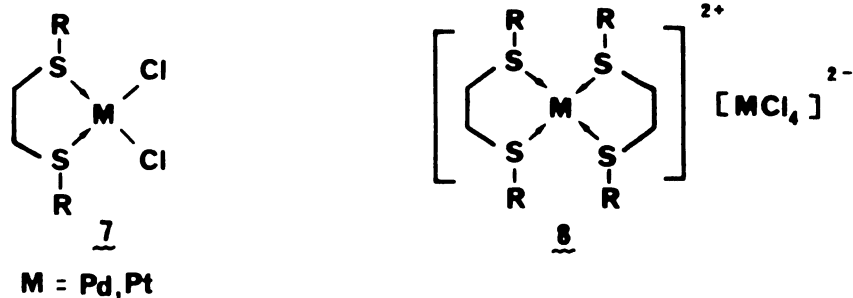
Cullen recently reported that the alkylferrocenylphosphine, (**6**) shown in Scheme 2, was more effective in asymmetric hydrogenation of acetamidoacrylic acids than the aryl analog<sup>25</sup>. He also concluded that rhodium complexes containing ferrocenylarsine ligands were not catalytically active in asymmetric hydrogenation.



Kumada was able to hydrogenate carbonyl compounds with optical yields ranging from 43 - 83% by introducing a hydroxyl group on to a chiral ferrocenylphosphine ligand. Previous attempts with other classes of phosphine ligands led to less than 10% stereoselectivity<sup>26</sup>. The high asymmetric induction obtained by Kumada can be ascribed to hydrogen bonding between the carbonyl group on the substrate and the hydroxy group on the chiral ligand. These attractive interactions increase the conformational rigidity of the diastereomeric transition state and consequently enhance the stereoselectivity of the reaction. Since chiral ferrocenylphosphines can be readily modified by introducing different functionality into the side chains<sup>27</sup> they have distinct advantages over other classes of phosphine ligands in that they may be tailored to "fit" specific substrates.

In contrast to tertiary phosphines, there has been very little interest in the chemistry of metal complexes containing organic sulfides. Two recent reviews deal with the coordination chemistry of thioether ligands with transition metals<sup>28</sup>. Two structures are possible, one where a single thioether ligand chelates to the metal, ( $\eta$ ) or alternatively where two ligands chelate to the metal, as in ( $\eta$ ), to give a complex similar to Magnus' green salt.

Traditionally metal sulfides have been used as catalysts in hydrosulfurization<sup>29</sup> but recently there has been much interest in the catalytic activity of transition metal sulfide complexes.

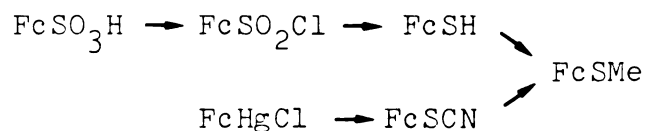


Many metal clusters with thiolato bridges have recently been reported<sup>30</sup>. A binuclear rhodium complex  $[\text{Rh}_2(\mu\text{S}-t\text{Bu})_2(\text{POMe}_3)_4]$  was reported to be catalytically active in the hydroformylation of 1-hexene<sup>31</sup>. In addition  $\eta^3$ -allyl metal sulfur clusters,  $[\eta^3\text{-C}_3\text{H}_5\text{MS}(\eta^3\text{-C}_3\text{H}_5\text{M}') ]_x$  where M, M' = Pd, Pt, were found to selectively hydrogenate acetylenes to olefins and to isomerize olefins<sup>32</sup>. Rakowski-DuBois has recently reported molybdenum dimers of the type  $(\text{CpMoS})_2\text{S}_2\text{CR}_2$ , R = H, alkyl, which reduce acetylenes to olefins and catalyze the hydrogenation of molecules containing C = N, N = N and C = S bonds<sup>33</sup>.

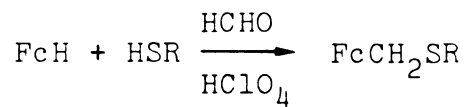
Very few thioether transition metal complexes have however proved to be effective catalysts. James<sup>34</sup> has reported that  $\text{RhCl}_3(\text{SEt}_2)_3$  hydrogenates maleic acid but as sulfur ligands are weaker  $\pi$ -acceptors than phosphine ligands, Rh(I) sulfide complexes can be reduced by hydrogen to rhodium metal. James has also prepared chelating chiral sulfoxide ligands and has found that ruthenium complexes are active in asymmetric hydrogenation<sup>35</sup>.

The object of this research was to develop a new class of chelating ferrocenyl ligands. The recent interest in transition metal sulfides led to the investigation of the preparation of ferrocenylsulfides.

A few ferrocenylsulfide complexes are known in the literature. Pauson<sup>36</sup> has prepared methylthioferrocene from ferrocenesulfonic acid whereas Russian workers<sup>37</sup> prepared this complex from thiocyanatoferrocene.



Ferrocenylmethylsulfides have recently been prepared from ferrocene and mercaptans in a one step synthesis<sup>38</sup>.

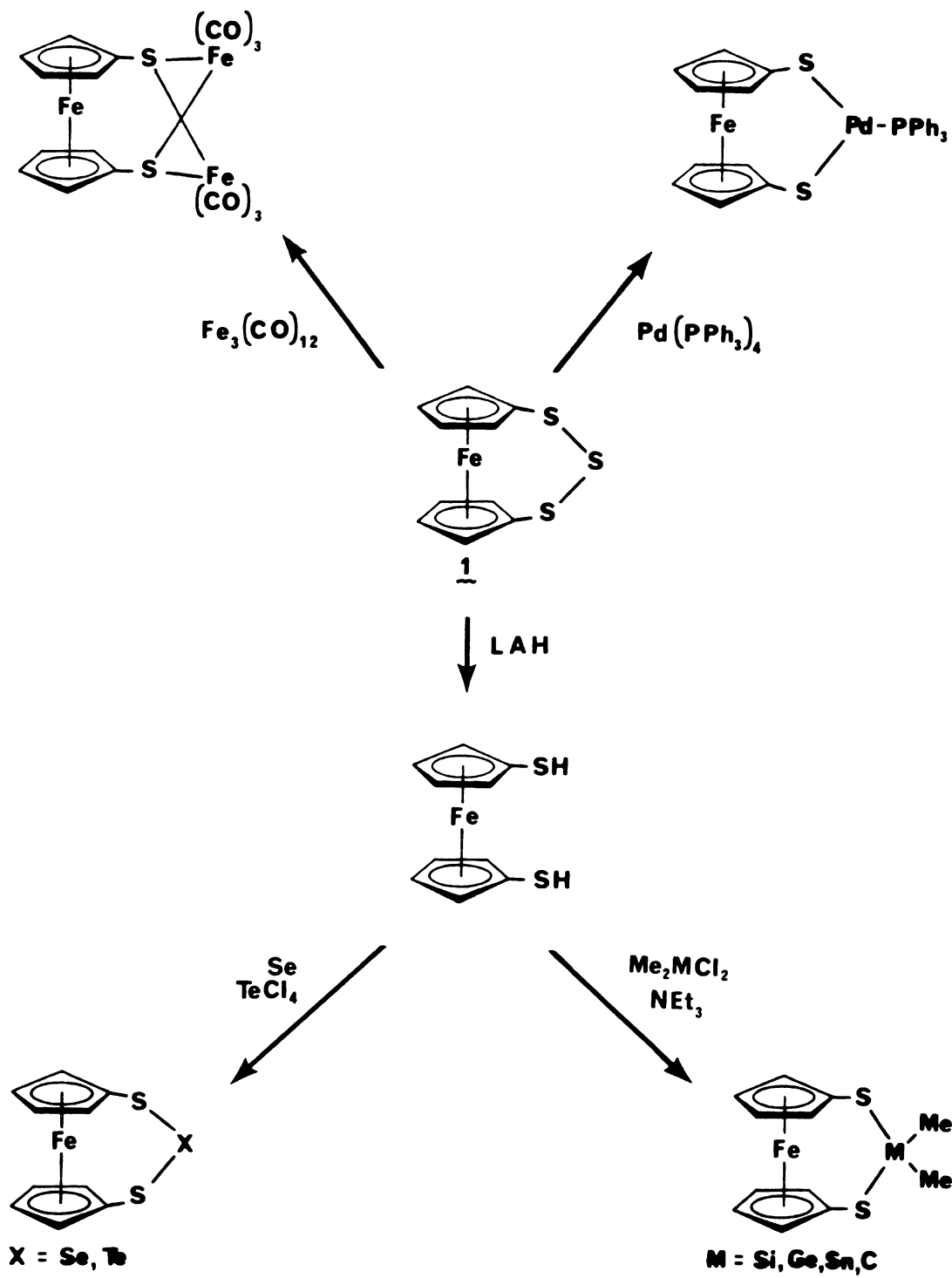


These procedures are limited to the preparation of specific ferrocenylsulfide complexes. Elschenbroich<sup>39</sup> reported the preparation of 1,1'-bis(methylthiobenzene)chromium by dilithiating bis(benzene)chromium followed by subsequent reaction with dimethyldisulfide. An approach similar to that used by Elschenbroich was used in this research to produce a one-pot, high yield, general synthesis of disubstituted ferrocenylsulfides. In addition the reaction of tetraalkylthiuram disulfides with mono and dilithioferrocene

was examined. The preparation of a chiral ferrocenylsulfide derivative is also outlined.

A few ferrocenylsulfide metal complexes have been prepared from 1,2,3-trithia[3]ferrocenophanes as shown in Scheme 3. Davison<sup>40</sup> has prepared a series of 1,3-dithia[3]ferrocenophanes with C, Si, Ge and Sn bridges from 1,1'-dithiolferrocene. Similarly Se and Te can be incorporated as bridges<sup>9</sup>. Seyferth has recently shown that transition metals readily insert into sulfur-sulfur bonds<sup>41</sup>. Reaction of (1) with  $\text{Pd}(\text{Ph}_3)_4$ <sup>42</sup> and  $\text{Fe}_3(\text{CO})_{12}$ <sup>43</sup> has resulted in unusual metal complexes with a chelating ferrocenyldithiolate ligand.

In the last section the reactivity of the ferrocenylsulfide derivatives as bidentate ligands was examined. Palladium and platinum halides were complexed with the ferrocenylsulfide ligands and the physical properties of the heterobimetallic compounds were examined.



Scheme 3

## II. EXPERIMENTAL

### General Techniques

Air-sensitive reagents were manipulated in a prepurified argon or nitrogen atmosphere. Hexane was freshly distilled from calcium hydride. 1,1'-Bis(diphenylphosphino)ferrocene, (fdpp), was prepared according to Davison's procedure<sup>8</sup> and (fdpp)PdCl<sub>2</sub> was prepared following Kumada's procedure<sup>17</sup>. (Fdpp)PtCl<sub>2</sub> was similarly prepared. Bis(benzonitrile) complexes, [(PhCN)<sub>2</sub>MX<sub>2</sub>], where M = Pd,Pt; X = Cl,Br, were prepared according to published procedures<sup>45</sup>.

Infrared spectra (IR) were obtained on a Perkin-Elmer 457 grating spectrophotometer or a Perkin-Elmer 239B spectrophotometer by using Nujol or Fluorolube mulls between CsBr plates. Ultraviolet and visible spectra (UV-vis) were recorded by use of a Cary 17 spectrophotometer and acetonitrile solutions. Mass spectra (MS) were obtained by means of a Finnigan 4000 instrument with an Incos data system at 70 eV. Electrochemical measurements were made with a PAR 174 polarograph, coupled to a Hewlett-Packard Model 7045A fast X-Y recorder, by cyclic voltammetry techniques. All melting points were determined by using a



Thomas-Hoover capillary melting point apparatus and are uncorrected. Elemental analyses were performed by Galbraith Laboratories, Inc., Knoxville, Tennessee.

Proton NMR spectra were obtained by use of a Bruker WM-250 spectrometer at 250 MHz. Unless otherwise noted, all NMR spectra were recorded in chloroform- $d_1$  solutions with chemical shifts reported in parts per million downfield from a tetramethylsilane internal standard. Carbon-13 NMR (broadband proton decoupled and gated decoupled) were obtained by use of a Bruker WM-250 spectrometer at 62.9 MHz. Carbon-13 NMR spectra were recorded in methylene chloride with deuterium oxide as an external lock and chemical shifts, referenced to methylene chloride, are uncorrected for volume susceptibilities. A pulse width (PW) of 6  $\mu$ s and a relaxation delay (RD) of 2 s were parameters that were generally used.

Platinum-195 NMR spectra were recorded with a Bruker WH-180 spectrometer with a mid-range frequency probe operating at 38.7 MHz. The spectra were obtained with a pulse width (PW) of 30  $\mu$ s and a sweep width (SW) of 40,000. The frequency offset (Ol) was set at zero and the synthesizer frequency (SY) was varied from 70,725,000 to 70,740,000.  $\text{Na}_2\text{PtCl}_6$  was used as the reference and as all signals are upfield of the reference they are reported as negative values. The chemical shifts were calculated by using the following equations:

$$\begin{aligned} \text{Absolute frequency} &= \text{Instrument frequency} - 2(\text{SY}) \\ &+ 01 + \text{cursor frequency} - (\text{SW}/2) \end{aligned}$$

$$\text{Shift(ppm)} = (\text{Abs freq}_{(\text{sample})} - \text{Abs freq}_{(\text{ref})})/38.7$$

A single crystal of 1,1'-bis(isobutylthio)ferrocene-palladiumdichloride was prepared for crystallographic studies by slow evaporation of the mixed solvent system methylene chloride/hexane at 25°C. It crystallizes in the orthorhombic space group Pbc<sub>a</sub> with eight molecules per unit cell. Crystal data are as follows:  $a = 22.168(11)$ ,  $b = 11.855(7)$ ,  $c = 16.131(6)$  Å;  $M = 539.69$ ;  $\rho_c = 1.691$  g cm<sup>-3</sup>. Lattice dimensions were determined by using a Picker FACS-I diffractometer and MoK $\alpha_1$  ( $\lambda = 0.70926$  Å) radiation.

Intensity data were measured using MoK $\alpha$  radiation ( $2\theta_{\text{max}} = 60^\circ$ ) yielding 6182 total unique data and, based on  $I > 2\sigma(I)$ , 3689 observed data. The data were reduced<sup>46</sup>; and refinement was by full-matrix least-squares techniques<sup>47</sup>; and the structures were solved by direct methods<sup>48</sup>. The final R value was 0.046. The final difference Fourier map showed densities ranging from +1.13 to -1.01 with no indication of missing atoms.

#### 1,1'-Bis(methylthio)ferrocene (9)

Ferrocene (3g, 16 mmol) was added to a solution of N,N,N',N'-tetramethylethylenediamine (TMEDA) (5.1 mL,

33 mmol) and 1,6 M n-butyllithium in hexane (20.67 mL, 33 mmol) in oxygen-free hexane (100 mL) in a 250 mL round bottom flask equipped with a side arm and serum cap, under nitrogen. The solution was stirred for 3 h then dimethyldisulfide (2.96 mL, 33 mmol) in about 20 mL benzene was added slowly via cannula to the bright orange solution at  $-10^{\circ}\text{C}$  and the solution was stirred overnight. The resulting brown solution was then filtered under nitrogen and the filtrate was evaporated to dryness. (Addition of water to destroy the excess lithio species resulted in a green then black/blue oil which could be ferricenium). Unreacted ferrocene was removed by sublimation ( $80^{\circ}\text{C}/10^{-1}$  mm) and (9) was obtained as a brown oil in a 70% yield.  $^1\text{H}$  NMR:  $\delta$ 4.29 (t, 4H,  $\text{H}_{2,5}$ ), 4.21 (t, 4H,  $\text{H}_{3,4}$ ) 2.30 (s, 6H,  $\text{CH}_3$ );  $^{13}\text{C}$  NMR: ( $\text{CH}_2\text{Cl}_2/\text{D}_2\text{O}$ ):  $\delta$ 85.21 (s,  $\text{C}_1$ ), 71.72 (d, J = 177.6 Hz,  $\text{C}_{3,4}$ ), 69.59 (d, J = 176.6 Hz,  $\text{C}_{2,5}$ ), 19.35 (q, J = 139.5 Hz,  $\text{CH}_3$ ). Mass spec: m/e (rel intensity), 278 (39,  $\text{M}^+$ ), 232 (85), 217 (71), 186 (20), 152 (16), 121 (2), 56 (100, Fe).

#### 1,1'-Bis(isobutylthio)ferrocene (10)

1,1'-Dilithioferrocene (36 mmol) was prepared as described above. Isobutyldisulfide (13.9 mL, 72 mmol) in 40 mL benzene was added slowly via cannula to the orange solution at  $-10^{\circ}\text{C}$ . After being stirred overnight at room temperature the solution became clear brown and 10 mL water

was added. The organic layer was separated, dried and evaporated to dryness. Unreacted ferrocene was removed by sublimation ( $80^{\circ}\text{C}/10^{-1}\text{ mm}$ ) to give 10 g of (10), (75% yield). Yellow flakes can be obtained by recrystallizing from hexane at  $-78^{\circ}\text{C}$ , mp =  $33-34^{\circ}\text{C}$ .  $^1\text{H}$  NMR:  $\delta$ 4.28 (5, 4H,  $\text{H}_{2,5}$ ), 4.20 (t, 4H,  $\text{H}_{3,4}$ ), 2.50 (d,  $J = 6.9\text{ Hz}$ , 4H,  $\text{CH}_2$ ), 1.72 (m,  $J = 6.9\text{ Hz}$ , 2H, CH), 0.97 (d,  $J = 6.9\text{ Hz}$ , 12H,  $\text{CH}_3$ );  $^{13}\text{C}$  NMR: ( $\text{CH}_2\text{Cl}_2/\text{D}_2\text{O}$ ),  $\delta$ 82.76 (s,  $\text{C}_1$ ), 74.11 (d,  $J = 172.9\text{ Hz}$ ,  $\text{C}_{3,4}$ ), 70.31 (d,  $J = 177.5\text{ Hz}$ ,  $\text{C}_{2,5}$ ), 46.40 (t,  $J = 137.8\text{ Hz}$ ,  $\text{CH}_2$ ), 28.51 (d,  $J = 128.5\text{ Hz}$ , CH), 21.68 ppm (q,  $J = 125.8\text{ Hz}$ ,  $\text{CH}_3$ ); Mass spec: m/e (rel intensity) 362 (45,  $\text{M}^+$ ), 274 (72), 218 (88), 152 (50), 121 (89), 56 (99), 41 (100).

Anal. Calcd. for  $\text{C}_{18}\text{H}_{20}\text{S}_2\text{Fe}$ : C, 59.66; H, 7.23.

Found: C, 59.60; H, 7.21.

#### 1,1'-Bis(isopropylthio)ferrocene (11)

Isopropyldisulfide (17.96 mL, 113 mmol) in about 150 mL hexane was slowly added via cannula to 1,1'-dilithioferrocene (54 mmol) at  $-78^{\circ}\text{C}$ . After being stirred at room temperature for two days 100 mL water was added to the cloudy yellow solution to give a clear brown solution. The organic layer was separated, dried and evaporated to give a brown oil. Unreacted ferrocene was removed by sublimation ( $80^{\circ}\text{C}/10^{-1}\text{ mm}$ ). About 13 g of (11) was obtained as a brown oil (73% yield). Traces of the disulfide can be removed by

crystallization from hexane at low temperature.  $^1\text{H}$  NMR:  $\delta$ 4.31 (t, 4H,  $\text{H}_{2,5}$ ), 4.24 (t, 4H,  $\text{H}_{3,4}$ ), 2.86 (m,  $J = 6.7$  Hz, 2H, CH), 1.16 (d,  $J = 6.7$  Hz, 12H,  $\text{CH}_3$ );  $^{13}\text{C}$  NMR:  $\delta$ ( $\text{CH}_2\text{Cl}_2/\text{D}_2\text{O}$ ), 79.14 (s,  $\text{C}_1$ ), 76.20 (d,  $J = 178$  Hz,  $\text{C}_{3,4}$ ), 70.96 (d,  $J = 176$  Hz,  $\text{C}_{2,5}$ ), 39.64 (d,  $J = 142$  Hz, CH), 23.41 (q,  $J = 126.9$  Hz,  $\text{CH}_3$ ); Mass spec: m/e (rel intensity), 334 (100,  $\text{M}^+$ ), 292 (19), 260 (22), 250 (26), 218 (43), 195 (42), 152 (38), 121 (27), 97 (35).

1,1'-Bis(phenylthio)ferrocene ( $\text{12}$ )

Phenyldisulfide (18 g, 82 mmol) in about 80 mL benzene was added slowly via cannula to 1,1'-dilithioferrocene (40 mmol) at  $-10^\circ\text{C}$ . The solution was stirred overnight at room temperature to give a cloudy yellow solution. About 30 mL water was added and ( $\text{12}$ ) which precipitated out from the benzene/hexane layer was filtered and washed with petroleum ether to remove the unreacted ferrocene. About 13 g (80% yield) of ( $\text{12}$ ) was obtained and an analytically pure sample was obtained by recrystallizing from  $\text{CH}_2\text{Cl}_2$  to give yellow needles, mp =  $172\text{--}173^\circ\text{C}$ .  $^1\text{H}$  NMR:  $\delta$ 4.49 (t, 4H,  $\text{H}_{2,5}$ ), 4.44 (t, 4H,  $\text{H}_{3,4}$ ), 7.08 (m, 10H, Ph);  $^{13}\text{C}$  NMR: ( $\text{CH}_2\text{Cl}_2/\text{D}_2\text{O}$ ),  $\delta$ 140.27 (s,  $\text{C}_1$  of Ph), 128.68 (d,  $J = 161$  Hz, Ph), 126.38 (d,  $J = 161$  Hz, Ph), 125.17 (d,  $J = 161$  Hz, Ph), 77.77 (s,  $\text{C}_1$ ), 76.34 (d,  $J = 181$  Hz,  $\text{C}_{3,4}$ ), 71.91 (d,  $J = 177.5$  Hz,  $\text{C}_{2,5}$ ); Mass spec.: m/e

(rel intensity), 402 (100,  $M^+$ ), 56 (74, Fe).

Anal. Calcd. for  $C_{22}H_{18}S_2Fe$ : C, 65.67; H, 4.48; S, 15.92

Found: C, 65.69; H, 4.36; S, 16.01

1,1'-Bis(benzylthio)ferrocene (13)

Benzyl disulfide (27.7 g, 112 mmol) in 200 mL benzene was added slowly via cannula to 1,1'-dilithioferrocene (54 mmol) at  $-40^\circ C$ . After being stirred at room temperature overnight the bright yellow suspension was filtered and washed with water. Unreacted ferrocene and benzyl disulfide were sublimed ( $80^\circ C/10^{-1}$  mm) from the sticky yellow powder. The yellow solid is recrystallized from  $CH_2Cl_2$ /hexane to give 10.2 g of (13) (50% yield). The filtrate was evaporated and after sublimation an additional 9 g was isolated to give a total yield of 83%.  $^1H$  NMR:  $\delta$ 7.19 (m), 7.11 (m, Ph), 4.12 (t, 4H,  $H_{2,5}$ ), 4.10 (t, 4H,  $H_{3,4}$ ), 3.72 (s, 4H,  $CH_2$ );  $^{13}C$  NMR: ( $CH_2Cl_2/D_2O$ ,  $28^\circ C$ ),  $\delta$ 138.8 (s,  $C_1$  of Ph), 128.87 (d,  $J = 164$  Hz, Ph), 128.25 (d,  $J = 161$  Hz, Ph), 126.80 (d,  $J = 168$  Hz, Ph), 81.16 (s,  $C_1$ ), 74.68 (d,  $J = 178$  Hz,  $C_{3,4}$ ), 70.57 (d,  $J = 177$  Hz,  $C_{2,5}$ ), 42.12 (t,  $J = 142$  Hz,  $CH_2$ ); Mass spec: m/e (rel intensity), 430 (100,  $M^+$ ), 339 (28,  $M^+ - CH_2Ph$ ), 243 (39), 152 (6), 91 (18).

Anal. Calcd. for  $C_{24}H_{22}S_2Fe$ : C, 66.97; H, 5.15

Found: C, 67.18; H, 5.12

1,1'-Bis(isopentylthio)ferrocene (14)

Isopentyldisulfide (7.4 mL, 33 mmol) in about 50 mL hexane was added slowly via cannula to 1,1'-dilithioferrocene (16 mmol) at  $-40^{\circ}\text{C}$ . After being stirred at room temperature overnight 100 mL water was added to the bright yellow solution. The organic layer was separated, dried and evaporated to give a light brown oil. Unreacted ferrocene was removed by sublimation ( $80^{\circ}\text{C}/10^{-1}$  mm) and traces of the disulfide were removed by recrystallization from hexane at low temperature to give 4.5 g of (14), 71% yield.  $^1\text{H}$  NMR:  $\delta$ 4.26 (t, 4H,  $\text{H}_{2,5}$ ), 4.18 (t, 4H,  $\text{H}_{3,4}$ ), 2.59 (t, 4H,  $\alpha\text{CH}_2$ ), 1.42 (m, 4H,  $\beta\text{CH}_2$ ), 1.65 (m, 2H, CH), 0.86 (d, 6H,  $\text{CH}_3$ );  $^{13}\text{C}$  NMR:  $\delta$ 81.41 (s,  $\text{C}_1$ ), 77.50 (d,  $\text{C}_{3,4}$ ), 70.03 (d,  $\text{C}_{2,5}$ ), 38.33 (t,  $\alpha\text{CH}_2$ ), 34.89 (t,  $\beta\text{CH}_2$ ), 26.67 (d, CH), 21.96 (q,  $\text{CH}_3$ ); Mass spec: m/e (rel intensity), 390 (100,  $\text{M}^+$ ), 286 (16), 249 (18), 218 (16), 152 (19), 121 (14), 97 (19).

1,1'-Bis(diphenylphosphino)ferrocene (15)<sup>8</sup>

$^{13}\text{C}$  NMR: ( $\text{CH}_2\text{Cl}_2/\text{D}_2\text{O}$ ),  $\delta$ 139.02 (d,  $^1\text{J}_{\text{CP}} = 10.7$  Hz, s,  $\text{C}_1$ ), 133.29 (d,  $^2\text{J}_{\text{CP}} = 18.5$  Hz, d,  $\text{J}_{\text{CH}} = 161$  Hz, Ph), 128.49 (d,  $^3\text{J}_{\text{CP}} = 18.5$  Hz, d,  $\text{J}_{\text{CH}} = 161$  Hz, Ph), 128.22 (d,  $^4\text{J}_{\text{CP}} = 25$  Hz, d,  $\text{J}_{\text{CH}} = 161$  Hz, Ph), 76.63 (d,  $^1\text{J}_{\text{CP}} = 8$  Hz,  $\text{C}_1$ ), 73.68 (d,  $^2\text{J}_{\text{CP}} = 14$  Hz, d,  $\text{J}_{\text{CH}} = 177$  Hz,  $\text{C}_{3,4}$ ), 72.71 (d,  $\text{J}_{\text{CH}} = 175$  Hz,  $\text{C}_{2,5}$ ).

### Preparation of Metal Complexes

The complexes  $\text{Fe}(\text{C}_5\text{H}_4\text{SR})_2\text{MX}_2$  where  $\text{R} = \text{Me}, \text{CHMe}_2, \text{CH}_2\text{CHMe}_2, \text{Ph}, \text{CH}_2\text{Ph}$ ;  $\text{M} = \text{Pd}, \text{Pt}$ ;  $\text{X} = \text{Cl}, \text{Br}$ , were prepared from benzene solutions of the appropriate  $(\text{PhCN})_2\text{MX}_2$  species and a slight excess of the ferrocenylsulfide,  $\text{Fe}(\text{C}_5\text{H}_4\text{SR})_2$ , in an approximate 1:1.1 molar ratio. The resulting precipitate was filtered, washed with benzene, then petroleum ether and then recrystallized from methylene chloride/hexane by slow evaporation.

#### 1,1'-Bis(isobutylthio)ferrocenepalladiumdichloride (16)

Shiny black crystals decomposed at 182-183°C.  $^1\text{H}$  NMR: (72°C),  $\delta$ 5.28 (br, 4H,  $\text{H}_{2,5}$ ), 4.42 (t, 4H,  $\text{H}_{3,4}$ ), 2.98 (d,  $J = 6.8$  Hz, 4H,  $\text{CH}_2$ ), 1.80 (m,  $J = 6.8$  Hz, 2H, CH), 1.01 (d,  $J = 6.8$  Hz, 12H,  $\text{CH}_3$ );  $^{13}\text{C}$  NMR: ( $\text{CH}_2\text{Cl}_2/\text{D}_2\text{O}$ ),  $\delta$ 79.32 (s,  $\text{C}_1$ ), 76.23 (d,  $J = 184$  Hz,  $\text{C}_{3,4}$ ), 71.72 (br d,  $J = 178$  Hz,  $\text{C}_{2,5}$ ), 49.50 (t,  $J = 145.5$  Hz,  $\text{CH}_2$ ), 26.42 (d,  $J = 134$  Hz, CH), 21.38 (q,  $J = 126.7$  Hz,  $\text{CH}_3$ ); IR (Nujol): 370 (sh), 365 (w), 307 (s), 290 (sh)  $\text{cm}^{-1}$ . Anal. Calcd. for  $\text{C}_{18}\text{H}_{26}\text{Cl}_2\text{S}_2\text{FePd}$ : C, 40.06; H, 4.86; Cl, 13.14; S, 11.88. Found: C, 40.14; H, 5.00; Cl, 13.35; S, 12.01.



1,1'-Bis(isobutylthio)ferrocenepalladiumdibromide (17)

Shiny black needles decomposed at 185-187°C.  $^1\text{H}$  NMR: (23°C),  $\delta$ 5.30 (br, 4H,  $\text{H}_{2,5}$ ), 4.40 (s, 4H,  $\text{H}_{3,4}$ ), 3.06 (br, s, 4H,  $\text{CH}_2$ ), 1.81 (m,  $J = 6.7$  Hz, 2H, CH), 1.01 (d,  $J = 6.7$  Hz, 12H,  $\text{CH}_3$ );  $^{13}\text{C}$  NMR: ( $\text{CH}_2\text{Cl}_2/\text{D}_2\text{O}$ ),  $\delta$ 79.48 (s,  $\text{C}_1$ ), 76.36 (d,  $J = 176$  Hz,  $\text{C}_{3,4}$ ), 71.85 (d,  $J = 177$  Hz,  $\text{C}_{2,5}$ ), 52.85 (t,  $\text{CH}_2$ ), 26.89 (d,  $J = 129$  Hz, CH), 21.39 (q,  $J = 126$  Hz,  $\text{CH}_3$ ); IR (Nujol): 365 (w), 222 (s)  $\text{cm}^{-1}$ .  
Anal. Calcd. for  $\text{C}_{18}\text{H}_{26}\text{Br}_2\text{S}_2\text{FePd}$ : C, 34.39; H, 4.17; Br, 25.42. Found: C, 34.50; H, 4.18; Br, 23.18.

1,1'-Bis(isobutylthio)ferroceneplatinumdichloride (18)

Yellow needles decomposed at 218-220°C.  $^1\text{H}$  NMR: (101°C),  $\delta$ 5.14 (t, 4H,  $\text{H}_{2,5}$ ), 4.43 (t, 4H,  $\text{H}_{3,4}$ ), 3.08 (br, s, 4H,  $\text{CH}_2$ ), 1.92 (m, 2H, CH), 1.01 (d,  $J = 6.5$  Hz, 12H,  $\text{CH}_3$ );  $^{13}\text{C}$  NMR: ( $\text{CH}_2\text{Cl}_2/\text{D}_2\text{O}$ ),  $\delta$ 80.22 ( $\text{C}_1$ ), 75.93 ( $\text{C}_{3,4}$ ), 73.36 ( $\text{C}_{2,5}$ ), 70.81 ( $\text{C}_{2,5}$ ), 48.21 ( $\text{CH}_2$ ), 26.55 (CH), 21.85 ( $\text{CH}_3$ ); IR (Nujol): 372 (w), 323 (s), 310 (m)  $\text{cm}^{-1}$ .  
Anal. Calcd. for  $\text{C}_{18}\text{H}_{26}\text{Cl}_2\text{S}_2\text{FePt}$ : C, 34.41; H, 4.17; Cl, 11.28. Found: C, 34.43; H, 4.20; Cl, 11.39.

1,1'-Bis(isobutylthio)ferroceneplatinumdibromide (19)

Yellow flakes decomposed at 225-227°C.  $^1\text{H}$  NMR:  $\delta$ 5.45 (br, 2H,  $\text{H}_{2,5}$ ), 4.86 (br, 2H,  $\text{H}_{2,5}$ ), 4.58 (br, 2H,  $\text{H}_{3,4}$ ), 4.34 (br, 2H,  $\text{H}_{3,4}$ ), 2.94 (br, 4H,  $\text{CH}_2$ ), 1.89 (br, 2H, CH),

1.04 (br, d, 12H, CH<sub>3</sub>); <sup>13</sup>C NMR: (45°C), δ80.09 (C<sub>1</sub>), 75.32 (C<sub>3,4</sub>), 71.35 (br, C<sub>2,5</sub>), 49.21 (CH<sub>2</sub>), 26.42 (CH), 21.54 (CH<sub>3</sub>). IR (Nujol): 372 (w), 364 (w) cm<sup>-1</sup>.

1,1'-Bis(isopropylthio)ferrocenepalladiumdichloride (20)

Brown needles decomposed at 192-193°C. <sup>1</sup>H NMR: (50°C), δ5.3 (br, 4H, H<sub>2,5</sub>), 4.45 (br, s, 4H, H<sub>3,4</sub>), 4.04 (m, J = 6.8 Hz, 2H, CH), 1.23 (d, J = 6.8 Hz, 12H, CH<sub>3</sub>); IR (Nujol): 380 (w), 360 (w), 320 (s), 305 (s) cm<sup>-1</sup>.

Anal. Calcd. for C<sub>16</sub>H<sub>22</sub>Cl<sub>2</sub>S<sub>2</sub>FePd: C, 37.56; H, 4.33; Cl, 13.86. Found: C, 37.56, H, 4.40, Cl, 14.00.

1,1'-Bis(isopropylthio)ferrocenepalladiumdibromide (21)

Brown needles decomposed at 188-190°C. <sup>1</sup>H NMR: δ5.23 (br, 4H, H<sub>2,5</sub>), 4.45 (br, 4H, H<sub>3,4</sub>), 4.17 (m, J = 6.7 Hz, 2H, CH), 1.24 (br, 12H, CH<sub>3</sub>); IR (Nujol): 380 (w), 360 (w), 225 (s) cm<sup>-1</sup>.

Anal. Calcd. for C<sub>16</sub>H<sub>22</sub>Br<sub>2</sub>S<sub>2</sub>FePd: C, 32.00; H, 3.69; Br, 26.61. Found: C, 32.19; H, 3.65; Br, 26.43.

1,1'-Bis(isopropylthio)ferroceneplatinumdichloride (22)

Yellow flakes decomposed at 223-225°C. <sup>1</sup>H NMR: δ5.51 (s, 2H, H<sub>2,5</sub>), 4.72 (s, 2H, H<sub>2,5</sub>), 4.56 (s, 2H, H<sub>3,4</sub>), 4.28 (s, 2H, H<sub>3,4</sub>), 4.27 (m, J = 6.4 Hz, 2H, CH), 1.37 (d, 6H, CH<sub>3</sub>), 1.12 (d, 6H, CH<sub>3</sub>); IR (Nujol): 383 (w), 365 (w),

328 (s), 315 (s)  $\text{cm}^{-1}$ .

1,1'-Bis(isopropylthio)ferroceneplatinumdibromide (23)

Yellow flakes decomposed at 214-216°C.  $^1\text{H}$  NMR:  $\delta$ 5.54 (br, 2H,  $\text{H}_{2,5}$ ), 4.75 (br, 2H,  $\text{H}_{2,5}$ ), 4.60 (br, 2H,  $\text{H}_{3,4}$ ), 4.31 (br, 2H,  $\text{H}_{3,4}$ ), 4.27 (m,  $J = 6.7$  Hz, 2H, CH), 1.39 (br, 6H,  $\text{CH}_3$ ), 1.16 (br, 6H,  $\text{CH}_3$ ); IR (Nujol): 389 (w), 370 (w), 220 (s)  $\text{cm}^{-1}$ .

Anal. Calcd. for  $\text{C}_{16}\text{H}_{22}\text{Br}_2\text{S}_2\text{FePt}$ : C, 27.88; H, 3.22; Br, 23.19. Found: C, 28.08; H, 3.41; Br, 23.35.

1,1'-Bis(methylthio)ferrocenepalladiumdichloride (24)

Brown powder decomposed at 192-198°C. IR (Nujol): 355 (w), 340 (w), 310 (s), 290 (sh)  $\text{cm}^{-1}$ .

1,1'-Bis(methylthio)ferrocenepalladiumdibromide (25)

Dark brown powder decomposed at 209-213°C. IR (Nujol): 343 (w), 205 (m)  $\text{cm}^{-1}$ .

1,1'-Bis(methylthio)ferroceneplatinumdichloride (26)

Yellow powder decomposed at 239-244°C. IR (Nujol): 345 (w), 323 (s), 305 (s)  $\text{cm}^{-1}$ .

1,1'-Bis(methylthio)ferroceneplatinumdibromide (27)

Yellow crystals decomposed at 225-230°C. IR (Nujol): 340 (w), 208 (s)  $\text{cm}^{-1}$ .

Anal. Calcd. for  $\text{C}_{12}\text{H}_{14}\text{Br}_2\text{S}_2\text{FePt}$ : C, 22.77; H, 2.23; Br, 25.24. Found: C, 22.90; H, 2.15; Br, 24.99.

1,1'-Bis(benzylthio)ferrocenepalladiumdichloride (28)

Shiny black needles decomposed at 223-225°C.  $^1\text{H}$  NMR: (50°C),  $\delta$ 7.22 (m), 7.19 (m), 7.06 (m, Ph), 5.00 (br, 4H,  $\text{H}_{2,5}$ ), 4.34 (br, s, 4H,  $\text{H}_{3,4}$ ), 4.32 (s,  $\text{CH}_2$ ); IR (Nujol): 358 (m), 335 (w), 315 (s), 300 (s)  $\text{cm}^{-1}$ .

Anal. Calcd. for  $\text{C}_{24}\text{H}_{22}\text{Cl}_2\text{S}_2\text{FePd}$ : C, 47.43; H, 3.65; Cl, 11.67. Found: C, 47.66; H, 3.65; Cl, 11.90.

1,1'-Bis(benzylthio)ferrocenepalladiumdibromide (29)

Shiny black needles decomposed at 206-207°C.  $^1\text{H}$  NMR:  $\delta$ 7.24 (m), 7.05 (m, Ph), 4.96 (v, br, 4H,  $\text{H}_{2,5}$ ), 4.40 (s, 4H,  $\text{CH}_2$ ), 4.33 (br, 4H,  $\text{H}_{3,4}$ ); IR (Nujol): 353 (m), 345 (sh), 230 (s)  $\text{cm}^{-1}$ .

Anal. Calcd. for  $\text{C}_{24}\text{H}_{22}\text{Br}_2\text{S}_2\text{FePd}$ : C, 41.38; H, 3.18; Br, 22.94. Found: C, 41.45; H, 3.19; Br, 22.69.

1,1'-Bis(benzylthio)ferroceneplatinumdichloride (30)

Yellow flakes decomposed at 224-225°C.  $^1\text{H}$  NMR: (50°C),  $\delta$ 7.34 (s), 7.20 (m), 7.04 (m, Ph), 5.45 (v, br, 4H,  $\text{H}_{2,5}$ ),

4.60 (br, 4H, H<sub>3,4</sub>), 4.43 (s, 4H, CH<sub>2</sub>); IR (Nujol): 360 (m), 350 (m), 332 (s), 312 (s) cm<sup>-1</sup>.

Anal. Calcd. for C<sub>24</sub>H<sub>22</sub>Cl<sub>2</sub>S<sub>2</sub>FePt: C, 41.39; H, 3.18; Cl, 10.18. Found: C, 41.21; H, 3.17; Cl, 9.90.

1,1'-Bis(benzylthio)ferroceneplatinumdibromide (31)

Yellow flakes decomposed at 198-200°C. <sup>1</sup>H NMR: δ7.23 (m), 7.20 (m), 7.02 (m, Ph), 5.53 (v, br, 2H, H<sub>2,5</sub>), 4.56 (br, s, 4H, CH<sub>2</sub>), 4.44 (br, 2H, H<sub>2,5</sub>), 4.12 (br, 4H, H<sub>3,4</sub>); IR (Nujol): 358 (m), 348 (m), 215 (s) cm<sup>-1</sup>.

Anal. Calcd. for C<sub>24</sub>H<sub>22</sub>Br<sub>2</sub>S<sub>2</sub>FePt: C, 36.71; H, 2.82; Br, 20.35. Found: C, 36.67; H, 2.81; Br, 20.12.

1,1'-Bis(phenylthio)ferrocenepalladiumdichloride (32)

Brown powder decomposed at 198-201°C. <sup>1</sup>H NMR: δ7.38 (m, 10H, Ph), 5.27 (v, br, 4H, H<sub>2,5</sub>), 4.65 (br, s, 4H, H<sub>3,4</sub>); IR (Nujol): 323 (vs), 308 (vs), 278 (s), 262 (s) cm<sup>-1</sup>.

1,1'-Bis(phenylthio)ferrocenepalladiumdibromide (33)

Shiny black needles decomposed at 188-189°C. <sup>1</sup>H NMR: δ7.35 (m, 10H, Ph), 5.41 (br, t, 4H, H<sub>2,5</sub>), 4.64 (t, 4H, H<sub>3,4</sub>); IR (Nujol): 316 (s) cm<sup>-1</sup>.

Anal. Calcd. for C<sub>22</sub>H<sub>18</sub>Br<sub>2</sub>S<sub>2</sub>FePd: C, 39.52; H, 2.71; Br, 23.90. Found: C, 39.45; H, 2.82; Br, 22.30.

1,1'-Bis(phenylthio)ferroceneplatinumdichloride (34)

Yellow needles decomposed at 210-213°C.  $^1\text{H}$  NMR:  $\delta$ 7.42 (m), 7.38 (s, Ph), 5.31 (br, s, 4H,  $\text{H}_{2,5}$ ) 4.64 (br, s, 4H,  $\text{H}_{3,4}$ ); IR (Nujol): 350 (s), 329 (s), 317 (s), 312 (s)  $\text{cm}^{-1}$ .

Anal. Calcd. for  $\text{C}_{22}\text{H}_{18}\text{Cl}_2\text{S}_2\text{FePt}$ : C, 39.54; H, 2.72; Cl, 10.61. Found: C, 39.74; H, 2.79; Cl, 10.66.

1,1'-Bis(phenylthio)ferroceneplatinumdibromide (35)

Yellow plates decomposed at 245-247°C.  $^1\text{H}$  NMR:  $\delta$ 7.38 (m, 10H, Ph), 5.30 (v br, 4H,  $\text{H}_{2,5}$ ), 4.61 (br, 4H,  $\text{H}_{3,4}$ ); IR (Nujol): 349 (sh), 324 (w), 266 (m)  $\text{cm}^{-1}$ .

Anal. Calcd. for  $\text{C}_{22}\text{H}_{18}\text{Br}_2\text{S}_2\text{FePt}$ : C, 34.89; H, 2.40; Br, 21.20. Found: C, 34.94; H, 2.51; Br, 21.23.

N,N-dimethyl- $\alpha$ -ferrocenylethylamine (36)

(36) was prepared and resolved using (R)-(+)-tartaric acid as described by Ugi<sup>49</sup>. The amine (36), can be recrystallized from petroleum ether to give a yellow powder, mp = 35°C.  $^1\text{H}$  NMR:  $\delta$ 4.11 (m, 4H,  $\text{C}_5\text{H}_4$ ), 4.08 (s, 5H, Cp), 3.55 (q,  $J$  = 6.8 Hz, 1H, CH), 2.05 (s, 6H,  $\text{NMe}_2$ ), 1.42 (d,  $J$  = 6.8 Hz, 3H,  $\text{CH}_3$ );  $^{13}\text{C}$  NMR:  $\delta$ 85.8 (s,  $\text{C}_1$ ), 68.3 (d), 67.5 (d,  $J$  = 176 Hz, Cp), 66.4 (d), 66.18 (d), 65.7 (d), 57.6 (d,  $J$  = 141 Hz, CH), 39.4 (q,  $J$  = 133 Hz,  $\text{NMe}_2$ ), 14.8 (q,  $J$  = 128 Hz,  $\text{CHMe}$ ).

(R)- $\alpha$ -[(S)-2-benzylthioferrocenyl]ethyldimethylamine (37)

The amine (36), (1.5 g, 5.8 mmol) was placed in a 200 mL flask equipped with a side arm and containing 40 mL diethylether. n-Butyllithium (4.0 mL, 6.4 mmol) was added slowly via syringe to the solution which was at  $-40^{\circ}\text{C}$ . The orange solution was allowed to warm to room temperature slowly and then stirred for an additional 1 h. Benzylidisulfide (1.45 g, 5.9 mmol) dissolved in about 70 mL warm hexane was added dropwise via cannula to the orange solution at  $-78^{\circ}\text{C}$ . The yellow solution was allowed to reach room temperature and then refluxed overnight. The reaction mixture was cooled and then 20 mL water was added. The organic layer was separated, dried and evaporated to give a dark oily residue. The oil was chromatographed on  $\text{Al}_2\text{O}_3/5\% \text{H}_2\text{O}$ , by eluting first with hexane and then with  $\text{CH}_2\text{Cl}_2$  to give 0.88 g of (37), (40% yield) as a brown oil.  $^1\text{H NMR}$ :  $\delta$ 7.18 (m, 5H, Ph), 4.10 (m, 3H,  $\text{C}_5\text{H}_3$ ), 4.06 (s, 5H, Cp), 3.90 (m, 2H,  $\text{CH}_2$ ), 2.21 (s, 6H,  $\text{NMe}_2$ ), 1.38 (d,  $J = 6.8 \text{ Hz}$ , 3H,  $\text{CHMe}$ );  $^{13}\text{C NMR}$ :  $\delta$ 138.9 (s), 129.1 (d), 128.3 (d), 126.7 (d, Ph), 79.3, 74.5, 71.6, 69.99 (d, Cp), 67.99, 67.03, 56.4 (d,  $\text{CHMe}$ ), 41.45 (t,  $\text{SCH}_2\text{Ph}$ ), 39.95 (q,  $\text{NMe}_2$ ), 10.88 (q,  $\text{CHMe}$ ); Mass spec: m/e (rel intensity), 379 (68,  $\text{M}^+$ ), 334 (98,  $\text{M}^+ - \text{HNMe}_2$ ), 243 (100), 121 (73).

1,1'-Bis(dimethyldithiocarbamate)ferrocene (38)

Ferrocene (10 g, 53.7 mmol) was added to a solution of N,N,N',N'-tetramethylethylenediamine (16.85 mL, 112 mmol) and 1,6 M n-butyllithium in hexane (68 mL, 112 mmol) in oxygen free hexane (200 mL) in a 1 l-round bottom flask, equipped with a side arm and serum cap, under nitrogen. The solution was stirred at least 3 h, or until bright orange, then tetramethylthiuram disulfide (26.5 g, 110 mmol) in 500 mL benzene was added slowly via cannula to the solution which was at  $-40^{\circ}\text{C}$ . The solution was allowed to reach room temperature and was stirred overnight to give a black/grey solution. Water (90 mL) was added and the solution was filtered. The grey precipitate was washed with water and then chromatographed on alumina. The yellow band, eluted with  $\text{CH}_2\text{Cl}_2$ , was evaporated to dryness to yield 16 g of (38), (70% yield). The filtrate was separated from the aqueous layer, dried and chromatographed. The first band, eluted with hexane, contained 0.95 g ferrocene whereas the second band eluted with  $\text{CH}_2\text{Cl}_2$  contained (38) and traces of the disulfide. The thiuram disulfide is removed by washing with benzene. Total yield was 18.2 g (80% yield). Compound (38) was recrystallized from  $\text{CH}_2\text{Cl}_2$ /hexane to give yellow crystals, mp =  $170\text{--}173^{\circ}\text{C}$ .  $^1\text{H}$  NMR:  $\delta$ 4.50 (t, 4H,  $\text{H}_{2,5}$ ), 4.38 (t, 4H,  $\text{H}_{3,4}$ ), 3.48 (s, 6H,  $\text{CH}_3$ ), 3.43 (s, 6H,  $\text{CH}_3$ );  $^{13}\text{C}$  NMR: ( $\text{CH}_2\text{Cl}_2/\text{D}_2\text{O}$ ),  $\delta$ 199.7 (CS), 77.4 ( $\text{C}_{2,5}$ ), 76.71 ( $\text{C}_1$ ), 71.98 ( $\text{C}_{3,4}$ ), 45.3 ( $\text{CH}_3$ ), 41.7 ( $\text{CH}_3$ ); Mass spec: m/e



(rel intensity), 424 (100,  $M^+$ ), 328 (53), 240 (42), 88 (65);  
IR (Fluorolube): 1480  $\text{cm}^{-1}$ .

Anal. Calcd. for  $\text{C}_{16}\text{H}_{20}\text{S}_4\text{N}_2\text{Fe}$ : C, 45.28; H, 4.75; N, 6.60; S, 30.22. Found: C, 45.29; H, 4.81; N, 6.57; S, 30.30.

1,1'-Bis(diethyldithiocarbamate)ferrocene (39)

Tetraethylthiram disulfide (32.68 g, 110 mmol) in 500 mL toluene was added slowly via cannula to 1,1'-dilithioferrocene (54 mmol) at  $-78^\circ\text{C}$ . The solution was allowed to reach room temperature and was stirred overnight to give a blackish solution. Water (100 mL) was added and the solution was filtered. The grey precipitate was washed with water then chromatographed on alumina. The yellow band eluted with  $\text{CH}_2\text{Cl}_2$  gave 13 g of (39), 50% yield. The brown filtrate, which contains ferrocene, thiuram disulfide and (39), was chromatographed to yield 4.5 g of (39), total yield 68%. Recrystallization from  $\text{CH}_2\text{Cl}_2$ /hexane gave yellow crystals that decomposed at  $160\text{--}163^\circ\text{C}$ , melted at  $181^\circ\text{C}$ .

$^1\text{H}$  NMR:  $\delta$ 4.52 (t, 4H,  $\text{H}_{2,5}$ ), 4.42 (t, 4H,  $\text{H}_{3,4}$ ), 3.99 (q,  $J = 7.0$  Hz, 2H,  $\text{CH}_2$ ), 3.85 (q,  $J = 7.0$  Hz, 2H,  $\text{CH}_2$ ), 1.39 (t,  $J = 7.0$  Hz, 3H,  $\text{CH}_3$ ), 1.26 (t,  $J = 7.0$  Hz, 3H,  $\text{CH}_3$ );

$^{13}\text{C}$  NMR: ( $\text{CH}_2\text{Cl}_2/\text{D}_2\text{O}$ ),  $\delta$ 197.5 (s, CS), 77.2 (d,  $J = 175$  Hz,  $\text{C}_{2,5}$ ), 76.1 (s,  $\text{C}_1$ ), 71.6 (d,  $J = 177$  Hz,  $\text{C}_{3,4}$ ), 49.4 (q,  $J = 134$  Hz,  $\text{CH}_3$ ), 46.9 (q,  $J = 134$  Hz,  $\text{CH}_2$ ), 12.5 (t,  $J = 126$  Hz,  $\text{CH}_3$ ), 11.2 (t,  $J = 126$  Hz,  $\text{CH}_3$ ); Mass spec: m/e

(rel intensity), 480 (54,  $M^+$ ), 384 (51), 268 (69), 116 (100), 85 (96), 60 (72); IR (Fluorolube):  $1480\text{ cm}^{-1}$ .  
Anal. Calcd. for  $C_{20}H_{28}N_2S_4Fe$ : C, 49.99; H, 5.87; N, 5.83; S, 26.69. Found: C, 49.90; H, 5.80; N, 5.75; S, 26.90.

1,1'-Bis(diisopropyldithiocarbamate)ferrocene (40)

Tetraisopropylthiuram disulfide (25 g, 71 mmol) in 250 mL toluene was added slowly via cannula to 1,1'-dilithioferrocene (35 mmol) at  $-78^\circ\text{C}$ . The solution was allowed to reach room temperature and was stirred overnight to give a black solution. Water (100 mL) was added and the solution was filtered. The green precipitate was washed with water (to remove ferricenium salts) and then chromatographed to give 15 g of (40), 79% yield. The green aqueous solution was reduced with sodium bisulfite and forms a brown solid after standing in air for 30 h. Complex (40) was recrystallized from  $CH_2Cl_2$ /hexane to give yellow crystals which decompose at  $180^\circ\text{C}$  and melt at  $225\text{--}226^\circ\text{C}$ .  $^1\text{H}$  NMR: ( $71^\circ\text{C}$ ),  $\delta$ 4.78 (br, CH), 4.46 (t, 4H,  $H_{2,5}$ ), 4.38 (t, 4H,  $H_{3,4}$ ), 1.47 (d,  $J = 6.5\text{ Hz}$ , 12H,  $CH_3$ );  $^{13}\text{C}$  NMR:  $\delta$ 198.0 (s, CS), 77.1 (d,  $J = 183\text{ Hz}$ ,  $C_{2,5}$ ), 76.1 (s,  $C_1$ ), 71.3 (d,  $J = 178\text{ Hz}$ ,  $C_{3,4}$ ), 53.3 (d,  $J = 137\text{ Hz}$ , CH), 19.7 (q,  $J = 127\text{ Hz}$ ,  $CH_3$ ); Mass spec: m/e (rel intensity), 536 (8,  $M^+$ ), 440 (8), 296 (14), 144 (31), 102 (100), 60 (56), 43 (92); IR (Fluorolube):  $1465\text{ cm}^{-1}$ .  
Anal. Calcd. for  $C_{24}H_{36}N_2S_4Fe$ : C, 53.77; H, 6.76  
Found: C, 53.77; H, 6.90.

Dimethyldithiocarbamateferrocene (41)

Ferrocene (6.14 g, 33 mmol) was added to a solution of TMEDA (5.1 mL, 33 mmol) and n-butyllithium (20.1 mL, 33 mmol) in 150 mL hexane and the solution was stirred for 3 h. Tetramethylthiuram disulfide (7.92 g, 33 mmol) in 120 mL benzene was added via cannula to the bright orange solution which had been cooled to  $-78^{\circ}\text{C}$ . The solution was allowed to reach room temperature, was stirred overnight and then 50 mL water was added to the brownish black solution. The solution was filtered and the sticky black precipitate was chromatographed on alumina. The first band, eluted with hexane, yielded 2.9 g of ferrocene. The second yellow band which was eluted with benzene gave 300 mg of an unidentified product.  $^1\text{H NMR}$ :  $\delta$ 4.28 (t), 4.19 (s), 4.15 (t); Mass spec: 402 (base peak). The third band, eluted with benzene, yielded 470 mg of (41) (9% yield based on the ferrocene reacted). Numerous additional bands were eluted with benzene and methylchloroform but the products were not isolated. Compound (41) was recrystallized from  $\text{CH}_2\text{Cl}_2$ /hexane to give yellow crystals which decompose at  $180\text{--}184^{\circ}\text{C}$ .  $^1\text{H NMR}$ :  $\delta$ 4.44 (t, 4H,  $\text{H}_{2,5}$ ), 4.34 (t, 4H,  $\text{H}_{3,4}$ ), 4.24 (s, 5H, Cp), 3.51 (s, 3H,  $\text{CH}_3$ ), 3.45 (s, 3H,  $\text{CH}_3$ );  $^{13}\text{C NMR}$ : ( $\text{CH}_2\text{Cl}_2/\text{D}_2\text{O}$ ,  $28^{\circ}\text{C}$ ),  $\delta$ 199.9 (CS), 75.66 ( $\text{C}_{2,5}$ ), 74.96 ( $\text{C}_1$ ), 70.34 ( $\text{C}_{3,4}$ ), 69.39 (Cp), 45.24 ( $\text{CH}_3$ ), 41.50 ( $\text{CH}_3$ ); Mass spec: m/e (rel intensity), 305 (87,  $\text{M}^+$ ),

240 (22,  $M^+ - Cp$ ), 217 (20), 209 (61), 121 (21) 88 (100,  $CSNMe_2$ ); IR (Fluorolube):  $1475\text{ cm}^{-1}$ .

Anal. Calcd. for  $C_{16}H_{20}S_4N_2Fe$ : C, 51.15; H, 4.95

Found: C, 51.36; H, 4.92.

### Dithyldithiocarbamateferrocene (42)

Bromoferrocene, prepared according to Rosenblum's<sup>6</sup> procedure, was dried in vacuo before use. Butyllithium (7.47 mL, 11.8 mmol) was added slowly via syringe to a solution of bromoferrocene (2.64 g, 10.0 mmol) in 70 mL dry diethylether which was cooled to  $-40^\circ\text{C}$ . After being stirred at room temperature for 20 min. tetraethylthiuram disulfide (3.27 g, 11.0 mmol) in 40 mL toluene was added slowly via cannula to the bright yellow solution which had been cooled to  $-78^\circ\text{C}$ . The solution was stirred for 12-18 h at room temperature to give a brown solution. Water, 20 mL, was added and the organic layer was separated, dried and chromatographed on alumina. The first yellow band, eluted with hexane, contained bromoferrocene and a small amount of ferrocene whereas the second yellow band, eluted with methylene chloride, yielded 2 g of (42), 60% yield. Complex (42) was recrystallized from  $CH_2Cl_2$ /hexane to give yellow crystals which melt at  $127.5\text{--}128.5^\circ\text{C}$ .  $^1H$  NMR:  $\delta$ 4.42 (t, 4H,  $H_{2,5}$ ), 4.33 (t, 4H,  $H_{3,4}$ ), 4.22 (s, 5H, Cp), 3.96 (q,  $J = 7\text{ Hz}$ ,  $CH_2$ ), 3.82 (q,  $J = 7\text{ Hz}$ ,  $CH_2$ ), 1.37 (t,  $J = 7\text{ Hz}$ ,  $CH_3$ ), 1.23 (t,  $J = 7\text{ Hz}$ ,  $CH_3$ );  $^{13}C$  NMR: ( $CH_2Cl_2/D_2O$ ,  $31^\circ\text{C}$ )

$\delta$ 198.7 (CS), 75.97 ( $C_{2,5}$ ), 75.22 ( $C_1$ ), 70.37 ( $C_{3,4}$ ), 69.48 (Cp), 49.61 ( $CH_2$ ), 47.19 ( $CH_2$ ), 12.56 ( $CH_3$ ), 11.53 ( $CH_3$ );  
Mass spec: m/e (rel intensity), 333 (18,  $M^+$ ), 237 (8),  
 217 (6), 116 (100,  $CSNet_2$ ), 88 (87), 60 (61); IR (Fluoro-  
 lube):  $1480\text{ cm}^{-1}$ .

Anal. Calcd. for  $C_{15}H_{19}NS_2Fe$ : C, 54.06; H, 5.75; N, 4.20  
Found: C, 53.95; H, 5.76; N, 4.29.

### Diisopropyldithiocarbamateferrocene (43)

Butyllithium (4.9 mL, 7.8 mmol) was slowly added via syringe to a solution of bromoferrocene (1.73 g, 6.5 mmol) in 100 mL dry diethylether. After being stirred at room temperature for 20 min, tetraisopropylthiuram disulfide (2.41 g, 6.8 mmol) in 80 mL hexane was added slowly via cannula to the bright orange solution which had been cooled to  $-78^\circ\text{C}$ . The solution was stirred at room temperature for 18 h to give a light brown reaction mixture. Water (30 mL) was added and then the organic layer was separated, dried and evaporated to dryness to give a brown oil which was chromatographed on alumina. The first yellow band, eluted with hexane, contained a small amount of bromoferrocene and 340 mg ferrocene. The second yellow band, eluted with methylene chloride, was concentrated and then the crystalline mass was washed briefly with benzene (to remove the disulfide). Yellow needles, recrystallized from methylene chloride/hexane, were obtained in 84% yield based on the

bromoferrocene reacted, mp = 189-190°C (dec).  $^1\text{H}$  NMR: (59°C),  $\delta$ 4.40 (t, 4H,  $\text{H}_{2,5}$ ), 4.33 (t, 4H,  $\text{H}_{3,4}$ ), 4.20 (s, 5H, Cp) 4.76 (septet, 1H, CH), 1.48 (d,  $J = 6.6$  Hz, 6H,  $\text{CH}_3$ );  $^{13}\text{C}$  NMR:  $\delta$ 198.0 (s, CS), 76.0 (d,  $\text{C}_{2,5}$ ), 75.2 (s,  $\text{C}_1$ ), 70.2 (d,  $\text{C}_{3,4}$ ), 69.4 (d, Cp), 54.1 (d, CH), 19.9 (q,  $\text{CH}_3$ ); Mass spec: m/e (rel intensity), 361 (100,  $\text{M}^+$ ), 218 (99), 217 (41), 144 (30), 121 (6), 102 (32).

Anal. Calcd. for  $\text{C}_{17}\text{H}_{23}\text{NS}_2\text{Fe}$ : C, 56.51; H, 6.42

Found: C, 56.69; H, 6.61.

Reaction of  $\text{Fe}(\text{C}_5\text{H}_4\text{SCSNET}_2)_2$ , (39), With  $(\text{PhCN})_2\text{PdCl}_2$

A benzene solution (40 mL) of  $(\text{PhCN})_2\text{PdCl}_2$  (300 mg, 783 mmol) was added slowly to a 100 mL benzene solution of  $\text{Fe}(\text{C}_5\text{H}_4\text{SCSNET}_2)_2$ , (39), (361 mg, 752 mmol) and stirred overnight. The light brown precipitate was filtered, washed with benzene and dried. The black brown product was slightly soluble in methylene chloride.

Reaction of  $\text{Fe}(\text{C}_5\text{H}_5)(\text{C}_5\text{H}_4\text{SCSNET}_2)$  (42), With  $(\text{PhCN})_2\text{PdCl}_2$

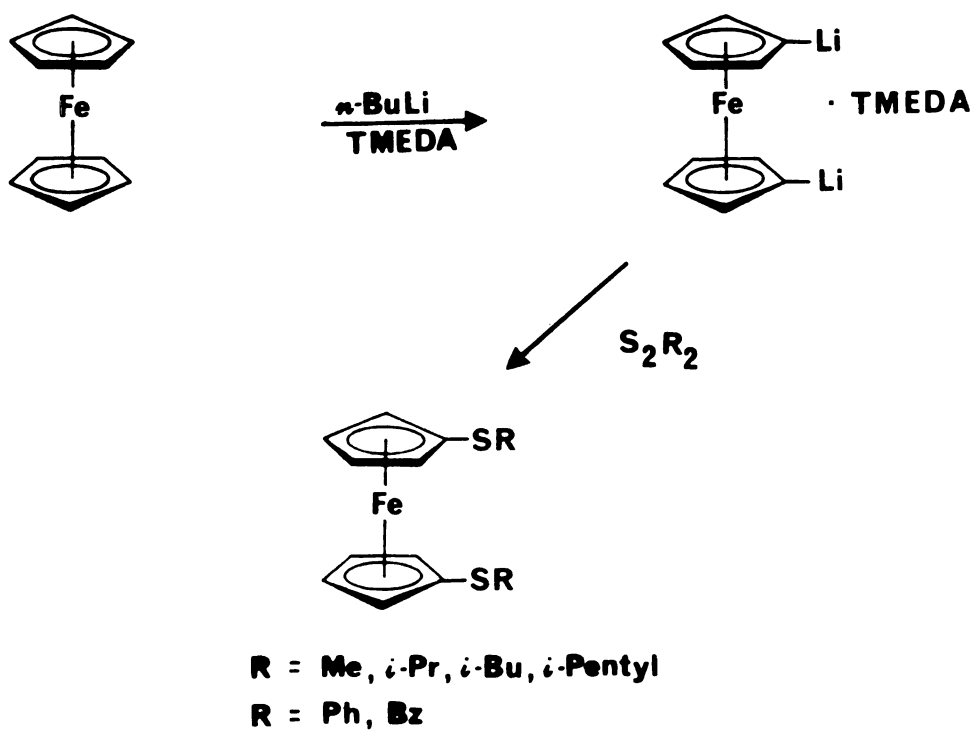
An identical procedure as given above was followed.  $(\text{PhCN})_2\text{PdCl}_2$  (115 mg, 0.3 mmol) was added to (42) (100 mg, 0.3 mmol) to give a red-brown precipitate which is soluble in methylene chloride and nitromethane.  $^1\text{H}$  NMR: ( $\text{CD}_3\text{NO}_2$ ),  $\delta$ 3.46 (br), 2.40, 2.04 (br,s), 1.52 (br), 1.30 (br), 0.87 (br); IR (Fluorolube):  $1550\text{ cm}^{-1}$ .

### III. RESULTS AND DISCUSSION

#### A. $\text{Fe}(\text{C}_5\text{H}_4\text{SR})_2$ ( $\text{R} = \text{Me}, i\text{Pr}, i\text{Bu}, i\text{Pent}, \text{Ph}, \text{Bz}$ )

##### 1. Preparation

Ferrocenylsulfide complexes of the type,  $\text{Fe}(\text{C}_5\text{H}_4\text{SR})_2$  where  $\text{R} = \text{Me}, i\text{Pr}, i\text{Bu}, i\text{Pent}, \text{Ph}, \text{Bz}$  have been prepared in a general, high yield, one step synthesis shown in Scheme 4. The appropriate disulfide is added slowly, via cannula,



Scheme 4

to a hexane solution of 1,1'-dilithioferrocene which was cooled to  $-40^{\circ}\text{C}$ . 1,1'-Dilithioferrocene is prepared in over 90% yield by reaction of stoichiometric quantities of n-butyllithium and tetramethylethylenediamine (TMEDA) with ferrocene. The metalation reagent was used as the in situ slurry even though use of the species isolated as a solid has been reported to lead to higher yields.<sup>8</sup>

1,1'-Bis(methylthio)ferrocene (9), 1,1'-bis(isopropylthio)ferrocene (11) and 1,1'-bis(isopentylthio)ferrocene (14) were isolated as yellow-brown oils whereas 1,1'-bis(phenylthio)ferrocene (12), 1,1'-bis(isobutylthio)ferrocene (10) and 1,1'-bis(benzylthio)ferrocene (13) were obtained as yellow crystals. All six derivatives are soluble in common organic solvents and are air stable in solution and the solid state.

The disulfide, t-butyldisulfide, failed to react with 1,1'-dilithioferrocene under the reaction conditions employed. This could be due to the steric crowding of the sulfur-sulfur bond by the bulky t-butyl groups which prevent nucleophilic cleavage of the sulfur-sulfur bonds.

The brown methyl sulfide derivative (9) turned green when water was added to destroy the excess lithio reagent. The aqueous layer was green which suggests that ferrocene or a ferrocene derivative was oxidized to the ferricenium analog. When the methyl sulfide (9) was filtered anaerobically the filtrate did not discolor in the presence of



water or oxygen. This suggests that a side product, present in the reaction mixture, is responsible for the discoloring.

## 2. $^1\text{H}$ NMR

The  $^1\text{H}$  NMR data of the ferrocenylsulfide complexes (9)-(14) is given in Table 2. The  $^1\text{H}$  NMR spectra of these compounds are typical of 1,1'-disubstituted ferrocenes. The resonances due to the ring protons consist of two "triplets" which is characteristic of an AA'BB' spin system where  $J_{AB}$  and  $J_{A'B'}$  (or  $J_{AB'}$ ) are equal and smaller than the chemical shift between A and B<sup>50</sup>. These "triplets" are slightly deshielded as expected for an electron withdrawing substituent<sup>16</sup>. Deuteration studies have indicated that the low field "triplet" is assigned to the protons in the 2 and 5 positions on the ring ( $\text{H}_{2,5}$ ) whereas the high field "triplet" is assigned to the ring protons in the 3 and 4 position ( $\text{H}_{3,4}$ )<sup>43</sup>.

## 3. $^{13}\text{C}$ NMR

$^{13}\text{C}$  NMR is a sensitive tool for measuring the electron density distribution on the cyclopentadienyl ring in ferrocene. Substituents on the ring induce screening of the nuclei in two different ways, one way being due to the magnetic anisotropy of the substituent and the second way due to the electronic effect of the substituent that

Table 2.  $^1\text{H}$  NMR Data for Ferrocenylsulfide Complexes,  $\text{Fe}(\text{C}_5\text{H}_4\text{SR})_2$  R = Me, iPr, iBu, iPent, Ph, Bz. Spectra obtained in  $\text{CDCl}_3$  at room temperature.

Compound	Ph	$\text{H}_{2,5}$	$\text{H}_{3,4}$	$\alpha\text{CH}_2$	$\beta\text{CH}_2$	CH	$\text{CH}_3$
$\text{Fe}(\text{C}_5\text{H}_4\text{SMe})_2$		4.29t	4.21t				2.30s
$\text{Fe}(\text{C}_5\text{H}_4\text{SCHMe}_2)_2$		4.31t	4.24t			2.86m	1.16d
$\text{Fe}(\text{C}_5\text{H}_4\text{SCH}_2\text{CHMe}_2)_2$		4.28t	4.20t	2.50d		1.72m	0.97d
$\text{Fe}(\text{C}_5\text{H}_4\text{SCH}_2\text{CH}_2\text{CHMe}_2)_2$		4.26t	4.18t	2.59t	1.42m	1.65m	0.86d
$\text{Fe}(\text{C}_5\text{H}_4\text{SPh})_2$	7.08m	4.49t	4.44t				
$\text{Fe}(\text{C}_5\text{H}_4\text{SCH}_2\text{Ph})_2$	7.19m	4.12t	4.10t	3.72s			
	7.11m						

consists of both resonance and inductive components.

The  $^{13}\text{C}$  NMR data for the ferrocenylsulfides (9)-(14) is presented in Table 3. A gated decoupled experiment, performed on the isopropyl derivative (11) simplifies the assignment of the  $^{13}\text{C}$  NMR spectra (shown in Figure 1). The gated decoupled spectrum confirms that the signal at 79 ppm is due to the substituted ring carbon,  $\text{C}_1$ , as this signal remains a singlet under proton coupled conditions. The resonances at 76 and 71 ppm are tentatively assigned to the nuclei at the  $\text{C}_{3,4}$  and  $\text{C}_{2,5}$  positions. Koridze<sup>51</sup> has assigned the signals in methoxyferrocene at 61.5 and 54.7 ppm to the  $\text{C}_{3,4}$  and  $\text{C}_{2,5}$  nuclei respectively on the basis of deuterium labelling studies. In general the  $\text{C}_{2,5}$  positions are primarily influenced by inductive effects and the magnetic anisotropy of the substituent whereas the  $\text{C}_{3,4}$  positions are more sensitive to resonance effects.<sup>52,53</sup> The assignments in the ferrocenylsulfide complexes (9)-(14) are tentative and deuteration studies must be employed to make unambiguous assignments of the ring carbons.

The chemical shift of the substituted ring carbon atom,  $\text{C}_1$ , reflects the inductive and field effects of the substituent and exhibits the widest range of values of any of the ring carbons. The  $\text{C}_1$  resonance of  $\text{Fe}(\text{C}_5\text{H}_4\text{SMe})_2$  is shifted downfield by 17 ppm, relative to ferrocene (68.2 ppm), whereas  $\text{Fe}(\text{C}_5\text{H}_4\text{SPh})_2$  is deshielded by 9 ppm. These

Table 3.  $^{13}\text{C}$  NMR Data for Ferrocenylsulfide Complexes,  $\text{Fe}(\text{C}_5\text{H}_4\text{SR})_2$ ,  $\text{R} = \text{Me}, \text{iPr}, \text{iBu}, \text{iPent}, \text{Ph}, \text{Bz}$ . Spectra obtained in  $(\text{CH}_2\text{Cl}_2/\text{D}_2\text{O})$  solution at room temperature.

Compound	Ph	$\text{C}_1$	$\text{C}_{3,4}$	$\text{C}_{2,5}$	$\text{CH}_2$	CH	$\text{CH}_3$
$\text{Fe}(\text{C}_5\text{H}_4\text{SMe})_2$		85.21	71.72	69.59			19.35
$\text{Fe}(\text{C}_5\text{H}_4\text{SCHMe}_2)_2$		79.14	76.20	70.96		39.64	23.41
$\text{Fe}(\text{C}_5\text{H}_4\text{SCH}_2\text{CHMe}_2)_2$		82.76	74.11	70.31	46.40	28.51	21.68
$\text{Fe}(\text{C}_5\text{H}_4\text{SCH}_2\text{CH}_2\text{CHMe}_2)_2$		81.41	77.50	70.03	38.33 $\alpha$ 34.89 $\beta$	26.67	21.96
$\text{Fe}(\text{C}_5\text{H}_4\text{SPh})_2$	140.27s 128.68d 126.38d 125.17d	77.77	76.34	71.91			
$\text{Fe}(\text{C}_5\text{H}_4\text{SCH}_2\text{Ph})_2$	138.80s 128.95d 128.30d 126.85d	81.16	74.68	70.57	42.12		
$\text{Fe}(\text{C}_5\text{H}_4\text{PPh}_2)_2$	139.00s 133.35d 128.51d 128.22d	76.63	73.68	72.71			

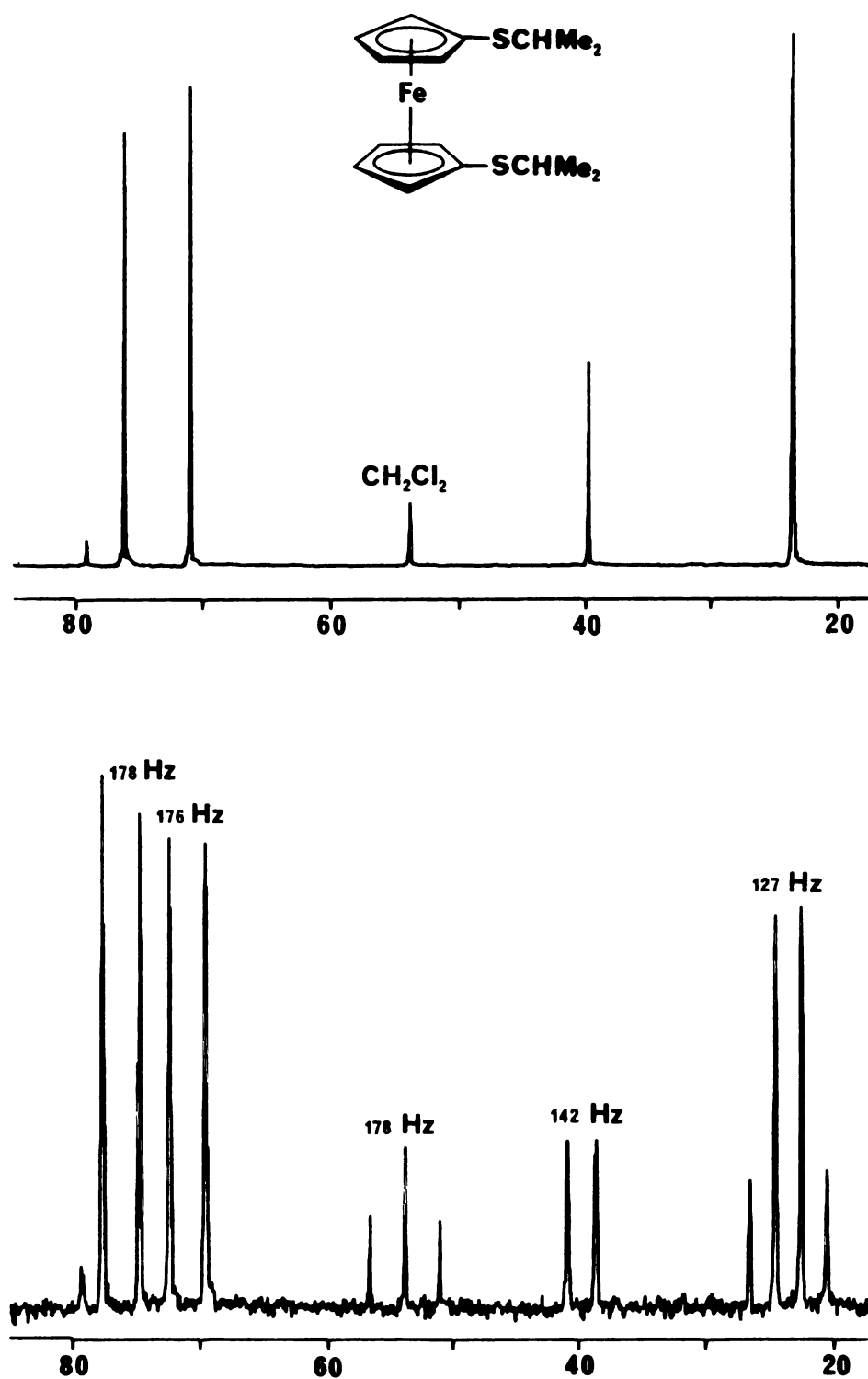


Figure 1. Proton decoupled (above) and gated decoupled (below)  $^{13}\text{C}$  NMR Spectra of  $\text{Fe}(\text{C}_5\text{H}_4\text{S-iPr})_2$ .

values are in contrast to methoxyferrocene where the  $C_1$  resonance is shifted downfield by over 59 ppm.

#### 4. Infrared Spectra

Table 4 contains the infrared data for the ferrocenyl-sulphide compounds (9)-(13). Inspection of Table 4 indicates that certain frequencies are common to all five compounds. These frequencies have been tentatively assigned by comparison with the vibrational spectra of ferrocene<sup>54</sup> and dimethylferrocene<sup>55</sup>.

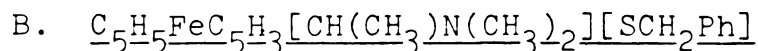
The high frequency infrared bands at 3090 and 2910  $cm^{-1}$  are assigned to C-H stretching frequencies. The strong absorption around 1440  $cm^{-1}$  may be associated with a C-C stretching mode whereas the strong bands observed at 1160, 888 and 820  $cm^{-1}$  are attributed to C-H deformation modes. The strong absorption that occurs at 1020  $cm^{-1}$  could be assigned to a ring breathing mode while the broad band in the 500-515  $cm^{-1}$  region may be associated with ring-metal vibrations such as an asymmetric ring-tilt and an asymmetric ring-metal stretch.

In the phenyl and benzyl analogs, (12) and (13), the absorptions due to the phenyl group are clearly visible. Strong absorption bands located between 730 and 680  $cm^{-1}$  result from out-of-plane C-H bending. In addition skeletal vibrations due to C-C ring stretching are found at 1580  $cm^{-1}$ . The stretching vibration assigned to the C-S linkage,

Table 4. Infrared Data for Ferrocenylsulfide Complexes,  
 $\text{Fe}(\text{C}_5\text{H}_4\text{SR})_2$ , R = Me, iPr, iBu, Ph, Bz.

R = Me	iPr	iBu	Ph	Bz
3090m	3085m	3095m	3080m	
2015s	2910br,s	2950br,s	2910br,s	2910m
2850m		2865m	2845m	
	1065br,m		1579s	1585m
	1440s	1463s	1438s	1445s
1420br,s	1410s	1414m	1408m	1412m
	1380s	1389s	1385m	1380m
	1365s	1364s	1358m	
1310m	1310m	1319m		
	1235br,s	1240m		1235m
			1189m	1194m
1163m	1155s	1164s	1168s	1161s
1103w	1100w		1078m	
			1062m	1060w
	1040m		1041m	1045w
1020s	1015s	1018s	1018s	1018s
			1010s	
964m	920m		963w	
885s	885s	888s	888s	885m
			863m	878s
				862m
		854m	845m	845m
817br,s	810br,s	815br,s	820s	815br,s
			732s	774s
				712br,s
			685s	692s
	640m		637m	620m
	615m			
			527m	577w
515br,s	500br,s	510br,s	501m	515m
				495m
			474m	478m
			455m	445m

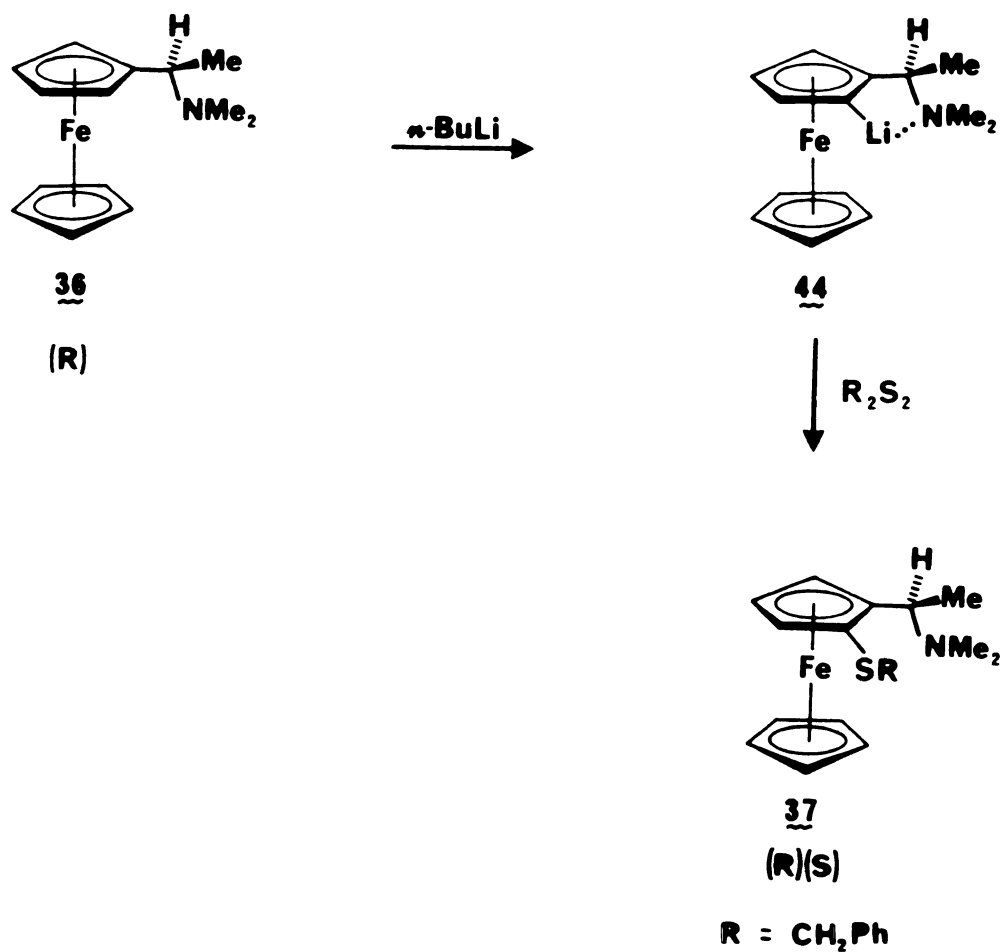
which occurs in the region of  $700 - 600 \text{ cm}^{-1}$ , is generally weak<sup>56</sup> and was not assigned for the ferrocenylsulphide complexes.



Chiral ferrocenylphosphine ligands, which have planar chirality due to a 1,2-unsymmetrically substituted cyclopentadienyl ring, are highly effective as ligands in transition metal catalyzed asymmetric synthesis. Though few sulfide complexes have been used as ligands in catalysis, the preparation of a chiral ferrocenylsulfide complex was undertaken so that its possible application to asymmetric synthesis may be investigated.

A chiral ferrocenylsulphide complex was readily prepared from N,N-dimethyl- $\alpha$ -ferrocenylethylamine, (36) (see Scheme 5). The amine (36) was prepared from ferrocene according to Ugi's procedure<sup>48</sup> and was resolved by using (R)-(+)-tartaric acid. As illustrated by Ugi<sup>56</sup>, the (R)-amine (36), is stereoselectively lithiated by butyllithium to give 96% of the (R)(R) isomer, (44). The (R)(R) derivative is thought to be stabilized by the coordination of the adjacent nitrogen atom in the side chain to the lithium atom. The lithiated ferrocene derivative is then treated with the disulfide and refluxed for at least three hours. The chiral ferrocenylsulphide, (37), is chromatographed on alumina, deactivated with 5% water, and is isolated in 40%





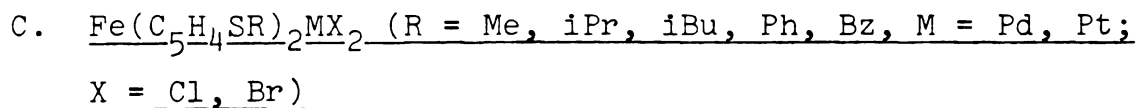
Scheme 5

yield as a brown oil. The chiral ferrocenylsulfide compound, (**37**) contains two elements of chirality. The (R) configuration refers to the asymmetric carbon atom while the (S) configuration refers to the planar chirality.

The presence of the asymmetric carbon atom in the amine, (**36**), gives rise to diastereotopic ring carbons. The  $^{13}\text{C}$

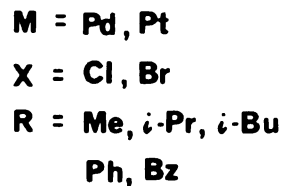
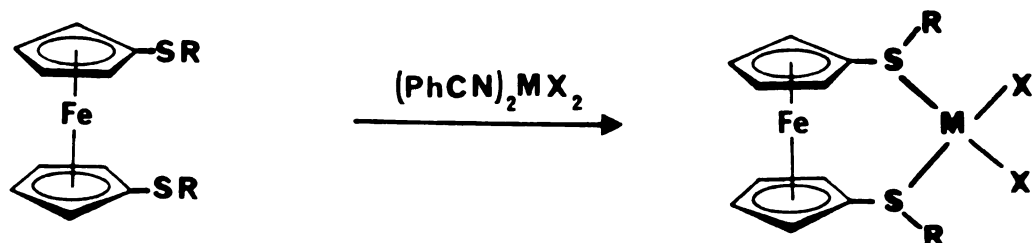
NMR spectrum of the amine, (36), contains five separate signals for the ring carbons at 85.8 ppm (assigned to  $C_1$  by a gated decoupling experiment), 68.3, 66.4, 66.14 and 65.7 ppm. This is in contrast to substituted ferrocenes without an element of chirality as one signal is attributed to the  $C_{2,5}$  nuclei and one to the  $C_{3,4}$  nuclei. In the chiral ferrocenylsulfide, (37), the benzylic protons are diastereotopic. Their diastereotopic nature was however not observed in the  $^1H$  NMR as the resonance due to the benzylic protons is partially obscured by the cyclopentadienyl ring protons.

Cullen<sup>57</sup> has determined the crystal structure of  $[(PPFA)Rh(NBD)]PF_6$ , where PPFA is (R,S)- $\alpha$ -(2-diphenylphosphinoferrocenyl)ethyldimethylamine; NBD is norbornadiene, and concluded that the chiral ferrocenylphosphine ligand coordinated to rhodium through both the phosphorous and nitrogen atoms. As there is much interest in ligands which have both "hard" and "soft" properties, investigation of the chelation of the chiral ferrocenylsulfide, (37), with transition metals would be of much interest. In addition it would be interesting to study the effectiveness of the chiral ferrocenylsulfide ligand in transition metal catalyzed asymmetric synthesis.



### 1. Preparation

Reaction of a benzene solution of the ferrocenylsulfide compounds, (9)-(13), with bis(benzonitrile) adducts of palladium and platinum chloride and bromide salts gave rise to the monosubstituted complexes, (16)-(35) (see Scheme 6). The heterobimetallic complexes are insoluble in benzene: the palladium ferrocenylsulphide complexes precipitated



Scheme 6

immediately while the platinum analogs precipitated after being stirred for a few days.

The isobutyl and isopropyl metal complexes are soluble in methylene chloride and chloroform whereas the benzyl derivatives are only slightly soluble in these solvents. The methyl and phenyl analogs are sparingly soluble in polar solvents such as acetonitrile, nitromethane and dimethylformamide. The platinum complexes are more soluble than the palladium species, especially the phenyl derivative as 1,1'-bis(phenylthio)ferrocenepalladiumdichloride is very sparingly soluble and tends to form a suspension. The palladium bromide analogs are more soluble than the chloride complexes.

Analytically pure samples were obtained by the slow evaporation of the mixed solvent system, methylene chloride/hexane. The isopropyl derivatives tend to trap one mole of methylene chloride in the crystal lattice as shown by the  $^1\text{H}$  NMR spectra and the elemental analysis of complex (22). The occluded solvent is removed by drying in vacuo at 90°C. The crystals tend to discolor once the solvent has been removed.

## 2. $^1\text{H}$ NMR

With the exception of the methyl metal complexes, (24)-(27), the bimetallic derivatives were sufficiently soluble to obtain  $^1\text{H}$  NMR spectra.  $^1\text{H}$  NMR data for the isobutyl metal complexes, (16)-(19), is presented in Table 5.

The ferrocenylsulfide ligand undergoes a significant

Table 5.  $^1\text{H}$  NMR and  $^{13}\text{C}$  NMR Data for  $\text{Fe}(\text{C}_5\text{H}_4\text{S-iBu})_2$  and Metal Derivatives,  $\text{PdCl}_2$ ,  $\text{PdBr}_2$ ,  $\text{PtCl}_2$  and  $\text{PtBr}_2$ .

$^1\text{H}$	Complex	$\text{H}_{2,5}$	$\text{H}_{3,4}$	$\text{CH}_2$	CH	$\text{CH}_3$	$\text{T}^\circ\text{C}$
	$\text{Fe}(\text{C}_5\text{H}_4\text{S-iBu})_2$	4.28	4.20	2.50	1.72	0.97	24°
	$\text{Fe}(\text{C}_5\text{H}_4\text{S-iBu})_2\text{PdCl}_2$	5.28	4.42	2.98	1.80	1.01	78°
	$\text{Fe}(\text{C}_5\text{H}_4\text{S-iBu})_2\text{PdBr}_2$	5.25	4.40	3.06	1.81	1.01	23°
	$\text{Fe}(\text{C}_5\text{H}_4\text{S-iBu})_2\text{PtCl}_2$	5.14	4.43	3.08	1.92	1.01	101°
	$\text{Fe}(\text{C}_5\text{H}_4\text{S-iBu})_2\text{PtBr}_2$	5.15	4.46	2.94	1.89	1.04	75°
$^{13}\text{C}$		$\text{C}_1$	$\text{C}_{3,4}$	$\text{C}_{2,5}$	$\text{CH}_2$	CH	$\text{CH}_3$
	$\text{Fe}(\text{C}_5\text{H}_4\text{S-iBu})_2$	82.76	74.11	70.31	46.40	28.51	21.68
	$\text{Fe}(\text{C}_5\text{H}_4\text{S-iBu})_2\text{PdCl}_2$	79.32	76.23	71.72	49.50	26.42	21.38
	$\text{Fe}(\text{C}_5\text{H}_4\text{S-iBu})_2\text{PdBr}_2$	79.48	76.36	71.85	52.85	26.89	21.39
	$\text{Fe}(\text{C}_5\text{H}_4\text{S-iBu})_2\text{PtCl}_2$	80.22	75.93	72.08	48.21	26.55	21.85
	$\text{Fe}(\text{C}_5\text{H}_4\text{S-iBu})_2\text{PtBr}_2$	80.09	75.32	71.35	49.21	26.42	21.54

change in the  $^1\text{H}$  NMR spectra upon complexing to platinum or palladium halides. Figure 2 indicates that the most striking difference in the  $^1\text{H}$  NMR spectra of the complexed ligand relative to the free ligand is the large downfield shift of the resonance due to the  $\text{H}_{2,5}$  ring protons. This deshielding was originally thought to be due to a severe tilting of the cyclopentadienyl rings where the alpha protons were further from the shielding iron atom<sup>59</sup>. The crystal structure of the isobutyl palladium complex, (16), (discussed in detail in a later section) however, indicated that the cyclopentadienyl rings were tilted  $2^\circ$  from the plane. The large downfield shift of the alpha protons is either due to the magnetic anisotropy or the inductive effect of the metal halide. A further difference between the  $^1\text{H}$  NMR spectra of the free and complexed isobutyl ligand is the deshielding of the alkyl protons. In particular, the resonance due to the methylene protons shifts from 2.50 to 2.98 ppm as shown in Figure 2.

Figure 3 illustrates the difference between the  $^1\text{H}$  NMR spectra of the isopropyl platinum and palladium chloride derivatives. The palladium complex exhibits a doublet at 1.23 ppm due to the methyl groups and a septet at 4.04 ppm due to the methine protons. The broad signal at 4.45 ppm and the extremely broad, low intensity signal at 5.23 ppm, which is partially obscured by the methylene chloride peak, are due to the ring protons. Both signals sharpen to give

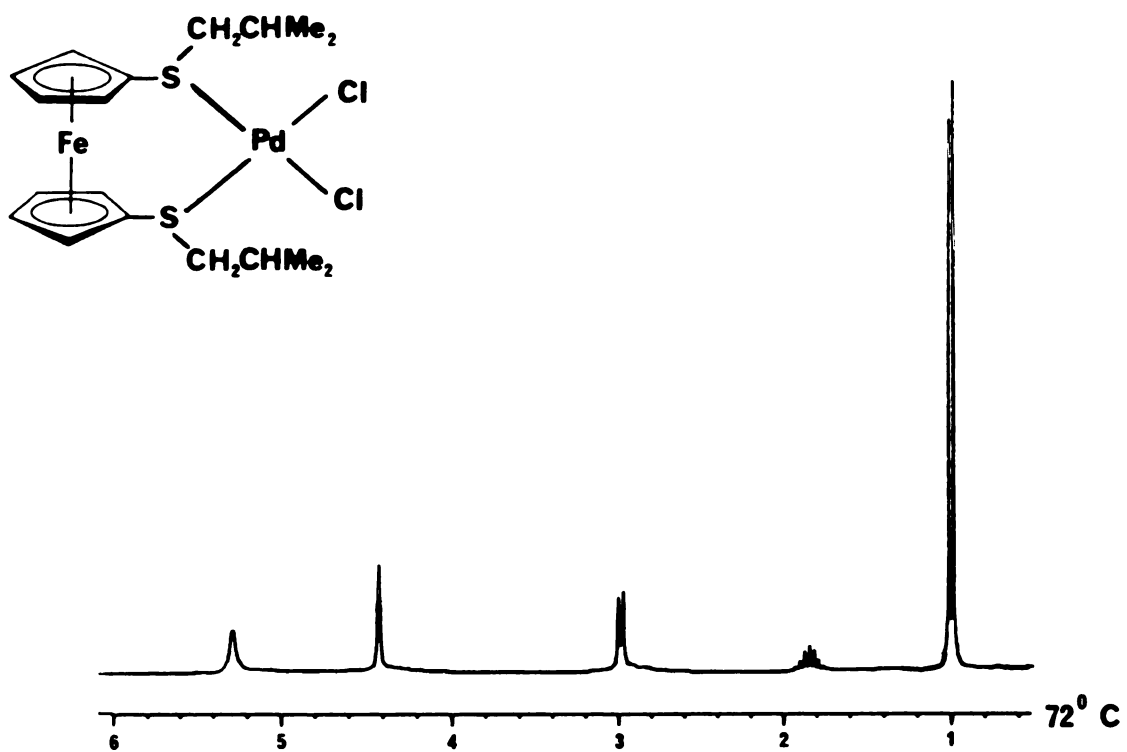
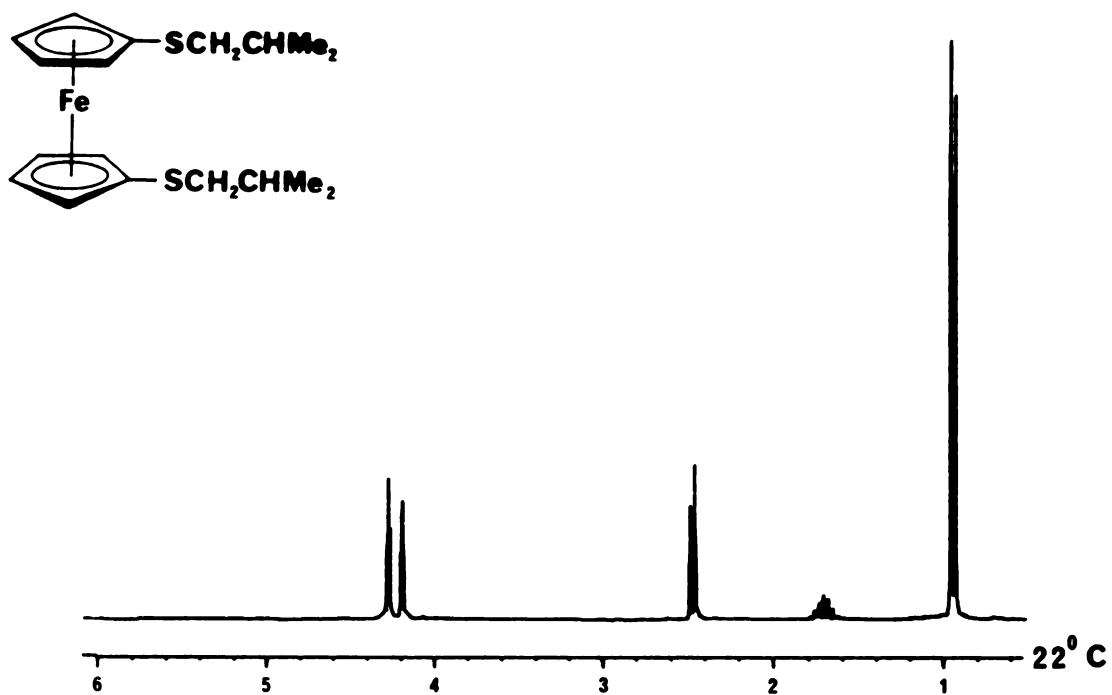


Figure 2.  $^1\text{H}$  NMR Spectra of  $\text{Fe}(\text{C}_5\text{H}_4\text{S-iBu})_2$  and  $\text{Fe}(\text{C}_5\text{H}_4\text{S-iBu})_2\text{PdCl}_2$ .

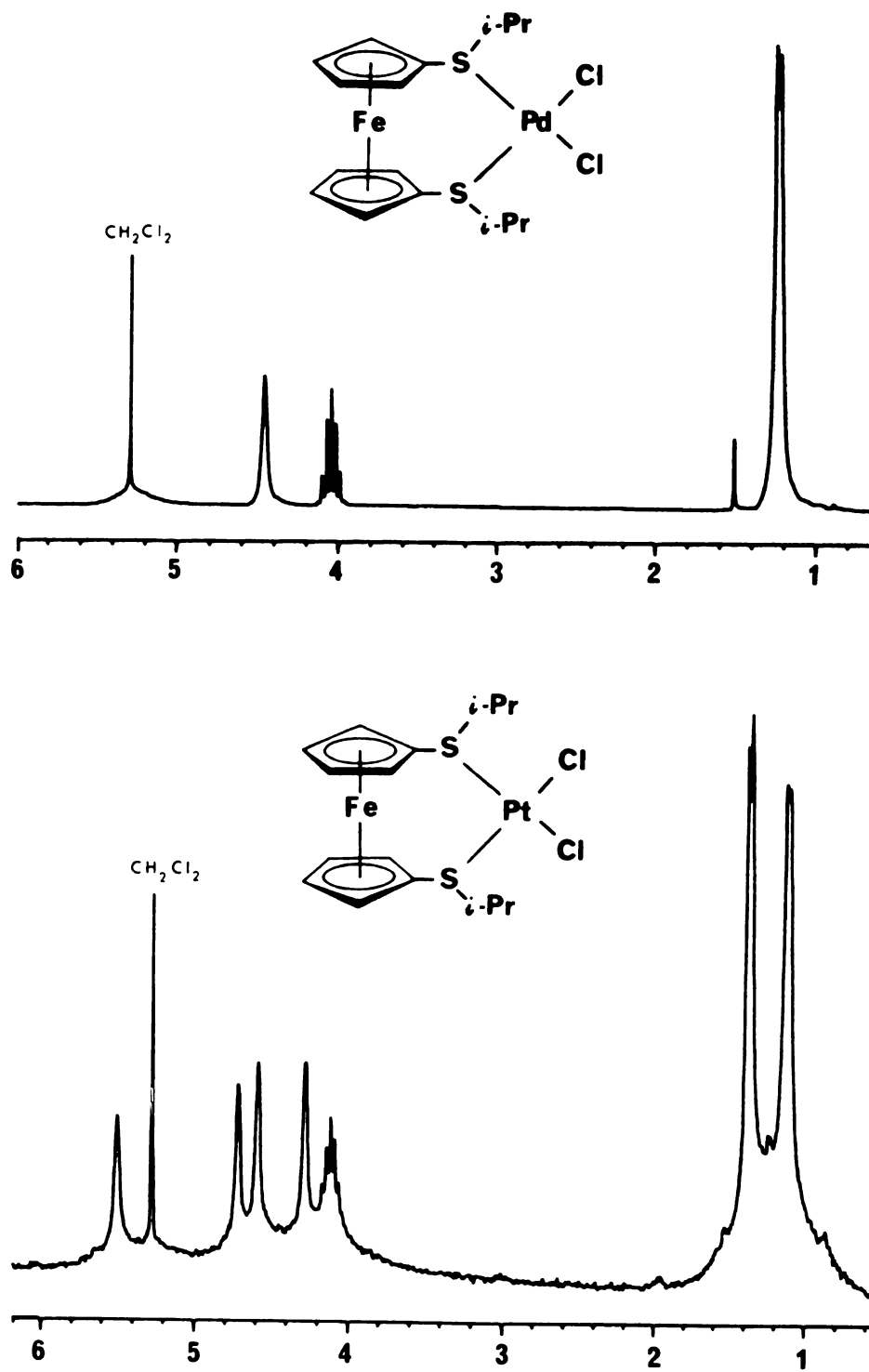


Figure 3.  $^1\text{H}$  NMR Spectra of  $\text{Fe}(\text{C}_5\text{H}_4\text{S}-i\text{Pr})_2\text{PdCl}_2$  and  $\text{Fe}(\text{C}_5\text{H}_4\text{S}-i\text{Pr})_2\text{PtCl}_2$ .



"triplets" at high temperature. The platinum analog exhibits a far more complex spectrum than the palladium compound. These differences are due to different rates of pyramidal sulfur inversion. This phenomenon is considered in detail in a later section. Both isopropyl complexes contain a peak at 5.28 ppm that is due to methylene chloride which is trapped in the crystal lattice.

In the  $^1\text{H}$  NMR spectra of the platinum complexes additional coupling from the  $^{195}\text{Pt}$  nucleus ( $I = 1/2$ , 33%) was anticipated. The methine region in Figure 3 should consist of a 1:4:1 proton resonance (in addition to coupling due to the methyl protons) where the outer signals are  $^{195}\text{Pt}$  satellites. At 250 MHz however  $^{195}\text{Pt}$ - $^1\text{H}$  coupling is not always observed due to the chemical shift anisotropy mechanism which dominates the relaxation of  $^{195}\text{Pt}$  at high field<sup>60</sup>.

### 3. $^{13}\text{C}$ NMR

$^{13}\text{C}$  NMR data were obtained only for the isobutyl complexes, (20)-(23) and the results are presented in Table 5. When the isobutyl ligand complexes to the metal halide the  $\text{C}_1$  chemical shift moves upfield by roughly 3 ppm whereas the  $\text{C}_{3,4}$  and  $\text{C}_{2,5}$  resonances move downfield by 1-2 ppm. This shift is consistent with the inductive effect of the electron-withdrawing metal halide as electron density is "drawn" towards the  $\text{C}_1$  atom (upfield shift) from the  $\text{C}_{2,5}$  and  $\text{C}_{3,4}$  nuclei (downfield shift)<sup>53</sup>. The signal due to the methylene

carbon moves downfield by 3-6 ppm while the resonance due to the methine carbon shifts upfield by at least 2 ppm upon complexation. The upfield shift of the methine carbon could be explained by a through space interaction rather than by a simple inductive effect.

#### 4. Infrared Spectra

The infrared spectra of the ferrocenylsulfide metal complexes are very similar to one another and to the free, uncomplexed ligand. Figure 4 illustrates representative spectra of the 1,1'-bis(phenylthio)ferrocene ligand, Figure (4a), and the corresponding platinum chloride and palladium bromide metal complexes, Figure (4b and 4c). Close inspection of the infrared spectra presented in Figure 4 reveals that the single absorption at  $820\text{ cm}^{-1}$  in the free ligand undergoes splitting in the metal complexes. There also appears to be additional splitting in the metal complexes in the  $500\text{ cm}^{-1}$  region where metal-ring vibrations occur.

The most striking change occurs in the low frequency region where metal-ligand vibrations are prevalent. Metal-sulfur vibrations are generally of low intensity and are found at higher frequencies than metal-halide stretches<sup>61</sup>. Table 6 contains the infrared data for the metal chloride and bromide complexes in the region  $400\text{-}200\text{ cm}^{-1}$ . Comparison of the chloride and bromide analogs, as shown in Figure 5, permits assignment of the metal-sulfur and the metal-halogen

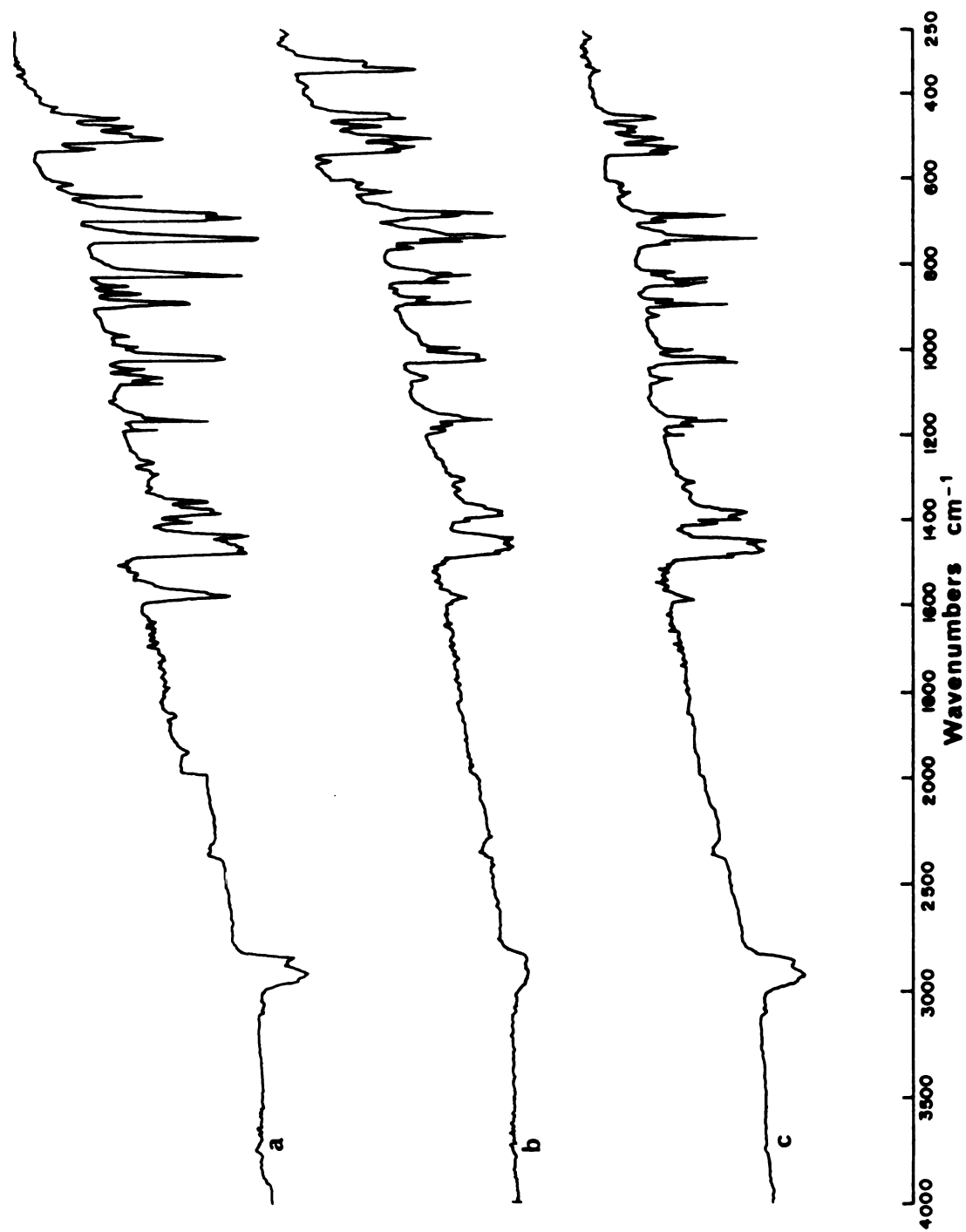


Figure 4. Infrared Spectra of (a)  $\text{Fe}(\text{C}_5\text{H}_4\text{SPh})_2$ , (b)  $\text{Fe}(\text{C}_5\text{H}_4\text{SPh})_2\text{PtCl}_2$  and (c)  $\text{Fe}(\text{C}_5\text{H}_4\text{SPh})_2\text{PdBr}_2$ .

Table 6. Infrared Data for  $\text{Fe}(\text{C}_5\text{H}_4\text{SR})_2\text{MX}_2$  ( $\text{R} = \text{Me}, \text{iPr}, \text{iBu}, \text{Ph}, \text{Bz}$ ;  $\text{M} = \text{Pd}, \text{Pt}$ ;  $\text{X} = \text{Cl}, \text{Br}$ ) in Region  $400\text{--}200\text{ cm}^{-1}$ . Measured as Nujol Mulls between CsBr Plates.

	Pd		Pt		
	Cl	Br	Cl	Br	
$\text{Fe}(\text{C}_5\text{H}_4\text{S-iBu})_2\text{MX}_2$	370sh 365w	365w	372w	372w 364w	(M-S)
	307s 290sh	222s	323s 310m	----- -----	(M-X)
$\text{Fe}(\text{C}_5\text{H}_4\text{SPh})_2\text{MX}_2$	360w	360w	372w	368w	(M-S)
	328s 320sh	210s	330s 318s	220m	(M-X)
$\text{Fe}(\text{C}_5\text{H}_4\text{SMe})_2\text{MX}_2$	355w 340w	343w	345w	340w	(M-S)
	310s 290sh	205m	323s 305s	208s	(M-X)
$\text{Fe}(\text{C}_5\text{H}_4\text{SCH}_2\text{Ph})_2\text{MX}_2$	358m 335w	353m 345sh	360m 350m	358m 348m	(M-S)
	315s 300s	230s	332s 312s	215s	(M-X)
$\text{Fe}(\text{C}_5\text{H}_4\text{S-iPr})_2\text{MX}_2$	380w 360w	380w 360w	383w 365w	389w 370w	(M-S)
	320s 305s	225s	328s 315s	220s	(M-X)
$(\text{PhSC}_3\text{H}_6\text{SPh})\text{MX}_2$	323vs 308vs	316s	350s 329s	349sh 324w	(M-S)
	278s 262s	----- -----	317s 312s	266m	(M-X)

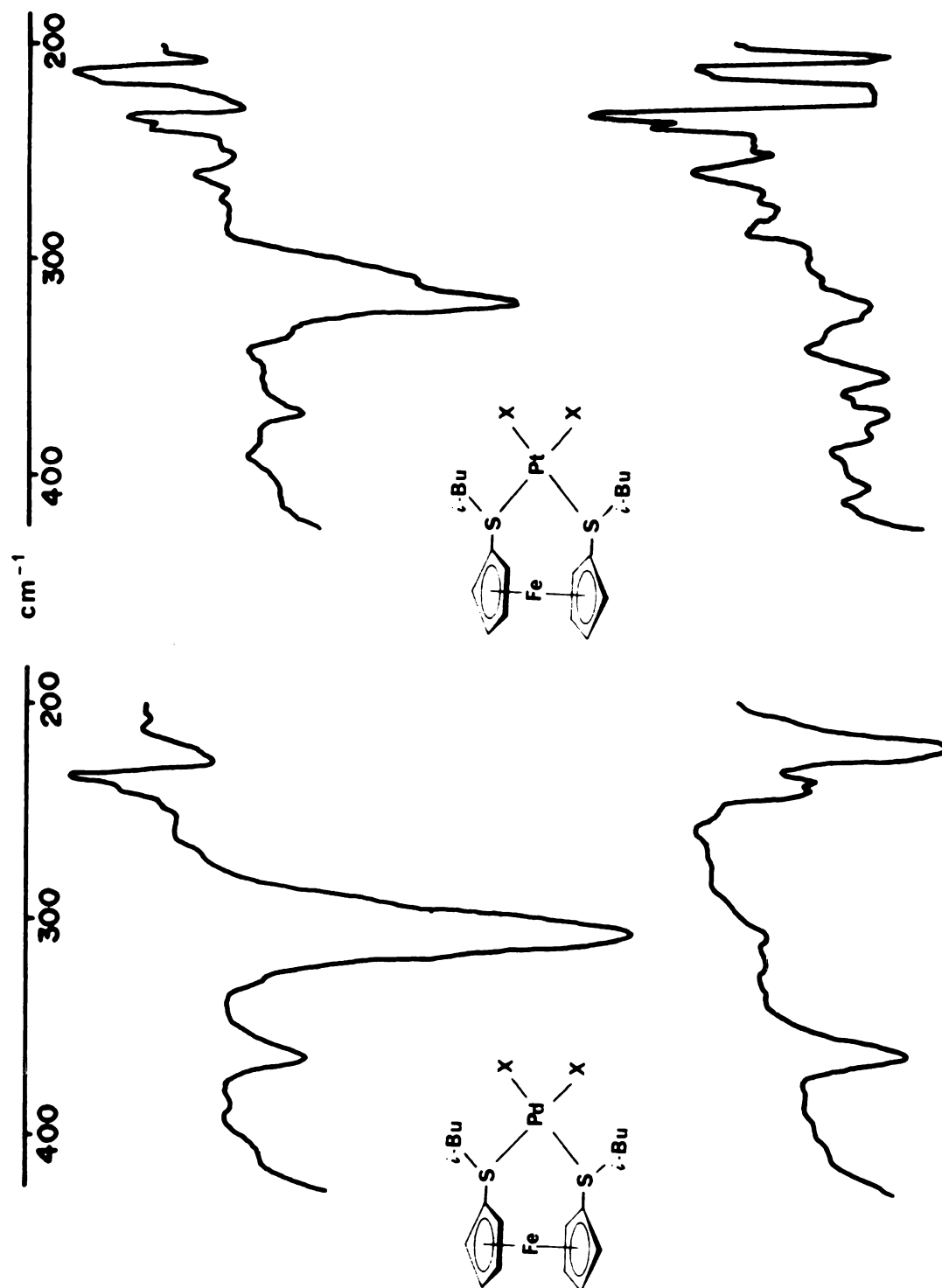


Figure 5. Far Infrared Region for  $\text{Fe}(\text{C}_5\text{H}_4\text{S}-i\text{Bu})_2\text{PdX}_2$  and  $\text{Fe}(\text{C}_5\text{H}_4\text{S}-i\text{Bu})_2\text{PtX}_2$  where X = Cl (above), and Br (below).

stretching frequencies. The metal-bromide stretch occurs at a lower frequency than the metal-chloride stretch and in some cases the metal-bromide stretch is not within range of the instrumentation used. The proposed assignments are in close agreement with those for the chelated thioether complex,  $(\text{PhSC}_3\text{H}_6\text{SPh})\text{MX}_2$  ( $\text{M} = \text{Pd}, \text{Pt}$ ;  $\text{X} = \text{Cl}, \text{Br}$ )<sup>62</sup>, (the last entry in Table 6) in addition to other values that have been reported<sup>61,63</sup>.

The metal-chloride stretches in complexes of the type  $\text{cis}(\text{PdCl}_2\text{L}_2)$ , where L is a phosphine, are found at lower frequencies than those given in Table 6<sup>64</sup>. One hesitates to correlate the higher metal-chloride stretch in the sulfide complexes with a weaker trans-influence of the sulfide ligands due to the possible coupling between the metal-chloride stretch and other vibrational modes within the molecule.

## 5. Ultraviolet and Visible Spectra

Table 7 contains the ultraviolet and visible spectral data for the complexes  $\text{Fe}(\text{C}_5\text{H}_4\text{SR})_2$  and  $\text{Fe}(\text{C}_5\text{H}_4\text{SR})_2\text{MX}_2$  where  $\text{R} = \text{iBu}, \text{Ph}, \text{Me}$ ;  $\text{M} = \text{Pd}, \text{Pt}$ ;  $\text{X} = \text{Cl}, \text{Br}$ . The methyl derivatives did not completely dissolve in acetonitrile solution and consequently the extinction coefficients for these compounds are unreliable.

In the electronic absorption spectrum of ferrocene the low energy bands at 440 nm ( $\epsilon = 91$ ) and 325 nm ( $\epsilon = 49$ )

Table 7. Electronic Absorption Spectra of Ferrocenylsulfide Complexes  $\text{Fe}(\text{C}_5\text{H}_4\text{SR})_2$ ,  $\text{Fe}(\text{C}_5\text{H}_4\text{SR})_2\text{MX}_2$  (R = iBu, Ph, Me; M = Pd, Pt; X = Cl, Br) at 24°C in MeCN Solution at approx. conc.  $8.0 \times 10^{-5}$  M.

	$\lambda_{\text{max}}$ (nm)	$\epsilon$ ( $\text{M}^{-1}\text{cm}^{-1}$ )		
$\text{Fe}(\text{C}_5\text{H}_4\text{S-iBu})_2$	425 <sup>a</sup> 300 <sup>a</sup> 352 <sup>b</sup> 210	190 1900 7000 32000		
$\text{Fe}(\text{C}_5\text{H}_4\text{SPh})_2$	430 248 220	500 32500 35000		
$\text{Fe}(\text{C}_5\text{H}_4\text{SMe})_2$	430 210	----- -----		
	Cl		Br	
	$\lambda_{\text{max}}$ (nm)	$\epsilon$ ( $\text{M}^{-1}\text{cm}^{-1}$ )	$\lambda_{\text{max}}$ (nm)	$\epsilon$ ( $\text{M}^{-1}\text{cm}^{-1}$ )
$\text{Fe}(\text{C}_5\text{H}_4\text{S-iBu})_2\text{PdX}_2$	400 330 262 210	760 2300 11600 30000	403 309 275 210	440  5100 30000
$\text{Fe}(\text{C}_5\text{H}_4\text{SPh})_2\text{PdX}_2$	400 <sup>a</sup>  245 210	800  1500 30000	433 317 255 210	500 1460 6900 30000
$\text{Fe}(\text{C}_5\text{H}_4\text{SMe})_2\text{PdX}_2$	400 <sup>a</sup> 319 254 210	----- 1600 5700 30000	400 309 270 210	210 820 1600 5000
$\text{Fe}(\text{C}_5\text{H}_4\text{S-iBu})_2\text{PtX}_2$	410  232 <sup>sh</sup> 210	440  14800 30000	420 300 234 210	390 2200 16900 30000

Table 7. Continued.

	Cl		Br	
	$\lambda_{\text{max}}$ (nm)	$\epsilon$ ( $\text{M}^{-1}\text{cm}^{-1}$ )	$\lambda_{\text{max}}$ (nm)	$\epsilon$ ( $\text{M}^{-1}\text{cm}^{-1}$ )
$\text{Fe}(\text{C}_5\text{H}_4\text{SPh})\text{PtX}_2$	420	950	428	660
	360	1220		
	300	2000	318	3400
	245	11900	278	14300
	210	30000	210	30000
$\text{Fe}(\text{C}_5\text{H}_4\text{SMe})_2\text{PtX}_2$	420	470		
	360	940	310	2800
	290	1200		
	242	11800	265 <sup>sh</sup>	12700
	210	30000	210	30000

<sup>a</sup>Difficult to ascertain exact maximum.<sup>b</sup>Inflection point.



have been attributed to spin allowed d-d transitions. In the near ultraviolet region the band at 200 nm ( $\epsilon = 51000$ ) has been assigned as a ligand-to-metal charge-transfer band and the shoulders at 265 nm and 240 nm have been assigned as metal-to-ligand charge-transfer transitions<sup>65</sup>.

The ferrocenylsulfide ligands exhibit an absorption at 425-430 nm ( $\epsilon = 10^2$ ) which is probably due to a d-d transition. The intensity of this band is significantly increased over the corresponding band in ferrocene. In the ferrocenylsulfide metal complexes the absorption due to the d-d transition is slightly blue shifted to 400-420 nm in comparison to ferrocene.

The ferrocenylsulfide palladium complexes exhibit an intense, well defined maximum around 260 nm whereas the platinum analogs have an inflection point in this region. This band could be associated with a metal-to-ligand charge-transfer band whereas the strong absorption at 210 nm is probably a ligand-to-metal charge-transfer transition.

## 6. Structure

The structure and numbering scheme of 1,1'-bis(isobutylthio)ferrocenepalladiumdichloride, (16), is shown in Figure 6 while a stereoview is given in Figure 7. Hydrogen atoms have been omitted for clarity. The positional parameters and anisotropic thermal parameters are given in Table 8 and Table 9, respectively. In (16) the palladium

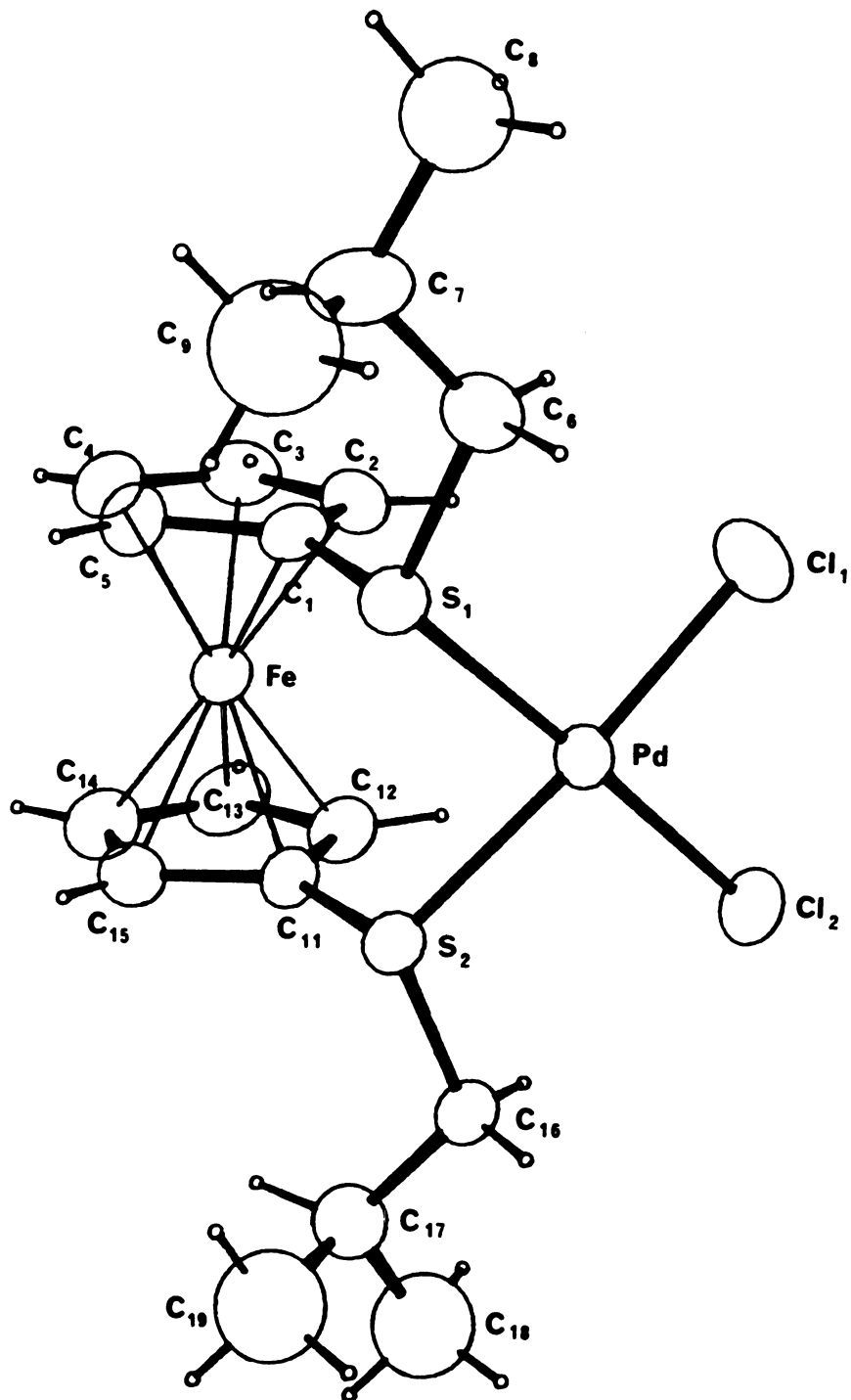


Figure 6. Structure and Numbering Scheme for  $\text{Fe}(\text{C}_5\text{H}_4\text{S-iBu})_2\text{-PdCl}_2$ .

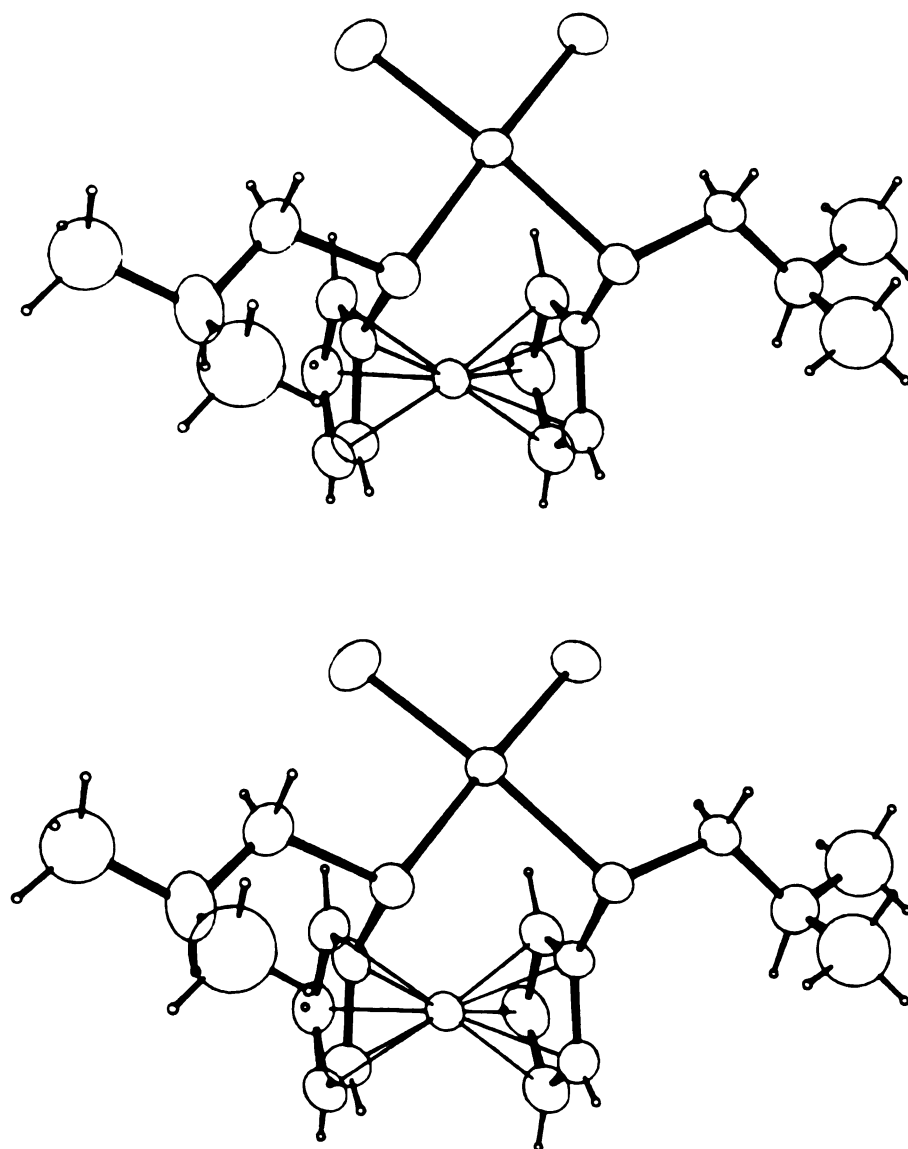


Figure 7. Stereoview of  $\text{Fe}(\text{C}_5\text{H}_4\text{S}-i\text{Bu})_2\text{PdCl}_2$ .

Table 8. Positional Parameters and Esd's for  $\text{Fe}(\text{C}_5\text{H}_4\text{S}-i\text{Bu})_2\text{-PdCl}_2$ .

Atom	X	Y	Z
Pd(1)	.02486(2)	.05361(3)	.09452(2)
Fe(1)	.03407(3)	-.00389(6)	.32654(4)
Cl(1)	-.04093(6)	.1867(1)	.04318(8)
Cl(2)	.10334(7)	.1636(1)	.0476(1)
S(1)	-.05094(6)	-.0531(1)	.15645(8)
S(2)	.08816(6)	-.0853(1)	.14708(8)
C(1)	-.0432(2)	-.0140(4)	.2609(3)
C(2)	-.0453(2)	-.0915(5)	.3294(3)
C(3)	-.0390(3)	-.0296(6)	.4017(4)
C(4)	-.0340(3)	.0855(5)	.3816(4)
C(5)	-.0366(2)	.0962(5)	.2944(3)
C(6)	-.1249(2)	.0076(5)	.1354(4)
C(7)	-.1754(3)	-.0400(5)	.1873(4)
C(8)	-.2299(4)	.0337(7)	.1748(6)
C(9)	-.1887(4)	-.1590(7)	.1643(5)
C(11)	.1028(2)	-.0401(4)	.2496(3)
C(12)	.1088(2)	.0711(5)	.2793(4)
C(13)	.1138(3)	.0653(6)	.3662(4)
C(14)	.1102(3)	-.0486(6)	.3895(4)
C(15)	.1044(3)	-.1151(5)	.3182(3)
C(16)	.1625(3)	-.0766(6)	.0997(4)
C(17)	.2065(3)	-.1648(5)	.1278(5)
C(18)	.2681(3)	-.1361(6)	.0899(5)
C(19)	.1877(4)	-.2819(7)	.1013(6)
H(2)	-.048(2)	-.165(4)	.327(3)
H(3)	-.036(2)	-.059(4)	.452(3)
H(4)	-.028(2)	.148(4)	.417(3)
H(5)	-.030(2)	.163(4)	.259(3)
H(6A)	-.130(3)	-.019(5)	.077(4)
H(6B)	-.122(2)	.084(4)	.140(3)
H(7)	-.170(2)	-.049(4)	.253(4)
H(12)	.110(2)	.139(4)	.248(3)
H(13)	.115(2)	.123(4)	.400(3)
H(14)	.111(2)	-.064(4)	.434(3)
H(15)	.101(2)	-.196(4)	.314(3)
H(16A)	.174(3)	-.000(5)	.104(4)
H(16B)	.153(3)	-.095(4)	.039(4)
H(17)	.201(3)	-.155(5)	.196(4)
H(8A)	-.2416	.0342	.1156
H(8B)	-.2203	.1119	.1939
H(8C)	-.2642	.0032	.2093
H(9A)	-.1527	-.206	.1732
H(9B)	-.2017	-.1618	.105

Table 8. Continued.

Atom	X	Y	Z
H(9C)	-.2229	-.1868	.2003
H(18A)	.2813	-.0606	.1092
H(18B)	.2647	-.1364	.0278
H(18C)	.2984	-.1945	.107
H(19A)	.1844	-.2858	.0410
H(19B)	.1475	-.2995	.128
H(19C)	.2182	-.3374	.1225

Table 9A. Anisotropic Thermal Parameters with Esd's for  $\text{Fe}(\text{C}_5\text{H}_4\text{S-iBu})_2\text{PdCl}_2$ .

The temperature factor has the form:  $T = -\text{SUM}(\text{H(I)}*\text{H(J)}*\text{BIJ*ASTAR(I)*ASTAR(J)})/4$ . Where H is the Miller Index, ASTAR is the reciprocal cell length, and I and J are cycled 1 through 3.

Atom	B11	B22	B33	B12	B13	B23
Pd(1)	2.57(1)	2.55(1)	2.00(1)	.03(1)	.20(1)	-.02(1)
Fe(1)	2.50(3)	2.97(3)	2.18(3)	.12(3)	-.13(3)	-.07(2)
Cl(1)	4.06(7)	2.95(5)	3.30(6)	.41(5)	-.33(5)	.50(5)
Cl(2)	3.97(7)	3.50(6)	4.74(8)	-.52(5)	1.24(6)	.29(5)
S(1)	2.51(5)	2.89(5)	2.28(5)	.01(4)	-.11(4)	.04(4)
S(2)	2.56(5)	3.15(5)	2.53(5)	.41(4)	.24(4)	-.10(4)
C(1)	2.4(2)	3.3(2)	2.0(2)	.3(2)	.1(2)	.3(2)
C(2)	2.6(2)	4.0(3)	2.8(2)	-.1(2)	.3(2)	.4(2)
C(3)	3.4(3)	6.8(4)	2.3(2)	.4(2)	.5(2)	.4(3)
C(4)	3.8(3)	5.2(3)	3.0(2)	1.4(2)	.1(2)	-1.3(2)
C(5)	3.1(3)	3.4(2)	3.1(2)	.8(2)	.0(2)	-.2(2)
C(6)	2.8(2)	3.4(3)	2.9(3)	.1(2)	-.3(2)	.5(2)
C(7)	2.7(2)	4.6(3)	4.8(3)	.6(2)	.6(2)	1.0(3)
C(11)	2.1(2)	3.6(2)	2.9(2)	.5(2)	-.2(2)	.1(2)
C(12)	2.9(2)	3.4(3)	3.6(3)	-.5(2)	.0(2)	.3(2)
C(13)	3.3(3)	4.9(3)	3.2(3)	-.8(2)	-.5(2)	-.7(3)

Table 9A. Continued.

Atom	B11	B22	B B33	B12	B13	B23
C(14)	3.0(2)	5.6(3)	2.5(3)	.5(2)	-.3(2)	.8(3)
C(15)	3.3(2)	3.6(3)	2.9(2)	.6(2)	.1(2)	.5(2)
C(16)	3.1(2)	5.3(4)	3.3(3)	.5(2)	1.0(2)	.3(3)
C(17)	2.9(3)	5.3(3)	5.6(4)	1.0(2)	.2(3)	-.5(3)

Table 9B. Isotropic Thermal Parameters with Esd's for  $\text{Fe}(\text{C}_5\text{H}_4\text{S}-i\text{Bu})_2\text{PdCl}_2$ .

The temperature factor has the form:  $T = -B * (\text{SIN}(\text{THETA})/\text{LAMBDA})^{**2}$   
Where theta is from the diffraction angle 2-theta, and lambda is the X-ray wavelength.

Atom	B	Atom	B	Atom	B
C(8)	7.5(2)	H(7)	4.4(13)	H(8C)	8.520
C(9)	7.6(2)	H(12)	2.1(10)	H(9A)	8.550
C(18)	6.3(2)	H(13)	1.6(10)	H(9B)	8.550
C(19)	8.2(2)	H(14)	2.9(13)	H(9C)	8.550
H(2)	3.0(13)	H(15)	2.2(10)	H(18A)	7.290
H(3)	3.3(12)	H(16A)	5.2(16)	H(18B)	7.290
H(4)	2.8(11)	H(16B)	4.8(14)	H(18C)	7.290
H(5)	2.7(11)	H(17)	8.0(20)	H(19A)	9.180
H(6A)	6.8(19)	H(8A)	8.520	H(19B)	9.180
H(6B)	2.9(12)	H(8B)	8.520	H(19C)	9.180

atom is in a square planar environment where the ferrocenylsulfide ligand chelates to the palladium atom through both sulfur atoms.

The bond distances and bond angles of the isobutyl palladium complex are presented in Table 10 and Table 11 and are fairly typical. The iron-carbon distances range from 2.011(5) Å to 2.051 Å with an average value of 2.036(6) Å that compares favorably with that of ferrocene<sup>66</sup>. The carbon-carbon distances in the cyclopentadienyl ring vary from 1.385(8) to 1.438(7) Å averaging at 1.410(5) Å, a value typical of ferrocene. The C-C-C bond angles within the two rings vary from 106.86(50) to 109.(52)°, with an average angle of 108.0° that is the typical angle for a regular, planar pentagon.

The Pd-S bond lengths are 2.329(1) and 2.324(2) Å which are comparable to the sum of the covalent radii (2.35 Å)<sup>67</sup>. This suggests that there is little or no  $\pi$ -bonding in the Pd-S bond. The Pd-Cl bond, which is trans to the sulfur atom, shows no apparent trans bond lengthening indicating that the thioether ligand has a negligible trans-influence<sup>68</sup>. The Pd-Cl bond distances have an average value of 2.303(2) Å that is almost equal to the sum of the Pauling covalent radii, 2.31 Å<sup>67</sup>.

Seyferth<sup>42</sup> recently reported a crystal structure of a heterobinuclear species  $(\text{Ph}_3\text{P})\text{PdFe}(\text{C}_5\text{H}_4\text{S})_2$  where thiolate groups chelate to palladium. The cyclopentadienylthiolato groups,  $(\text{C}_5\text{H}_4\text{S})$ , are tilted away from the plane parallel



Table 10. Selected Bond Distances (Å) with Esd's for  
 $\text{Fe}(\text{C}_5\text{H}_4\text{S}-i\text{Bu})_2\text{PdCl}_2$ .

Cl(1)-Pd	2.303(2)	H(2)-C(2)	0.873(45)
Cl(2)-Pd	2.302(2)	H(3)-C(3)	0.889(52)
S(1)-Pd	2.329(1)	H(4)-C(4)	0.948(47)
S(2)-Pd	2.324(2)	H(5)-C(5)	0.987(46)
C(1)-Fe	2.018(5)	H(6A)-C(6)	0.994(64)
C(2)-Fe	2.045(6)	H(6B)-C(6)	0.913(45)
C(3)-Fe	2.046(6)	H(7)-C(7)	1.073(58)
C(4)-Fe	2.046(6)	H(8A)-C(8)	0.989(00)
C(5)-Fe	2.033(6)	H(8B)-C(8)	1.000(01)
C(11)-Fe	2.011(5)	H(8C)-C(8)	1.009(00)
C(12)-Fe	2.028(6)	H(9A)-C(9)	0.985(00)
C(13)-Fe	2.051(6)	H(9B)-C(9)	0.999(00)
C(14)-Fe	2.039(6)	H(9C)-C(9)	1.010(00)
C(15)-Fe	2.045(6)	H(12)-C(12)	0.947(43)
C(1)-S(1)	1.756(5)	H(13)-C(13)	0.876(42)
C(6)-S(1)	1.822(6)	H(14)-C(14)	0.737(52)
C(11)-S(2)	1.768(5)	H(15)-C(15)	0.971(40)
C(16)-S(2)	1.818(6)	H(16A)-C(16)	0.942(55)
C(2)-C(1)	1.438(7)	H(16B)-C(16)	1.024(57)
C(5)-C(1)	1.421(7)	H(17)-C(17)	1.104(68)
C(3)-C(2)	1.385(8)	H(18A)-C(18)	0.992(00)
C(4)-C(3)	1.406(9)	H(18B)-C(18)	1.005(00)
C(5)-C(4)	1.414(8)	H(18C)-C(18)	1.004(00)
C(7)-C(6)	1.507(8)	H(19A)-C(19)	0.978(00)
C(8)-C(7)	1.505(9)	H(19B)-C(19)	1.010(00)
C(9)-C(7)	1.488(9)	H(19C)-C(19)	1.004(00)
C(12)-C(11)	1.409(7)	C(15)-C(14)	1.401(8)
C(15)-C(11)	1.419(7)	C(17)-C(16)	1.501(8)
C(13)-C(12)	1.409(8)	C(18)-C(17)	1.535(9)
C(14)-C(13)	1.403(9)	C(19)-C(17)	1.511(10)

Table 11. Selected Bond Angles (deg) with Esd's for  
 $\text{Fe}(\text{C}_5\text{H}_4\text{S-iBu})_2\text{PdCl}_2$ .

Cl(1)-Pd-Cl(2)	88.41(07)	Fe-C(1)-C(2)	70.27(26)
Cl(1)-Pd-S(1)	94.00(07)	Fe-C(1)-C(5)	70.03(27)
Cl(1)-Pd-S(2)	177.82(08)	S(1)-C(1)-C(2)	124.48(30)
Cl(2)-Pd-S(1)	173.79(08)	S(1)-C(1)-C(5)	128.12(29)
Cl(2)-Pd-S(2)	93.73(07)	C(2)-C(1)-C(5)	107.35(48)
S(1)-Pd-S(2)	83.92(06)	C(1)-C(2)-C(3)	107.79(48)
C(1)-Fe-C(2)	41.45(19)	C(2)-C(3)-C(4)	109.14(52)
C(1)-Fe-C(3)	68.29(24)	C(3)-C(4)-C(5)	108.24(53)
C(1)-Fe-C(4)	68.46(23)	C(1)-C(5)-C(4)	107.46(47)
C(1)-Fe-C(5)	41.08(19)	S(1)-C(6)-C(7)	114.62(30)
C(1)-Fe-C(11)	107.83(27)	C(6)-C(7)-C(8)	107.73(52)
C(1)-Fe-C(12)	121.47(29)	C(6)-C(7)-C(9)	111.27(58)
C(1)-Fe-C(13)	156.85(32)	C(8)-C(7)-C(9)	110.93(69)
C(1)-Fe-C(14)	161.50(34)	Fe-C(11)-S(2)	120.21(15)
C(1)-Fe-C(15)	125.00(30)	S(2)-C(11)-C(12)	128.21(32)
Pd-S(1)-C(1)	101.41(16)	S(2)-C(11)-C(15)	122.93(31)
Pd-S(1)-C(6)	110.77(19)	C(12)-C(11)-C(15)	108.59(50)
C(1)-S(1)-C(6)	99.35(31)	C(11)-C(12)-C(13)	107.43(48)
Pd-S(2)-C(11)	103.71(16)	C(13)-C(12)-C(15)	71.58(40)
Pd-S(2)-C(16)	110.69(20)	C(12)-C(13)-C(14)	108.02(53)
C(11)-S(2)-C(16)	102.10(33)	C(13)-C(14)-C(15)	109.07(52)
Fe-C(1)-S(1)	127.03(15)		

by  $19.6^\circ$ . Seyferth proposed the presence of a weak dative  $\text{Fe} \rightarrow \text{Pd}$  bond on the basis of a Fe-Pd distance of  $2.878(1)$  Å. In the isobutyl palladium complex, (16), the distance between the iron and palladium atom is  $3.81$  Å which suggests that there is no direct metal-metal interaction.

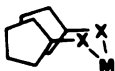
The two cyclopentadienyl rings are eclipsed and are slightly tilted with respect to each other, the dihedral angle being  $1.9^\circ$ . The planes containing the cyclopentadienyl rings are almost orthogonal to the plane containing the palladium, sulfur and chlorine atoms. The calculated least-squares planes and the torsion angles are given in Table 13 and Table 14, respectively.

Crystal structures of similar [3]ferrocenophanes such as 1,2,3-trithia-[3]ferrocenophane<sup>69</sup>, (1), 1,3-dithia-2-selena-[3]ferrocenophane<sup>9</sup>, (45), diiodocarbonylferrocene-1,1'-bis(dimethylarsine)nickel[II]<sup>70</sup>, (46), and 1,1'-bis(*t*-butylphosphino)ferrocene norbornadiene rhodium[I] perchlorate, (47)<sup>71</sup>, have been determined. In compound (46), the authors claim that the ferrocenylarsine ligand chelates to the nickel atom with a stepped conformation such that the Ni, Fe and two As atoms are not coplanar. A similar conformation is evident in the structure of the isobutyl palladium complex, (16), where the dihedral angle between the plane containing the iron and two sulfur atoms and the plane containing the palladium, two chlorine and two sulfur atoms is  $75.4^\circ$ . The dihedral angles of selected

Table 12. Dihedral Angle and Bridgehead Angle of Selected [3]ferrocenophanes.

Compound	X	M	Dihedral <sup>a</sup> Angle	Bridgehead Angle
$\text{Fe}(\text{C}_5\text{H}_4\text{S})_2\text{Se}$	S	Se	112.2°	100.5°
$\text{Fe}(\text{C}_5\text{H}_4\text{S})_2\text{S}$	S	S	110.9°	103.9°
$\text{Fe}(\text{C}_5\text{H}_4\text{S}-i\text{Bu})_2\text{PdCl}_2$	S	Pd	75.4°	84.0°
$\text{Fe}(\text{C}_5\text{H}_4\text{AsMe}_2)_2\text{Ni}(\text{CO})\text{I}_2$	As	Ni	46.6°	93.5°

<sup>a</sup>Dihedral angle obtained from least-squares planes calculation. Dihedral angle refers to angle between  $\text{FeX}_2$  plane and  $\text{MX}_2$  plane.



[3]ferrocenophanes is given in Table 12, shown above. In the trithiane, (1), and the selenium analog, (45), the larger dihedral and bridgehead angles are due to the steric bulk of the larger sulfur and selenium bridgehead atoms.

## 7. Dynamic NMR Studies

Variable temperature  $^1\text{H}$  NMR spectra of 1,1'-bis(iso-butylthio)ferrocenepalladiumdichloride, (16), are shown in Figure 8. At 72°C the ring protons give rise to an AA'BB' spin system that consists of two distorted "triplets" separated by 0.87 ppm. These "triplets" appear to coalesce at different temperatures with the alpha protons broadening at 39°C and the beta protons broadening at 15°C.

Table 13. Least-Squares Planes in  $\text{Fe}(\text{C}_5\text{H}_4\text{S}-i\text{Bu})_2\text{PdCl}_2$ .

Planes are in the form  $A \cdot X + B \cdot Y + C \cdot Z - D = 0$ ;  
plane constants with respect to crystallographic  
axes and X,Y,Z in fractional coordinates.

Plane	A	B	C	D
1	22.019	-1.184	-0.934	-1.199
2	22.060	-0.821	-1.132	2.030
3	1.399	5.984	13.888	1.710
4	2.355	11.325	-4.448	-1.417

Angles between planes:

1-2	1.9°
1-3	-87.8°
1-4	88.5°
2-3	-88.1°
2-4	86.6°
3-4	75.4°

Distances of atoms from planes:

Atom	Plane 1	Plane 2	Plane 3	Plane 4
Pd	1.595	-1.634	-.041*	1.663
Fe	1.651	-1.644	2.849	-.000*
Cl(1)	0.039	-3.134	-.052*	3.246
Cl(2)	3.237	0.061	0.073*	3.301
S(1)	-.007	-3.289	0.075*	-.000*
S(2)	3.104	-.183	-.055*	-.000*
C(1)	0.002*	-3.287	1.783	-.016
C(2)	-.004*	-3.335	2.223	-1.210
C(3)	0.005*	-3.317	3.630	-.799
C(4)	-.003*	-3.279	4.060	0.599
C(5)	-.001*	-3.254	2.896	1.108
C(6)	-1.693	-4.951	0.040	0.622
C(7)	-2.804	-6.092	0.397	-.283
C(8)	-4.069	-7.331	0.631	0.495
C(9)	-2.907	-6.235	-.631	-1.564
C(11)	3.285	-.005*	1.646	0.087
C(12)	3.256	0.001*	2.730	1.248
C(13)	3.277	0.003*	3.931	0.796
C(14)	3.314	-.007*	3.574	-.615
C(15)	3.338	0.007*	2.175	-1.067
C(16)	4.779	1.530	-.563	0.482
C(17)	5.820	2.513	-.648	-.536
C(18)	7.194	3.908	-.904	0.107
C(19)	5.584	2.239	-1.685	-1.787

\* Indicates an atom included in the calculation of the plane.

Table 14. Torsion Angles in  $\text{Fe}(\text{C}_5\text{H}_4\text{S}-i\text{Bu})_2\text{PdCl}_2$ .

Atoms	Angle
C1(1)-Pd(1)-S(1)-C(1)	-102.54
C1(1)-Pd(1)-S(1)-C(6)	2.17
C1(1)-Pd(1)-S(2)-C(11)	-102.22
C1(1)-Pd(1)-S(2)-C(16)	148.95
C1(2)-Pd(1)-S(1)-C(1)	10.08
C1(2)-Pd(1)-S(1)-C(6)	114.78
C1(2)-Pd(1)-S(2)-C(11)	88.93
C1(2)-Pd(1)-S(2)-C(16)	-19.90
Pd(1)-S(1)-C(1)-C(2)	-136.75
Pd(1)-S(1)-C(1)-C(5)	46.30
Pd(1)-S(1)-C(6)-C(7)	-167.42
Pd(1)-S(2)-C(11)-C(12)	-34.52
Pd(1)-S(2)-C(11)-C(15)	138.87
Pd(1)-S(2)-C(16)-C(17)	-178.44
S(1)-Pd(1)-S(2)-C(11)	-85.29
S(1)-Pd(1)-S(2)-C(16)	165.88
S(1)-C(1)-C(2)-C(3)	-178.65
S(1)-C(1)-C(5)-C(4)	178.15
S(1)-C(6)-C(7)-C(8)	168.97
S(1)-C(6)-C(7)-C(9)	-69.23
S(2)-Pd(1)-S(1)-C(1)	78.10
S(2)-Pd(1)-S(1)-C(6)	-177.19
S(2)-C(11)-C(12)-C(13)	173.92
S(2)-C(11)-C(15)-C(14)	-173.41
S(2)-C(16)-C(17)-C(18)	-173.37
S(2)-C(16)-C(17)-C(19)	65.99
C(1)-S(1)-C(6)-C(7)	-61.34
C(1)-C(2)-C(3)-C(4)	1.10
C(1)-C(5)-C(4)-C(3)	-.12
C(2)-C(1)-C(5)-C(4)	0.78
C(2)-C(3)-C(4)-C(5)	-.62
C(3)-C(2)-C(1)-C(5)	-1.16
C(11)-S(2)-C(16)-C(17)	71.68
C(11)-C(12)-C(13)-C(14)	-.75
C(11)-C(15)-C(14)-C(13)	-1.59
C(12)-C(11)-C(15)-C(14)	1.12
C(12)-C(13)-C(14)-C(15)	1.46
C(13)-C(12)-C(11)-C(15)	-.23

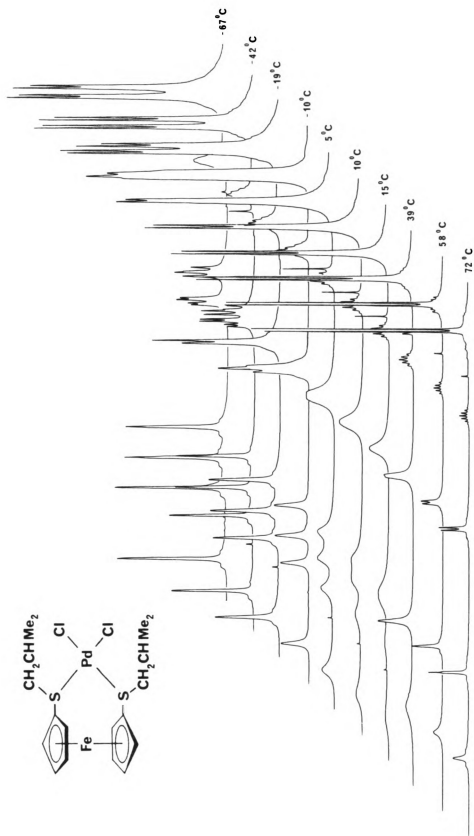


Figure 8. Variable temperature  $^1\text{H}$  NMR spectra for  $\text{Fe}(\text{C}_5\text{H}_4\text{S}-i\text{Bu})_2\text{PdCl}_2$ .

In the slow exchange limit, which occurs at  $-40^{\circ}\text{C}$ , the ring protons appear as four singlets. Enhancement of the low temperature spectrum indicates that the two low field singlets are in fact doublets and the two high field singlets are triplets.

The isobutyl protons also exhibit temperature dependent NMR spectra. At the fast exchange limit,  $72^{\circ}\text{C}$ , the doublet at 2.98 ppm is due to the methylene protons, the multiplet at 1.80 ppm is due to the methine protons and the doublet at 1.01 ppm is assigned to the methyl protons. As the temperature is lowered, the signals broaden with the methylene protons coalescing at around  $39^{\circ}\text{C}$ . At the slow exchange limit the methylene protons exist as four doublets. The methyl protons coalesce at around  $-10^{\circ}\text{C}$  and appear as two distinct doublets at  $-67^{\circ}\text{C}$ . The methine multiplet is broad at low temperature probably due to two overlapping multiplets.

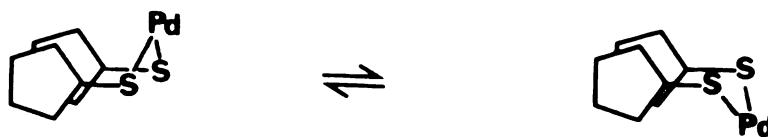
The temperature dependent NMR spectra could arise from two independent dynamic processes. A bridge reversal process has been observed in [3]ferrocenophanes with tri-chalcogen bridges. As discussed in the section dealing with the structure, the dihedral angle between the planes  $\text{Fe-S}_1\text{-S}_3$  and  $\text{S}_1\text{-S}_2\text{-S}_3$  is  $110.9^{\circ}$  in the trithiane, (1). The bridging sulfur,  $\text{S}_2$ , flips from one side of the  $\text{Fe-S}_1\text{-S}_3$  plane to the other side on the NMR time scale and gives rise to a fluxional molecule. This process is analogous



to the chair-to-chair reversal observed in six membered rings<sup>72</sup>.

In the dynamic NMR spectra of the trithiane, (1), the low temperature spectrum consists of four complex signals which, upon raising the temperature, collapse to give two distorted "triplets" at high temperature. At the slow exchange limit, bridge reversal is slow with respect to the NMR time scale and this gives rise to an ABCD spectrum where the four cyclopentadienyl ring protons are anisochronous. As the temperature is raised, bridge reversal becomes rapid relative to the NMR time scale and the spectrum consists of two distorted "triplets" arising from an AA'BB' spin system<sup>73</sup>.

The crystal structure of the isobutyl palladium complex, (16), indicated that the dihedral angle between the Fe-S<sub>1</sub>-S<sub>2</sub> plane and the S<sub>1</sub>-Pd-S<sub>2</sub> plane was 75.4°. Bridge reversal could occur in this complex in much the same way it occurs in the trithiane complex. The palladium atom could flip from one side of the Fe-S<sub>1</sub>-S<sub>2</sub> plane to the other side as illustrated in Scheme 7.



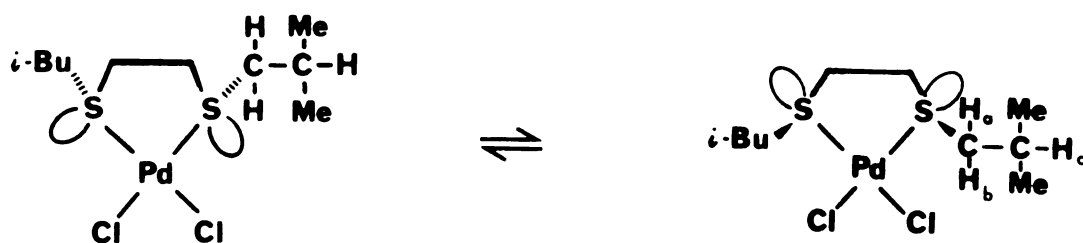
Scheme 7.

The change observed in the NMR spectra of (16), as shown in Figure 8, in the cyclopentadienyl proton region is very similar to that observed for the fluxional [3]-ferrocenophane, (1). Bridge reversal, where the palladium atom flips back and forth, could account for the temperature dependence of the NMR spectra of complex (16).

The second dynamic process is the pyramidal inversion of sulfur. Inversion rates at sulfur are often too slow to be observed on the NMR time scale, as for example in the sulfoxides, but recently Abel and coworkers<sup>74</sup> and other groups<sup>75</sup> have determined the barrier energies for sulfur inversion in a variety of palladium and platinum complexes.

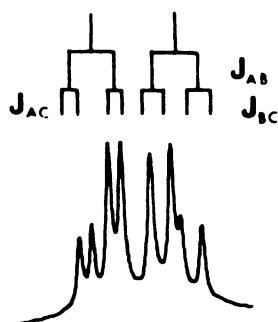
In a recent study Orrell<sup>76</sup> determined the inversion barriers at sulfur in compounds of the type  $\text{cis}[\text{MX}_2\text{L}]$ , ( $\text{M} = \text{Pd}, \text{Pt}$ ;  $\text{X} = \text{Cl}, \text{Br}, \text{I}$ ;  $\text{L} = \text{MeS}(\text{CH}_2)_2\text{SMe}, \text{MeS}(\text{CH}_2)_3\text{SMe}$ ). At low temperatures, in the absence of sulfur inversion, two diastereoisomers, meso and DL, were detected. When pyramidal inversion of sulfur is slow, the sulfur atoms are chiral and this leads to the presence of diastereoisomers.

Sulfur inversion could occur in the isobutyl palladium complex, (16), as illustrated in Scheme 8. The two sulfur atoms are centers of chirality and at low temperature, when pyramidal inversion is slow relative to the NMR time scale the methylene protons in the isobutyl groups are diastereotopic and give rise to an ABC spin system<sup>77</sup>. At  $-42^\circ\text{C}$



Scheme 8

two sets of doublets are observed for each methylene proton. Splitting pattern could be shown below where  $J_{AB}$  is 13 Hz and  $J_{AC}$  and  $J_{BC}$  are 5.4 Hz and 8.8 Hz.



When pyramidal inversion is rapid, at 72°C, there is the equivalent of a planar configuration at sulfur and the methylene protons are split only by the methine proton with  $J = 6.8$  Hz.

Activation parameters for the sulfur inversion process have recently been obtained for  $\text{Fe}(\text{C}_5\text{H}_4\text{S}-i\text{Bu})_2\text{PdX}_2$ ,

X = Cl, Br, from a total line shape analysis<sup>78</sup>. The  $\Delta G^\ddagger$  values are  $13.88 \pm 0.09$  and  $13.42 \pm 0.12$  kcal/mol for the chloride and bromide complex respectively. The difference in the energy barriers suggest that there is a measurable halogen trans-influence on the energy process.

Orrell proposes that the NMR spectral changes are due solely to sulfur inversion and that the bridge reversal of the palladium atom is fast on the NMR time scale even at  $-90^\circ\text{C}$ . In addition Orrell proposes that only one diastereoisomer is present and he favors the DL isomer as ring reversal is rapid. This is consistent with the crystallographic data as the DL isomer was the structure observed in the solid state. Variable temperature  $^{195}\text{Pt}$  NMR studies indicate that there are two diastereoisomers in a relative population of 10:1 at  $-35^\circ\text{C}$ . Only the major diastereoisomer however appears to be observed in the  $^1\text{H}$  NMR spectra.

Figure 9 shows the variable temperature  $^1\text{H}$  NMR spectra for the isobutyl platinum analog, (18). The same features are present as those in the palladium complex except that higher coalescence temperatures are observed for the platinum complex. This implies that the platinum complexes have a higher energy barrier than the palladium complexes and this suggests that the Pt-S bond is stronger than the Pd-S bond. Abel<sup>74a</sup> and Cross<sup>75b</sup> have observed a similar trend in other platinum and palladium derivatives.

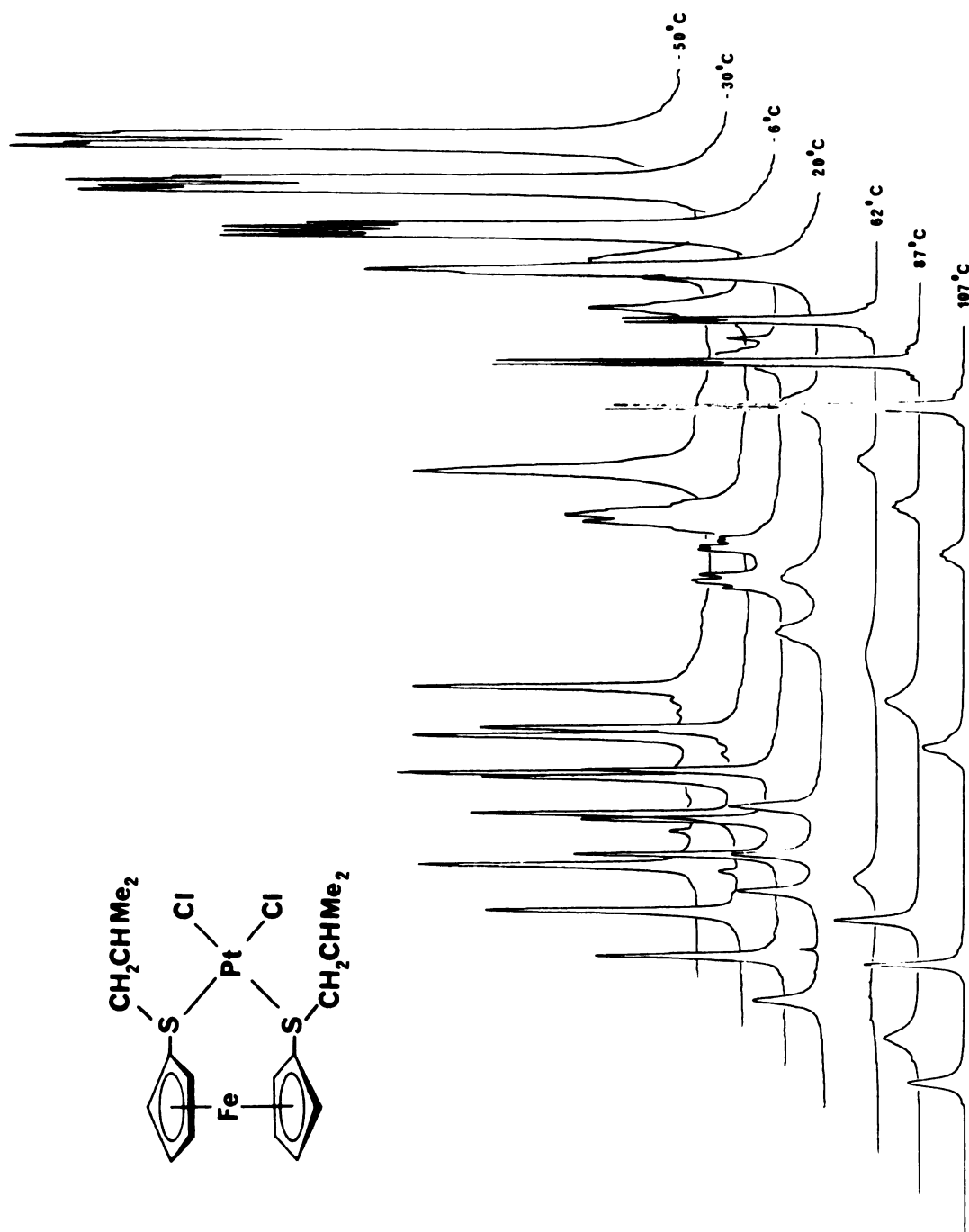


Figure 9. Variable temperature  $^1\text{H}$  NMR Spectra for  $\text{Fe}(\text{C}_5\text{H}_4\text{S}-i\text{Bu})_2\text{PtCl}_2$ .

The only significant difference between the dynamic NMR spectra of the palladium and platinum complexes occurs in the methylene region at low temperature. In the platinum complex the four sets of doublets which are visible at  $-6^{\circ}\text{C}$  appear to coalesce to give a single broad resonance at  $-50^{\circ}\text{C}$ . An explanation for this behavior awaits the results of Orrell's total line shape analysis.

Variable temperature  $^{13}\text{C}$  NMR data also suggests the presence of a dynamic process. The cyclopentadienyl ring carbon region is shown in Figure 10. At  $35^{\circ}\text{C}$  a sharp signal is observed for the substituted carbon,  $\text{C}_1$ , at 79.3 ppm and two broad signals are observed at 76.0 and 71.7 ppm for the  $\text{C}_{3,4}$  and  $\text{C}_{2,5}$  nuclei, respectively. The signal at 71.7 ppm coalesces at this temperature and at  $9^{\circ}\text{C}$  two separate signals are evident. The lower field signal at 76 ppm coalesces around  $-6^{\circ}\text{C}$  and gradually separates into two distinct signals. At  $-20.8^{\circ}\text{C}$  the carbon atoms in the alpha and beta positions,  $\text{C}_{2,5}$  and  $\text{C}_{3,4}$ , are magnetically non-equivalent and give rise to four separate signals. At  $-54.6^{\circ}\text{C}$  these four resonances are further split and now appear as four doublets. The signal due to the  $\text{C}_1$  carbon remains a sharp singlet with no indication of broadening from an overlapping signal. The additional splitting could be due to the sulfur inversion process, which is now slow on the NMR time scale, that produces diastereotopic carbon nuclei that are anisochronous.

Figure 10. Variable Temperature  $^{13}\text{C}$  NMR for  
 $\text{Fe}(\text{C}_5\text{H}_4\text{S-iBu})_2\text{PdCl}_2$  in Region from  
70-80 ppm.

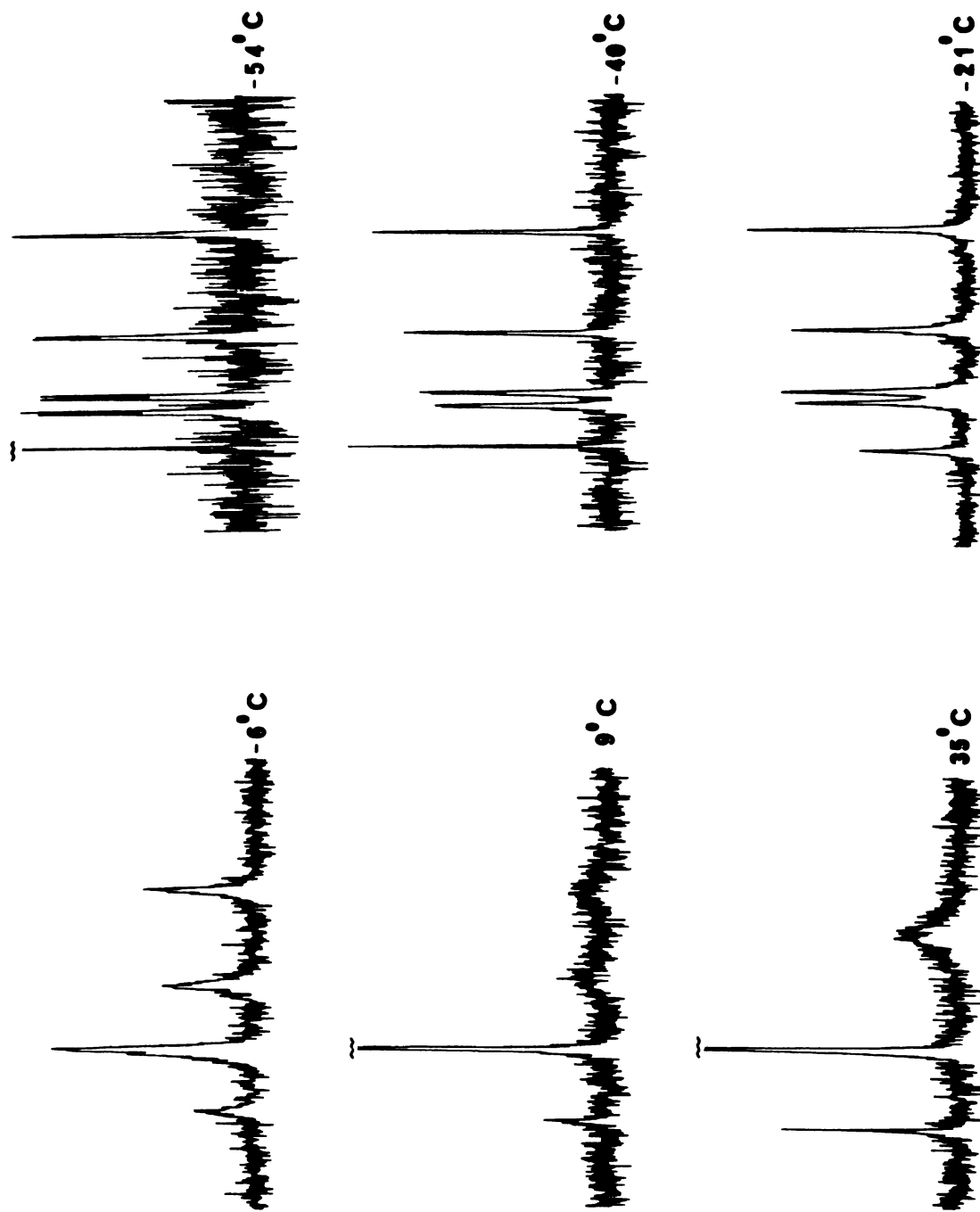


Figure 10.



8.  $^{195}\text{Pt}$  NMR

Table 15 contains the  $^{195}\text{Pt}$  NMR data for the ferrocenylsulfide complexes  $\text{Fe}(\text{C}_5\text{H}_4\text{SR})_2\text{PtX}_2$ ,  $\text{R} = \text{iBu}, \text{iPr}, \text{Ph}, \text{Bz}$ ;  $\text{X} = \text{Cl}, \text{Br}$  in chloroform- $\text{d}_1$  solutions at ambient temperature. The methylthioferrocene platinum complexes were too insoluble to obtain  $^{195}\text{Pt}$  NMR data.  $^{195}\text{Pt}$  ( $I = 1/2$ ) has a natural abundance of 33% and has roughly the same relative sensitivity as the  $^{13}\text{C}$  nucleus.

In Table 15 the  $^{195}\text{Pt}$  chemical shifts of the chloride complexes are found at 3,200 ppm whereas the bromide analogs are found 400 ppm further upfield. This is consistent with general trends where bromide complexes are found upfield of the chloride analogs<sup>79</sup>. As  $^{195}\text{Pt}$  chemical shifts are solvent and temperature dependent caution must be employed when data from different sources is compared.

1,1'-Bis(diphenylphosphino)ferroceneplatinumdichloride has a signal, a triplet with  $J_{\text{Pt-P}} = 3,374$  Hz due to coupling to two phosphorous atoms, about 1,100 ppm upfield from the corresponding ferrocenylsulfide complexes. This is consistent with previously reported data<sup>80</sup>, shown as the last two entries in Table 15, where the phosphine compound,  $[(\text{PMe}_3)_2\text{PtCl}_2]$ , is found about 900 ppm upfield from the sulfide complex,  $[(\text{SMe}_2)_2\text{PtCl}_2]$ . This suggests that sulfide ligands are weaker sigma donors than the phosphine analogs.

As  $^{195}\text{Pt}$  NMR is very sensitive to changes in the metal

Table 15.  $^{195}\text{Pt}$  NMR Data for Ferrocenylsulfideplatinum Complexes,  $\text{Fe}(\text{C}_5\text{H}_4\text{SR})\text{PtX}_2$ , R = iBu, iPr, Ph, Bz; X = Cl, Br. Measurements made in  $\text{CDCl}_3$  solution at room temperature.

Compound	Cl	Br
$\text{Fe}(\text{C}_5\text{H}_4\text{S-iBu})_2\text{PtX}_2$	-3,285 -3,353	-3,662 -3,759
$\text{Fe}(\text{C}_5\text{H}_4\text{S-iPr})_2\text{PtX}_2$	-3,253	-3,633
$\text{Fe}(\text{C}_5\text{H}_4\text{SPh})_2\text{PtX}_2$	-3,246	-3,658
$\text{Fe}(\text{C}_5\text{H}_4\text{SCH}_2\text{Ph})_2\text{PtX}_2$	-3,244	-3,622
$\text{Fe}(\text{C}_5\text{H}_4\text{PPh}_2)_2\text{PtCl}_2$	-4,374t	-----
cis- $[(\text{SMe}_2)_2\text{PtX}_2]^a$	-3,551	-3,879
cis- $[(\text{PMe}_3)_2\text{PtX}_2]^a$	-4,408	-4,636

<sup>a</sup>Obtained from Reference 80, measured in  $\text{CH}_2\text{Cl}_2$ .

coordination sphere we could expect to see two separate platinum resonances for the diastereoisomers obtained from slow inversion at the sulfur centers. For the isobutyl platinum compound, (18), two distinct signals, separated by 74 ppm, were observed at room temperature in a 17:1 ratio. Variable temperature measurements of this complex indicate that the relative populations of the diastereoisomers increase as the temperature decreases. Figure 11

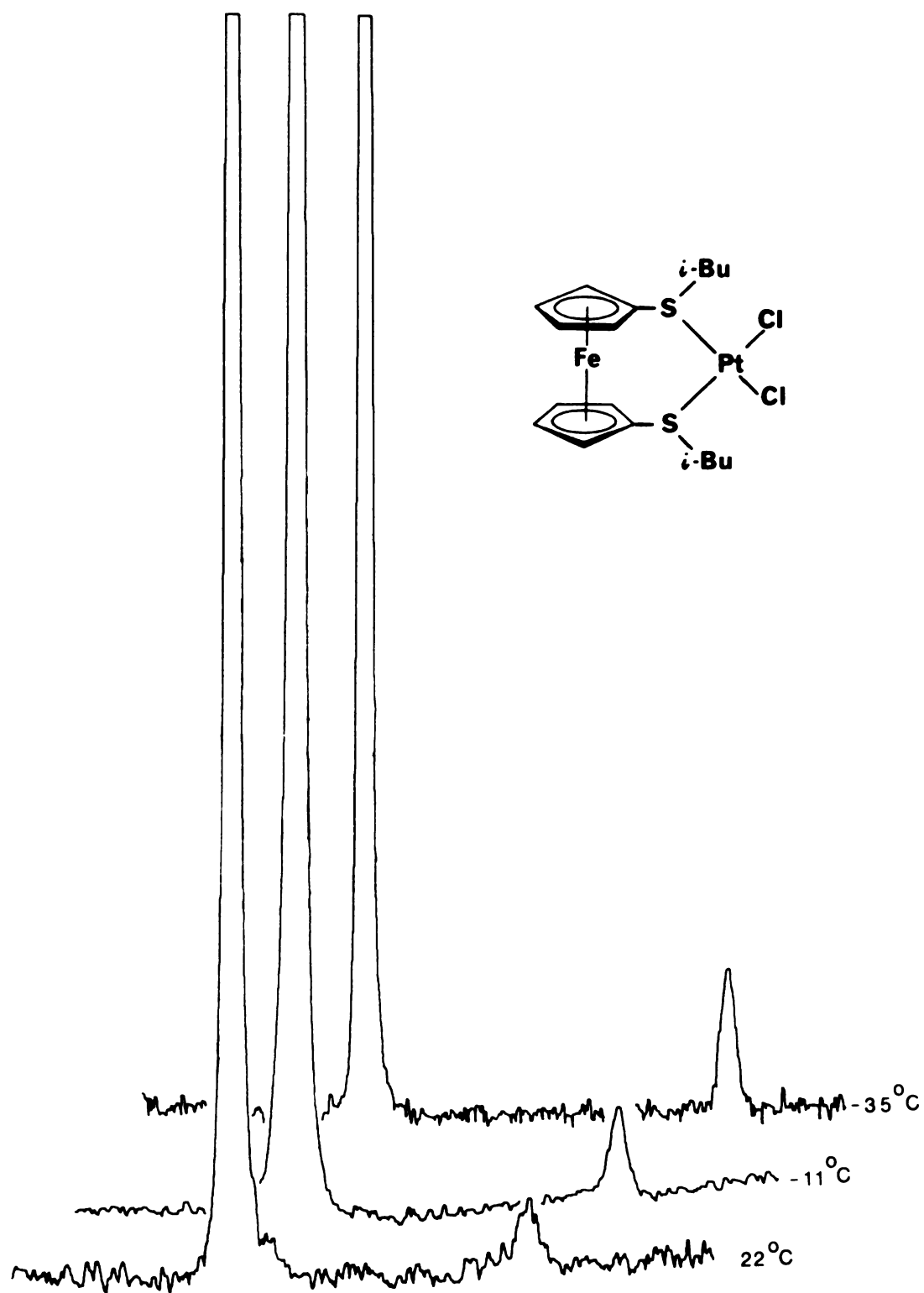


Figure 11. Variable Temperature  $^{195}\text{Pt}$  NMR Spectra for  $\text{Fe}(\text{C}_5\text{H}_4\text{S}-i\text{Bu})_2\text{PtCl}_2$ .

shows that at  $-35^{\circ}\text{C}$  two signals in an approximate 10:1 ratio were observed. A set of variable temperature data was also obtained for the isopropyl platinum compound, (22) and is presented in Figure 12. The spectrum at  $-10^{\circ}\text{C}$  indicates the presence of two diastereoisomers in a 70:1 ratio. This large ratio suggests that the isomer found upfield is very much a minor diastereoisomer. Pregosin<sup>81</sup> has observed two  $^{195}\text{Pt}$  resonances, separated by 51 ppm, for the two diastereoisomers of trans-dichloro-[(S)-N-methyl- $\alpha$ -methylbenzylamine](ethylene)platinum[II].

## 9. Electrochemistry

The electrochemistry of the complexes  $\text{Fe}(\text{C}_5\text{H}_4\text{SR})_2$  and  $\text{Fe}(\text{C}_5\text{H}_4\text{SR})_2\text{MCl}_2$  where  $\text{R} = \text{iBu}, \text{Ph}, \text{Me}$ ;  $\text{M} = \text{Pd}, \text{Pt}$  has been examined by cyclic voltammetry. All measurements were made in either DMF or  $\text{CH}_2\text{Cl}_2$  solutions with 0.1 M  $[\text{nBu}_4\text{N}][\text{ClO}_4]$  as a supporting electrolyte. A platinum "flag" electrode or a glassy carbon electrode was used as the working electrode and values were recorded relative to a standard calomel reference electrode (SCE). Sweep rates were varied from 100 mV/s to 200 mV/s over a potential range of +2.0 to -1.5 V.

Well defined, one-electron reversible redox waves were observed for the oxidation of the iron atom in the ferrocenylsulfide complexes, (9), (10), (12), and the platinum analogs in DMF and  $\text{CH}_2\text{Cl}_2$  solutions respectively.

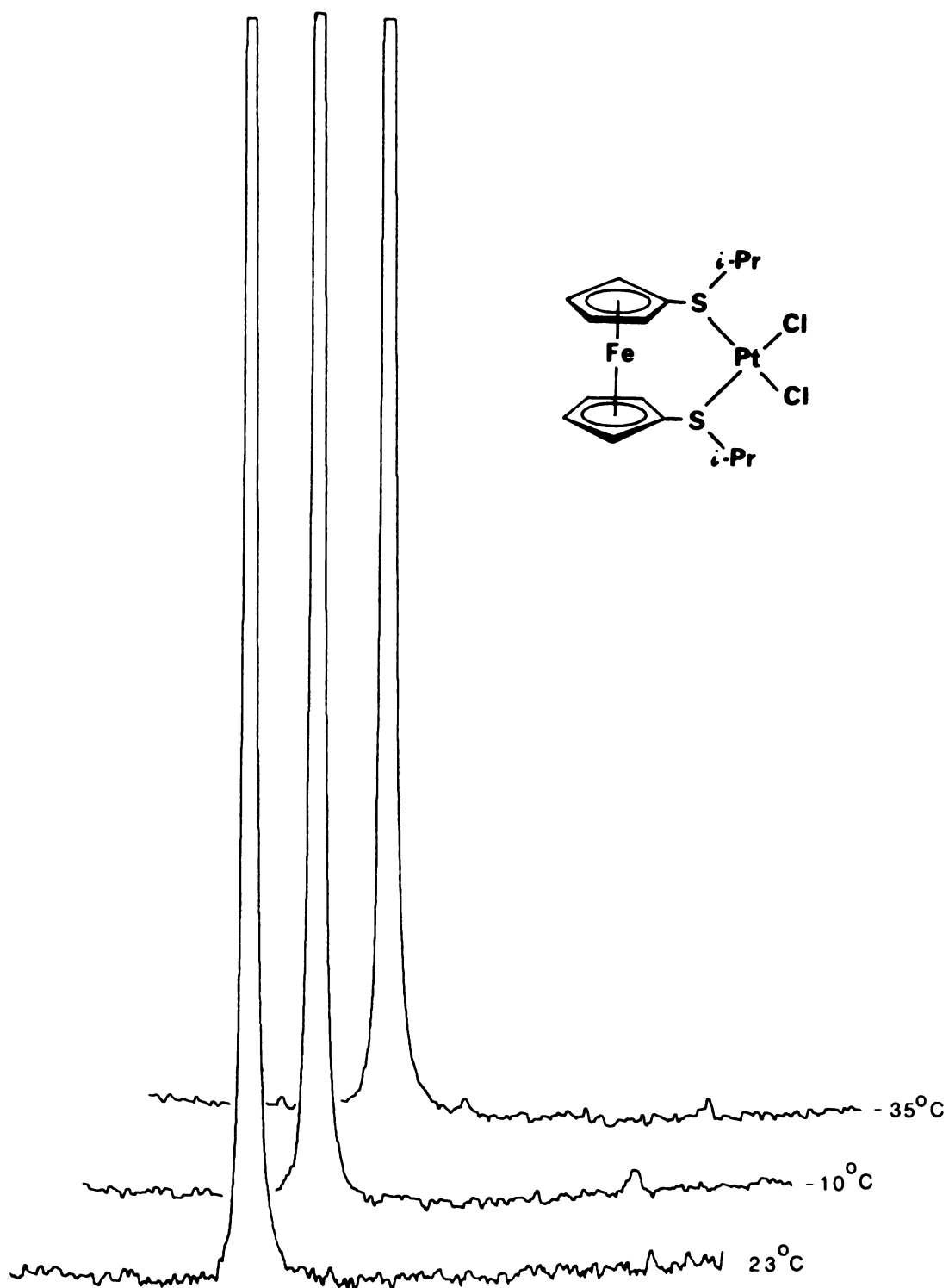


Figure 12. Variable Temperature  $^{195}\text{Pt}$  NMR Spectra for  $\text{Fe}(\text{C}_5\text{H}_4\text{S}-i\text{Pr})_2\text{PtCl}_2$ .

The palladium complexes, which are sparingly soluble in these solvents (especially the phenyl derivative), gave poorly defined redox waves with large peak separations. Representative cyclic voltammograms are shown in Figure 13.

Examination of the electrochemical data given in Table 16 indicates that  $E_{1/2}$  for the ferrocene ligands becomes increasingly positive in the order S-iBu < SMe < SPh < PPh<sub>2</sub>. This is consistent with ferrocene being stabilized by electron withdrawing substituents. Upon complexation to palladium or platinum,  $E_{1/2}$  for the ferrocenyl group increases by +0.4 to +0.59 V. This increase could be attributed to a through space electrostatic interaction with the positive charge on Pd or Pt or alternatively could be viewed as Pd or Pt withdrawing electron density from the ferrocenyl group through the sulfide bridges.

The theoretical difference in peak potentials for anodic and cathodic waves ( $\Delta E_p$ ) is 57 mV for a reversible one-electron process. This difference can however be affected by the cell design and the solvent. In Table 16 peak separations are as large as 350 mV. McCleverty<sup>82</sup> has reported peak separations of up to 230 mV for the reversible oxidation of Cr(CO)<sub>5</sub>L complexes, where L is a phosphine, in CH<sub>2</sub>Cl<sub>2</sub> solution. In addition Kotz<sup>83</sup> has reported a peak separation of 310 mV for the reversible system FcPPh<sub>2</sub> in CH<sub>2</sub>Cl<sub>2</sub> solution. Moreover, under the experimental conditions employed, ferrocene, a completely

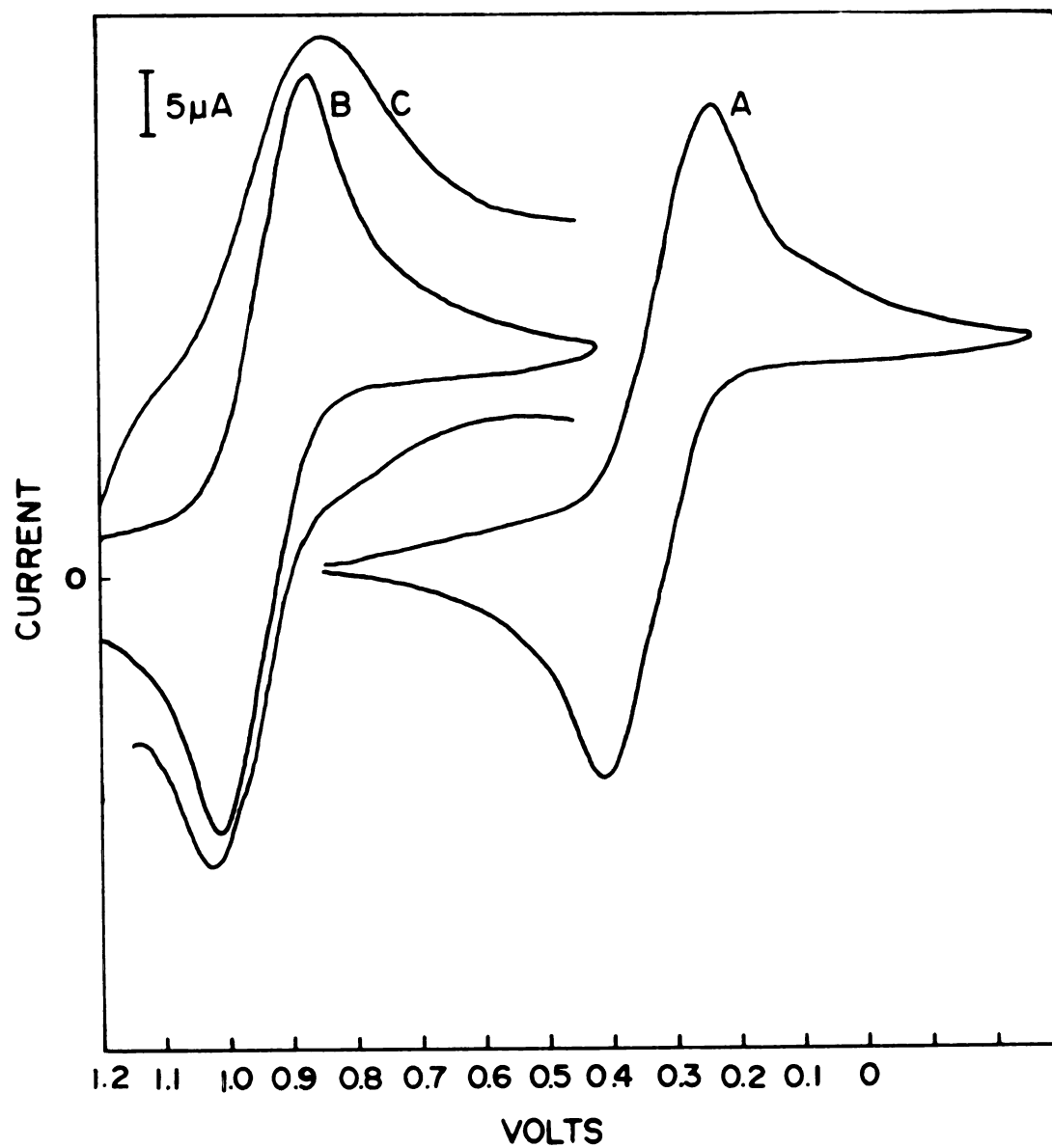


Figure 13. Cyclic Voltammograms of (A)  $\text{Fe}(\text{C}_5\text{H}_4\text{S-iBu})_2$ , (B)  $\text{Fe}(\text{C}_5\text{H}_4\text{S-iBu})_2\text{PtCl}_2$  and (C)  $\text{Fe}(\text{C}_5\text{H}_4\text{S-iBu})_2\text{-PdCl}_2$ .

Table 16. Cyclic Voltammetry Data for Ferrocenylsulfide Complexes.

Compound	$E_{1/2}$ (V) <sup>a</sup>	$\Delta E_p$ (mV) <sup>b</sup>	$i_c/i_a$ <sup>c</sup>	$E_{1/2}$ (V) <sup>a</sup>
$\text{Fe}(\text{C}_5\text{H}_5)_2$	0.34	250	1.00	
$\text{Fe}(\text{C}_5\text{H}_4\text{S}-i\text{Bu})_2$	0.33 0.37	170 150	0.96 0.97 <sup>d</sup>	
$\text{Fe}(\text{C}_5\text{H}_4\text{SMe})_2$	0.35 0.35	350 105	0.84 0.92 <sup>d</sup>	
$\text{Fe}(\text{C}_5\text{H}_4\text{SPh})_2$	0.52 0.56	125 200	1.03 <sup>e</sup> 0.93 <sup>d</sup>	
$\text{Fe}(\text{C}_5\text{H}_4\text{PPh}_2)_2$	0.52 0.53	120 120	0.64 0.45 <sup>e</sup>	
$\text{Fe}(\text{C}_5\text{H}_4\text{S}-i\text{Bu})_2\text{PdCl}_2$	0.94 0.86	175 145	0.88 0.78	-0.79 <sup>e</sup> -0.89 <sup>e</sup>
$\text{Fe}(\text{C}_5\text{H}_4\text{SMe})_2\text{PdCl}_2$	0.86	270	1.20	-0.66
$\text{Fe}(\text{C}_5\text{H}_4\text{SPh})_2\text{PdCl}_2$	0.85	360	----	(-1.45)
$\text{Fe}(\text{C}_5\text{H}_4\text{PPh}_2)_2\text{PdCl}_2$	0.93	120	0.93	-1.20
$\text{Fe}(\text{C}_5\text{H}_4\text{S}-i\text{Bu})_2\text{PtCl}_2$	0.94 0.94	180 145	1.01 1.00	-1.64 <sup>e</sup>
$\text{Fe}(\text{C}_5\text{H}_4\text{SMe})_2\text{PtCl}_2$	0.94 0.93	150 165	0.99 1.10	-1.50 <sup>e</sup>
$\text{Fe}(\text{C}_5\text{H}_4\text{SPh})_2\text{PtCl}_2$	1.03 1.06	135 165	1.03 0.97	-1.38 <sup>e</sup>
$\text{Fe}(\text{C}_5\text{H}_4\text{PPh}_2)_2\text{PtCl}_2$	0.92 0.93	145 160	1.04 1.03	-1.61 <sup>e</sup>

<sup>a</sup> $E_{1/2}$  values were calculated as the average of the cathodic and anodic peak potential. <sup>b</sup> $\Delta E_p$  is the difference between the cathodic and anodic peak. <sup>c</sup>Ratio of peak currents cathodic ( $i_c$ ) vs. ( $i_a$ ) anodic waves. <sup>d</sup>Measured in DMF/0.1 M  $n\text{-Bu}_4\text{NClO}_4$  at 25° at Pt electrode vs. SCE. Other measurements made in  $\text{CH}_2\text{Cl}_2$ . <sup>e</sup>Measured in  $\text{CH}_2\text{Cl}_2$ /0.1 M  $n\text{-Bu}_4\text{NClO}_4$  at glassy carbon electrode vs. SCE.



reversible system, has a peak separation of 250 mV. These results suggest that despite the large differences in cathodic and anodic peak potentials, ferrocenylsulfide complexes can be considered to undergo a chemically reversible one-electron process.

The sulfur complexes appear to adsorb on the platinum electrode as in some cases the platinum surface was discolored after use. This adsorption could account for the ratio of the cathodic and anodic current ( $i_c/i_a$ ) being less than unity, particularly for the free ligands, as voltammograms may exhibit enhancement of the peak currents in the presence of weakly adsorbed material<sup>84</sup>. The fact that  $i_c/i_a$  is close to unity suggests that the process is chemically reversible.

In the ferrocenyl platinum and palladium complexes an irreversible wave was observed at -0.6 to -1.64 V and has been attributed to  $\text{Pd}^{3/2+}$  or  $\text{Pt}^{3/2+}$ .  $E_{1/2}$  for platinum is more negative than the corresponding value for palladium and this is consistent with polarographic and voltammetric data obtained for palladium and platinum bis-1,2-dithiolene complexes<sup>85</sup>. The large negative  $E_{1/2}$  for palladium and platinum suggest that the ferrocenyl group is a strong electron donor.

Ferrocene itself has only recently been reduced electrochemically but ferrocene derivatives with electron-withdrawing groups, such as carboxy groups, are readily

reduced<sup>86</sup>. The large positive  $E_{1/2}$  value for  $\text{Fe}(\text{C}_5\text{H}_4\text{S-iBu})_2\text{-PdCl}_2$ , (16), suggests that the iron atom in this complex may be readily reduced. After a dimethoxyethane solution of (16) was stirred in the presence of a sodium amalgam for two days, the brown solution turned yellow and a fine metallic precipitate was observed. These results suggest that as the palladium atom was reduced the ferrocenyl-sulfide ligand was cleaved.

D.  $\text{Fe}(\text{C}_5\text{H}_4\text{SCSNR}_2)_2$  and  $\text{Fe}(\text{C}_5\text{H}_5)(\text{C}_5\text{H}_4\text{SCSNR}_2)$  (R = Me, Et, iPr)

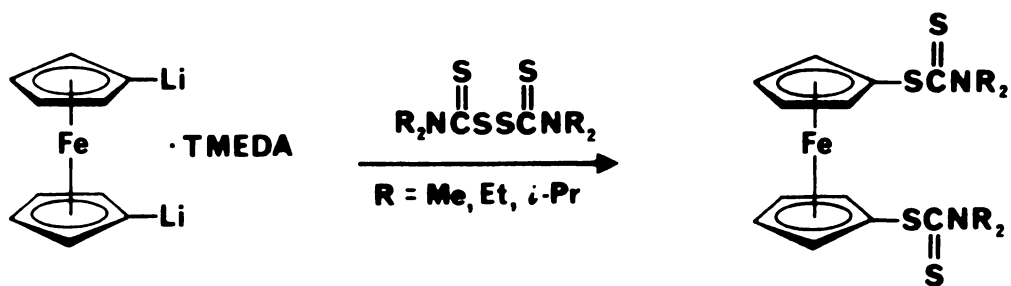
### 1. Preparation

Dithiocarbamates and thiuram disulfides have been used as fungicides, pesticides, vulcanization accelerators, antioxidants, flotation agents and high-pressure lubricants and as drugs in medicine<sup>87</sup>. In particular complexes of heavy metals with thiuram disulfides are effective fungicides and seed disinfectants. The rich and diverse chemistry of dithio acid and dithiolate complexes has been extensively covered in many reviews<sup>88</sup>.

Tetraalkylthiuram disulfides undergo nucleophilic attack at the disulfide linkage by cyanide ions, amines and Grignard reagents<sup>89</sup>. Recently Cava<sup>90</sup> reported that aryllithium derivatives react with tetraisopropylthiuram disulfide to give dithiocarbamate esters that were

precursors to aromatic thiols.

Reaction of dilithioferrocene with a series of tetraalkylthiuram disulfides gave rise to a high yield preparation of bis(dialkyldithiocarbamate)ferrocene derivatives. A solution of the tetraalkylthiuram disulfide was added slowly via cannula to a hexane slurry of dilithioferrocene which had been cooled to  $-78^{\circ}\text{C}$  (see Scheme 9).

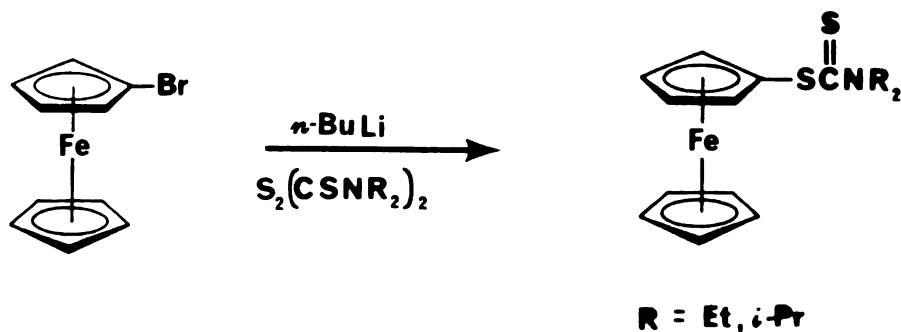


Scheme 9

In contrast to the results obtained by Cava only the desired product and no thioamide derivative was observed. The thioamide species arises from competing nucleophilic attack at the thione carbon rather than at the sulfur-sulfur bond in the tetraalkylthiuram disulfide.

A series of monosubstituted dialkyldithiocarbamate-ferrocene derivatives was also prepared by reaction of tetraalkylthiuram disulfide with lithioferrocene. Difficulty was encountered when lithioferrocene was prepared

from ferrocene and a mixture of *n*-butyllithium and TMEDA. Dimethyldithiocarbamateferrocene was isolated in 9% yield by using this procedure. At least six different products were observed when chromatography was employed in isolating the dimethyl derivative. One product, which was obtained from the second band on the column, has spectral data consistent with the binuclear complex, Fc-S-Fc, where two ferrocene moieties are linked through a sulfur atom. An alternative route where lithioferrocene is generated from bromoferrocene gave monosubstituted dialkyldithiocarbamateferrocene derivatives in 60-80% yields as shown in Scheme 10.



Scheme 10

On one occasion a very concentrated solution of bromoferrocene (about 2 g in 10 mL ether) was lithiated and after addition of tetraalkylthiuram disulfide, biferrocene which was identified by NMR and mass spectrometry was obtained.

Consistent results were obtained when dilute solutions of bromoferrocene were used.

## 2. $^1\text{H}$ NMR

$^1\text{H}$  NMR data for the dialkyldithiocarbamateferrocene derivatives, (38) - (43), is given in Table 17. The  $^1\text{H}$  NMR spectra of these complexes are very similar to the spectra obtained for the ferrocenylsulfide compounds in the previous section. Two apparent "triplets" are observed for the cyclopentadienyl ring protons that is consistent with an AA'BB' spin system. The "triplets" are slightly deshielded as anticipated for the electron withdrawing dithiocarbamate substituent.

The  $^1\text{H}$  NMR spectra for the mono and bis(diethyldithiocarbamate)ferrocene species are shown in Figure 14 and are identical except that a singlet at 4.22 ppm is observed for the unsubstituted cyclopentadienyl ring in the mono substituted ferrocene. Two separate signals are observed for the N,N-dialkyl protons due to restricted rotation around the carbamate C-N bond. This process will be examined more closely at a later stage.

## 3. $^{13}\text{C}$ NMR

The  $^{13}\text{C}$  NMR data for the dialkyldithiocarbamateferrocene complexes is presented in Table 18. During acquisition

Table 17.  $^1\text{H}$  NMR Data for  $\text{Fe}(\text{C}_5\text{H}_4\text{SCSNR}_2)_2$  and  $\text{Fe}(\text{C}_5\text{H}_5)(\text{C}_5\text{H}_4\text{SCSNR}_2)$  Complexes (R = Me, Et, iPr).

Compound	T $^\circ\text{C}$	H <sub>2,5</sub>	H <sub>3,4</sub>	C <sub>5</sub> H <sub>5</sub>	CH	CH <sub>2</sub>	CH <sub>3</sub>
$\text{Fe}(\text{C}_5\text{H}_4\text{SCSNMe}_2)_2$	22	4.50t	4.38t				3.48s 3.43s
$\text{Fe}(\text{C}_5\text{H}_4\text{SCSNEt}_2)_2$	22	4.52t	4.42s			3.99q 3.85q	1.39t 1.26t
$\text{Fe}(\text{C}_5\text{H}_4\text{SCSNIPr}_2)_2$	71	4.46t	4.38t		4.78m		1.47d
$\text{Fe}(\text{C}_5\text{H}_5)(\text{C}_5\text{H}_4\text{SCSNMe}_2)$	22	4.44t	4.34t	4.24s			3.51s 3.45s
$\text{Fe}(\text{C}_5\text{H}_5)(\text{C}_5\text{H}_4\text{SCSNEt}_2)$	22	4.42t	4.34t	4.22s		3.96q 3.82q	1.37t 1.23t
$\text{Fe}(\text{C}_5\text{H}_5)(\text{C}_5\text{H}_4\text{SCSNIPr}_2)$	59	4.40t	4.33t	4.20s	4.76m		1.48d

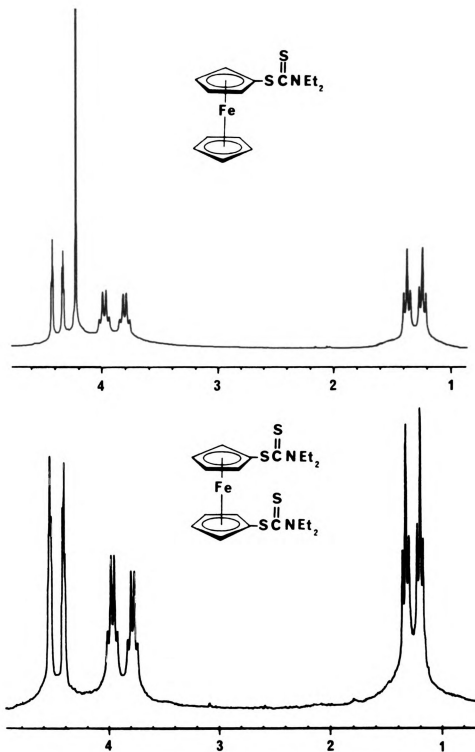


Figure 14.  $^1\text{H}$  NMR Spectra of  $\text{Fe}(\text{C}_5\text{H}_5)(\text{C}_5\text{H}_4\text{SCSNet}_2)$  (above) and  $\text{Fe}(\text{C}_5\text{H}_4\text{SCSNet}_2)_2$  (below).

Table 18.  $^{13}\text{C}$  NMR Data for  $\text{Fe}(\text{C}_5\text{H}_4\text{SCSNR}_2)_2$  and  $\text{Fe}(\text{C}_5\text{H}_5)(\text{C}_5\text{H}_4\text{SCSNR}_2)$  (R = Me, Et, iPr).  
Measured in  $\text{CH}_2\text{Cl}_2/\text{D}_2\text{O}$  solution at ambient temperature unless otherwise shown.

Compound	C=S	C <sub>1</sub>	C <sub>2,5</sub>	C <sub>3,4</sub>	C <sub>5</sub> H <sub>5</sub>	CH	CH <sub>2</sub>	CH <sub>3</sub>
$\text{Fe}(\text{C}_5\text{H}_4\text{SCSNMe}_2)_2$	199.7	76.7	77.4	72.0				45.3 41.7
$\text{Fe}(\text{C}_5\text{H}_4\text{SCSNEt}_2)_2$	197.5	76.1	77.2	71.6			49.4 46.9	12.5 11.2
$\text{Fe}(\text{C}_5\text{H}_4\text{SCSNIPr}_2)_2^{\text{a}}$	198.0	76.1	77.1	71.3		53.3		19.7
$\text{Fe}(\text{C}_5\text{H}_5)(\text{C}_5\text{H}_4\text{SCSNMe}_2)$	199.9	75.0	75.7	70.3	69.4			45.2 41.5
$\text{Fe}(\text{C}_5\text{H}_5)(\text{C}_5\text{H}_4\text{SCSNEt}_2)$	198.7	75.2	76.0	70.4	69.5		49.6 47.2	12.6 11.5
$\text{Fe}(\text{C}_5\text{H}_5)(\text{C}_5\text{H}_4\text{SCSNIPr}_2)^{\text{b}}$	198.0	75.2	76.0	70.2	69.4	54.1		19.9

<sup>a</sup>Measured at 45°C.

<sup>b</sup>Measured at 47°C.



of the  $^{13}\text{C}$  NMR data the parameters  $\text{PW} = 4 \mu\text{s}$  and  $\text{RD} = 4\text{s}$  were used as the thiocarbonyl carbon has a long relaxation time,  $T_1$ . The low field signal at 199 ppm is attributed to the thiocarbonyl.

Figure 15 displays an expansion of the region from 70-80 ppm for  $\text{Fe}(\text{C}_5\text{H}_4\text{S-iPr})_2$ ,  $\text{Fe}(\text{C}_5\text{H}_4\text{SCSNIPr}_2)_2$  and  $\text{Fe}(\text{C}_5\text{H}_5)(\text{C}_5\text{H}_4\text{SCSNEt}_2)$ . Tentative assignments have been made for the cyclopentadienyl ring carbons. In Figure 15(A) the  $\text{C}_1$  resonance is found downfield at 79.14 ppm whereas in Figure 15(B) and (C) the  $\text{C}_1$  resonance is found upfield of the  $\text{C}_{2,5}$  signal at 76.1 and 75.2 ppm respectively. The major difference between the spectra in Figure 15 is that the  $\text{C}_{2,5}$  resonance is deshielded in Figure 15(B) and (C) whereas in Figure 15(A) the  $\text{C}_{2,5}$  resonance is located at 70.96 ppm. The downfield shift in the dialkyldithiocarbamateferrocene derivatives could be due to the magnetic anisotropy of the thiocarbonyl group<sup>91</sup>. In Figure 15(C) the peak at 69.5 ppm is due to the unsubstituted cyclopentadienyl ring.

The  $^{13}\text{C}$  NMR spectra, shown in Figure 16, illustrate that the dialkyl groups exhibit two separate signals at room temperature. This phenomenon is due to the restricted rotation around the carbamate C-N bond and will be discussed in detail later.

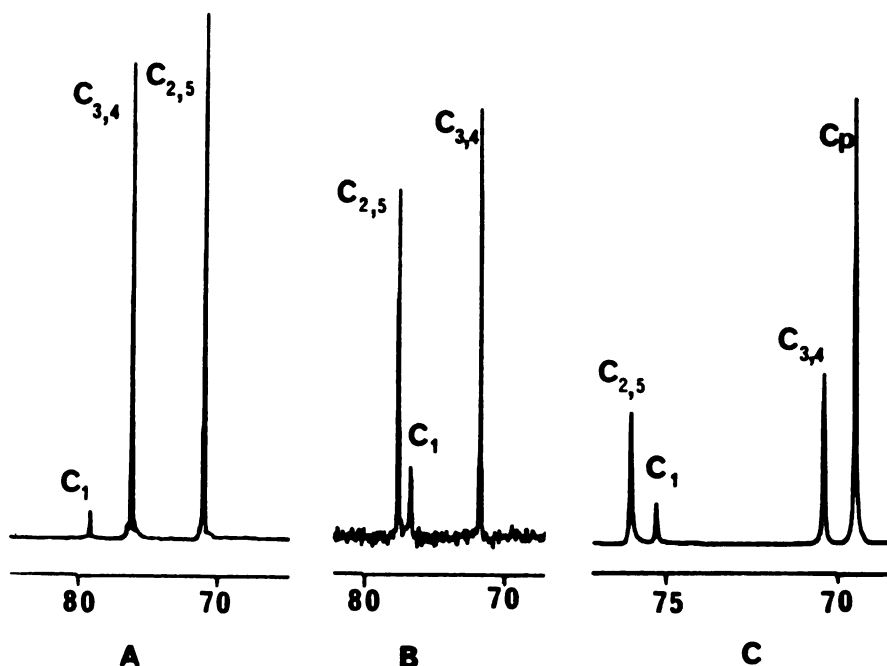


Figure 15.  $^{13}\text{C}$  NMR Spectra of (A)  $\text{Fe}(\text{C}_5\text{H}_4\text{S-iPr})_2$ , (B)  $\text{Fe}(\text{C}_5\text{H}_4\text{SCSNiPr}_2)_2$  and (C)  $\text{Fe}(\text{C}_5\text{H}_5)(\text{C}_5\text{H}_4\text{SCSNEt}_2)$ .

#### 4. Ultraviolet and Visible Spectra

Table 19 contains the absorption spectra of the dialkyl-dithiocarbamateferrocene derivatives. The absorption maxima are identical for the corresponding mono and bis-substituted ferrocene complexes except that the extinction coefficients for the bands centered at 270 and 240 nm are significantly lower for the monosubstituted species as shown in Figure 17.

Tentative assignments of the absorption maxima have been made. The band centered around 430 nm ( $\epsilon = 350 \text{ M}^{-1}\text{cm}^{-1}$ ) which corresponds to the d-d transition observed in ferrocene

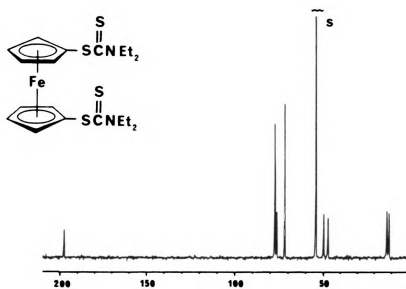
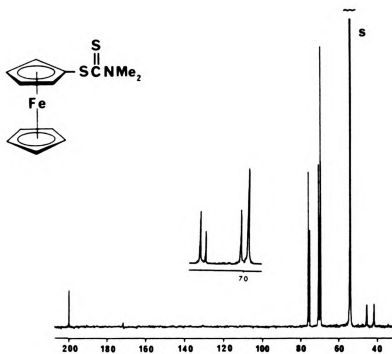


Figure 16.  $^{13}\text{C}$  NMR Spectra of  $\text{Fe}(\text{C}_5\text{H}_5)(\text{C}_5\text{H}_4\text{SCSMe}_2)$  (above) and  $\text{Fe}(\text{C}_5\text{H}_4\text{SCSEt}_2)_2$  (below).

Table 19. Electronic Absorption Spectra of  $\text{Fe}(\text{C}_5\text{H}_4\text{SCSNR}_2)_2$  and  $\text{Fe}(\text{C}_5\text{H}_5)(\text{C}_5\text{H}_4\text{SCSNR}_2)$  ( $\text{R} = \text{Me}, \text{Et}, \text{iPr}$ ) at  $24^\circ\text{C}$  in MeCN solution at approx. conc.  $8.0 \times 10^{-5} \text{ M}$ .

R	$\text{Fe}(\text{C}_5\text{H}_4\text{SCSNR}_2)_2$		$\text{Fe}(\text{C}_5\text{H}_5)(\text{C}_5\text{H}_4\text{SCSNR}_2)$	
	$\lambda_{\text{max}}$ (nm)	$\epsilon$ ( $\text{M}^{-1}\text{cm}^{-1}$ )	$\lambda_{\text{max}}$ (nm)	$\epsilon$ ( $\text{M}^{-1}\text{cm}^{-1}$ )
Me	430	360	437	410
	273	17400	272	12900
	241	24100	239sh	17000
	220	30000	210	30000
Et	435	380	435	300
	276	17200	274	12800
	245	25500	245	16900
	223sh	29700		
	205sh	32400	210	30000
iPr	437	370	437	310
	279	13500	274	12800
	248	22100	247	14300
	227	25600		
	205	31600	210	30000

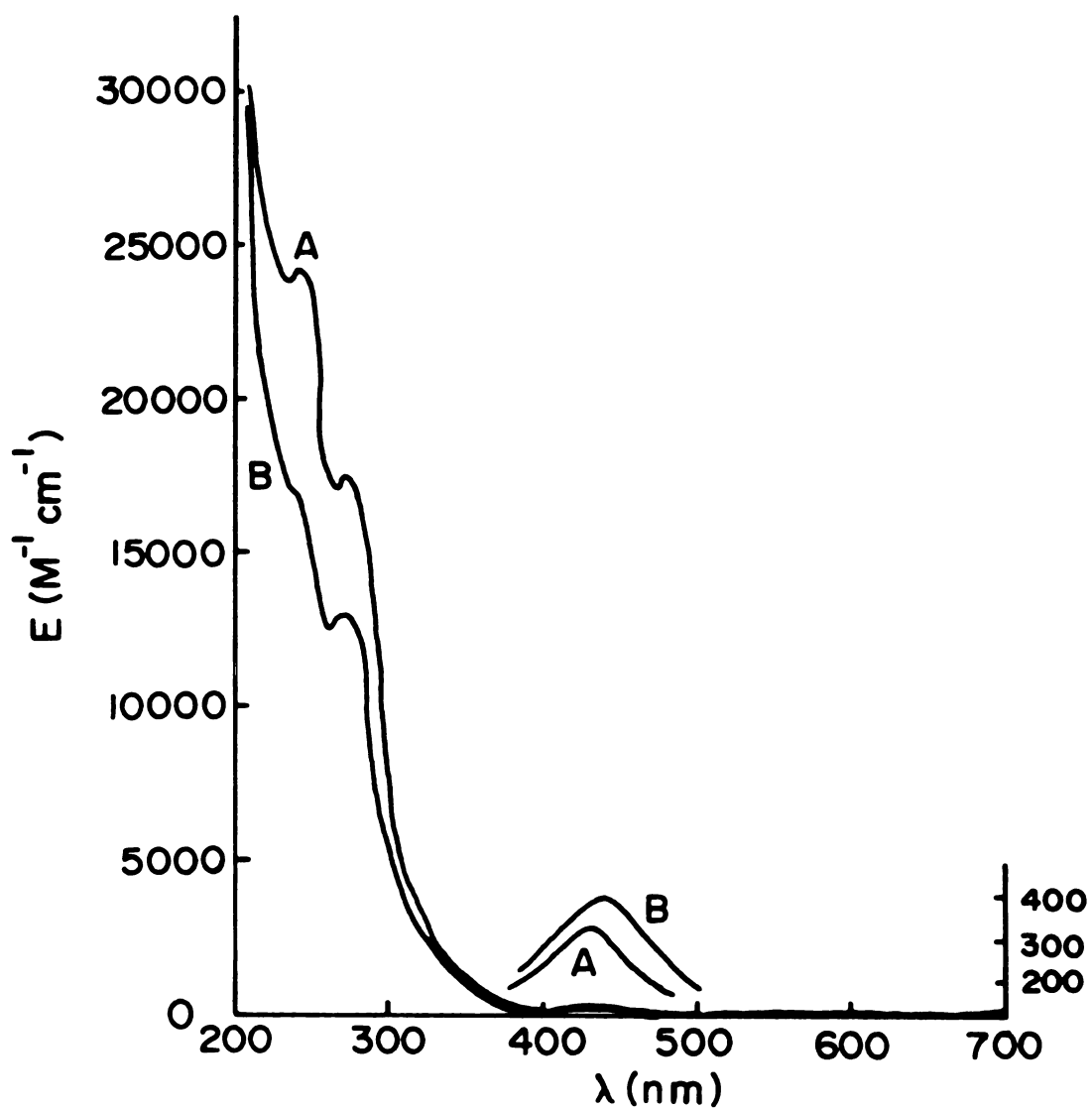
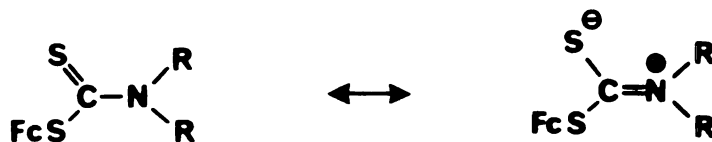


Figure 17. Ultraviolet-visible Spectra for (A)  $Fe(C_5H_4SCSNMe_2)_2$  and (B)  $Fe(C_5H_5)(C_5H_4SCSNMe_2)$ .

at 440 nm is very slightly blue shifted compared to ferrocene. Two well defined maxima at 270 and 240 nm are characteristic of dithiocarbamates and have been assigned as intraligand transitions<sup>92</sup>. The band at 272 - 279 nm ( $\epsilon \sim 10^4$ ) could be assigned to a  $n \rightarrow \sigma^*$  transition whereas the band at 239 - 248 nm ( $\epsilon \sim 10^4$ ) could be a  $\pi \rightarrow \pi^*$  transition. The high energy band located at 210 nm ( $\epsilon \sim 30,000$ ) is probably a ligand-to-metal charge-transfer band associated with ferrocene<sup>65</sup>.

### 5. Dynamic NMR Studies

Two resonance forms possible for the dialkyldithiocarbamateferrocene complexes are shown below.



The second resonance form introduces a degree of double bond character into the carbon-nitrogen bond which prevents free rotation around the C-N bond.

The  $^1\text{H}$  NMR and  $^{13}\text{C}$  NMR data in Table 17 and Table 18 respectively indicate that two separate signals are observed for the N,N-dialkyl protons for the methyl and ethyl dithiocarbamateferrocene derivatives, (38), (39), (41) and (42) at room temperature. When the temperature is raised

the two N,N-dialkyl signals coalesce and as the fast exchange limit is approached they sharpen to a single peak. The protons on the cyclopentadienyl rings show no variation with temperature.

The behavior of the alkyl protons is due to the restricted rotation around the carbamate C-N bond and a rough approximation of the barrier to rotation about this bond has been determined.

NMR parameters, rate constants and an approximate value of the barrier to rotation in compounds (38), (39), (41) and (42) are given in Table 20. The rate constant,  $k_c$ , at the coalescence temperature,  $T_c$ , was determined from the peak separation,  $\delta\nu$ , at slow exchange using equation  $k_c = \pi\delta\nu/\sqrt{2}$  or  $k_c = \pi[\delta\nu^2 + 6J^2]^{1/2}/\sqrt{2}$  for coupled systems<sup>93</sup>. An approximate rotational free energy barrier was obtained from the Eyring equation:  $\Delta G^\ddagger = 2.3RT[10.3 - \log(k_c/T_c)]$ . The values of the rotational barriers lie in a fairly narrow range from 15.75 to 16.15 kcal/mol and appear to be independent of the nature of the alkyl group.

Holloway<sup>94</sup> has determined rotational barriers about the carbamate C-N bond in a series of N,N-dialkyldithiocarbamate esters. Activation energies of 10 to 12 kcal/mol suggested that an appreciable amount of C-N double bond character was present. Holloway was able to correlate the C-N double bond character with the "thioureide" band between 1489 and 1498  $\text{cm}^{-1}$  in the infrared region. The "thioureide" band which

Table 20. NMR Parameters, Kinetic and Infrared Data for  $\text{Fe}(\text{C}_5\text{H}_4\text{SCSNR}_2)_2$  and  $\text{Fe}(\text{C}_5\text{H}_5)(\text{C}_5\text{H}_4\text{SCSNR}_2)$  where  $\text{R} = \text{Me}, \text{Et}$ .

	$\delta\nu$ (Hz)	$k_c$ ( $\text{s}^{-1}$ )	$T_c$ (K)	$\Delta G^\ddagger$ (kcal/mol)	IR ( $\text{cm}^{-1}$ )
$\text{Fe}(\text{C}_5\text{H}_4\text{SCSNMe}_2)_2$	16.48	36.61	314	16.15	1480
$\text{Fe}(\text{C}_5\text{H}_4\text{SCSNEt}_2)_2$	43.95	104.24	319	15.75	1480
$\text{Fe}(\text{C}_5\text{H}_5)(\text{C}_5\text{H}_4\text{SCSNMe}_2)$	17.70	39.32	312	16.00	1475
$\text{Fe}(\text{C}_5\text{H}_5)(\text{C}_5\text{H}_4\text{SCSNEt}_2)$	31.74	79.40	320	15.98	1480

has been assigned to the partial double character in the carbon-nitrogen bond was observed at  $1480 \text{ cm}^{-1}$  in the dialkyldithiocarbamateferrocene derivatives as shown in Table 20.

The variable temperature  $^1\text{H}$  NMR spectra for the isopropyl derivatives, ( $\text{40}$ ) and ( $\text{43}$ ), are considerably more complex and are shown in Figures 18 and 19 respectively. The NMR spectra for the mono and bisdiisopropyldithiocarbamateferrocene derivatives are very similar which suggests that in the disubstituted species the dithiocarbamate groups are on opposite sides and act independently of each other.

Various groups have studied methyl N,N-diisopropyldithiocarbamate,  $\text{MeSCSNiPr}_2$ <sup>95-98</sup>, and have concluded that



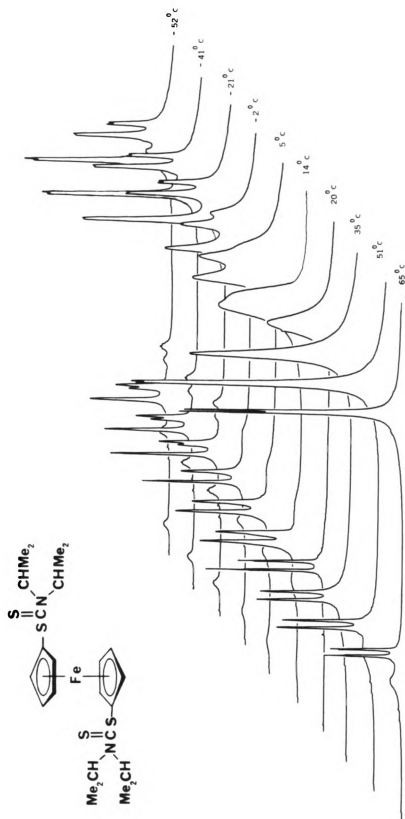


Figure 18. Variable temperature  $^1\text{H}$  NMR Spectra of  $\text{Fe}(\text{C}_5\text{H}_4\text{SCSNIPr}_2)_2$ .

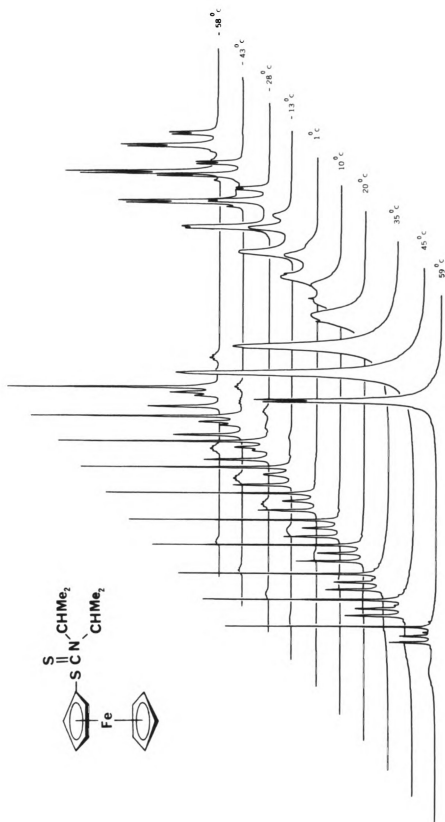


Figure 19. Variable temperature  $^1\text{H}$  NMR Spectra of  $\text{Fe}(\text{C}_5\text{H}_5)(\text{C}_5\text{H}_4\text{SCSNCMe}_2)_2$ .

hindered rotation occurs around the carbamate C-N bond and the isopropyl-nitrogen bonds. Similar processes seem to occur in the ferrocene derivatives. Figures 18 and 19 indicate that at high temperature the  $^1\text{H}$  NMR spectrum consists of a septet for the methine protons, a doublet for the isopropyl methyl groups and the signals associated with the ring protons. This spectrum is consistent with rapid rotation around the carbamate C-N and isopropyl-nitrogen bonds. As the temperature is lowered the signals broaden and at the slow exchange limit there are four methine septets and three methyl doublets clearly visible.

The low temperature spectra can be interpreted in terms of a mixture of the two conformers A and B which exist in different relative populations (see Figure 20). Conformer A is the preferred conformer as in conformer B there is significant interaction between the isopropyl methyl groups and the bulky ferrocene. Integration of the methine septets suggest that conformer A and conformer B are present in a 2.1:1 ratio.

Tentative assignments which are based on the magnetic anisotropy of the thiocarbonyl group are shown in Figure 21. The lowest field septet is assigned to  $\text{H}_c$  - the proton adjacent to the thiocarbonyl. The next lowest field septet is attributed to  $\text{H}_a$  which is adjacent to the C-SFc bond. The high field septets are assigned to  $\text{H}_d$  and  $\text{H}_b$ . Assignment of the isopropyl methyl resonances are extremely

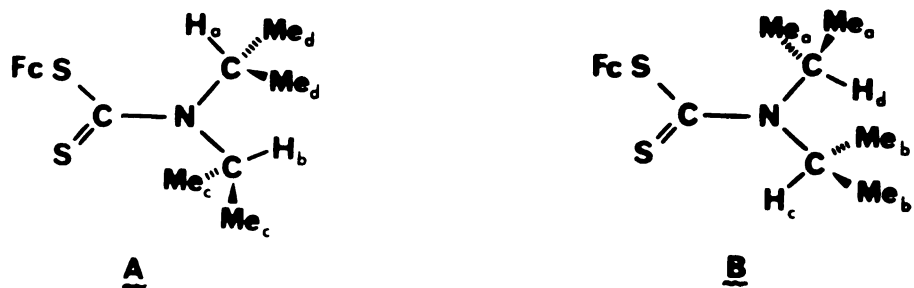


Figure 20. Conformers A and B of  $\text{Fe}(\text{C}_5\text{H}_5)(\text{C}_5\text{H}_4\text{SCSNiPr}_2)$ .

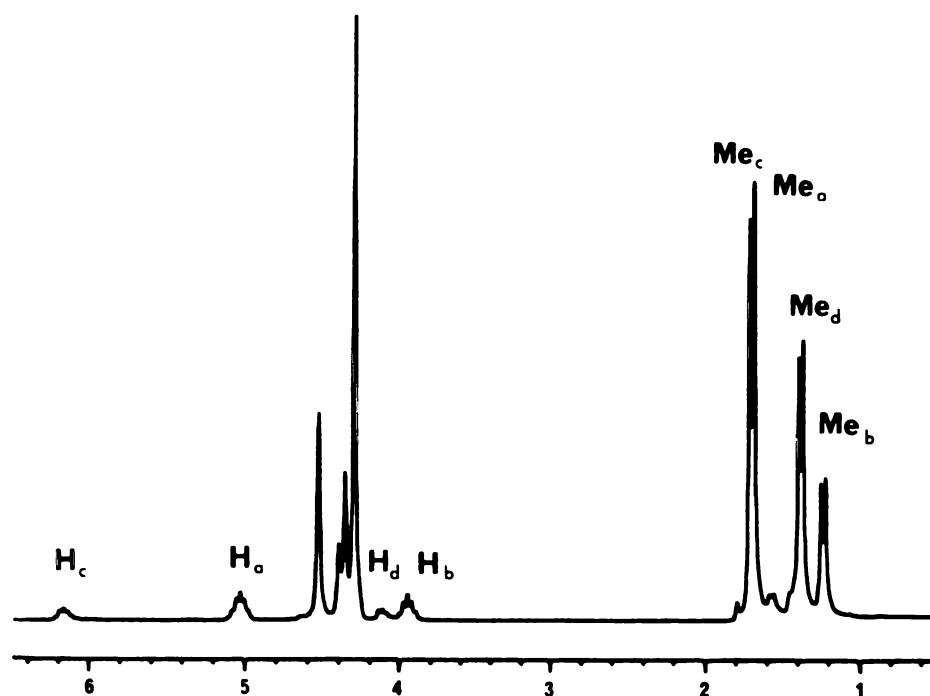


Figure 21. Slow exchange  $^1\text{H}$  NMR Spectrum of  $\text{Fe}(\text{C}_5\text{H}_5)(\text{C}_5\text{H}_4\text{SCSNiPr}_2)$ .

tentative especially since only three of the four methyl doublets are clearly visible. Spin decoupling experiments are necessary to provide more unambiguous assignments. Close examination of the isopropyl methyl region suggests that a third conformer is present in low concentration as has been observed in the  $\text{MeSCSNiPr}_2$  complex<sup>95,97</sup>. A resolution enhanced spectrum of the isopropyl methyl region is shown in Figure 22 and this clearly shows the presence of the third conformer.

The dynamic NMR studies suggest that in the methyl and ethyldithiocarbamateferrocene derivatives carbamate C-N bond rotation is observed whereas in the isopropyl analogs isopropyl-nitrogen bond rotation predominates. Sandström<sup>96</sup> has performed molecular mechanics calculations on  $\text{MeSCSNiPr}_2$  and has determined that the isopropyl groups rotate non-synchronously.

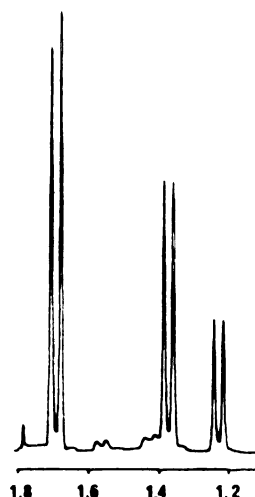
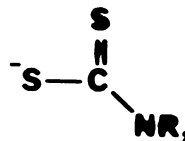
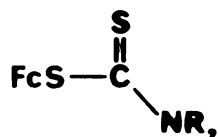


Figure 22. Resolution Enhanced  $^1\text{H}$  NMR Spectrum of  $\text{Fe}(\text{C}_5\text{H}_5)(\text{C}_5\text{H}_4\text{SCSNiPr}_2)$  at Slow Exchange.

6. Metal Complexes of  $\text{Fe}(\text{C}_5\text{H}_4\text{SCSNET}_2)_2$  and  $\text{Fe}(\text{C}_5\text{H}_5)-$   
 $(\text{C}_5\text{H}_4\text{SCSNET}_2)$

The dialkyldithiocarbamateferrocene derivatives, (38) to (43), are very similar to the ubiquitous dithiocarbamate ligands except that the ferrocene derivatives are neutral.



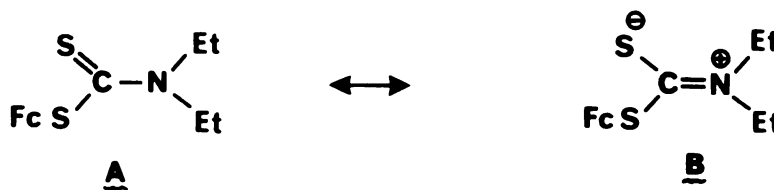
The dithiocarbamate ligand forms many metal complexes with many interesting properties such as a broad range of oxidation states<sup>88</sup>. The similarity between the dithiocarbamate ligands and the ferrocene derivatives led to the investigation of the preparation of palladium complexes of the ethyl derivatives, (39) and (42).

A benzene solution of bis(benzonitrile)palladiumdichloride was slowly added to a benzene solution of either complex (39) or compound (42). A red brown precipitate that formed immediately was filtered, washed with benzene and dried. The palladium complex obtained from  $\text{Fe}(\text{C}_5\text{H}_4\text{SCSNET}_2)_2$ , (39), was slightly soluble in methylene chloride but seemed to form a metallic film on the bottom of the flask on standing. Even though high dilution reaction conditions were employed there was probably an appreciable amount of polymeric product formed as the palladium could coordinate to two dithiocarbamate

moeities on different ferrocene units.

The palladium complex derived from  $\text{Fe}(\text{C}_5\text{H}_5)(\text{C}_5\text{H}_4\text{SCSNET}_2)$  was soluble in methylene chloride and nitromethane. Attempts to characterize the metal complex were not very successful. The  $^1\text{H}$  NMR spectrum, measured in nitromethane- $\text{d}_3$  solution, consisted of broad, featureless peaks which were not very informative. Attempts to obtain  $^{13}\text{C}$  NMR data failed as over a period of time a brown film coated the walls of the NMR tube. This was unfortunate as an upfield shift of the thiocarbonyl resonance would confirm that the palladium atom complexed to the thiocarbonyl sulfur<sup>99</sup>.

Infrared is helpful in characterizing the palladium complex and three specific regions are particularly helpful. As noted previously,  $\text{Fe}(\text{C}_5\text{H}_5)(\text{C}_5\text{H}_4\text{SCSNET}_2)$  displays an absorption at  $1480\text{ cm}^{-1}$  which has been described as the "thioureide" vibration and is attributed to the carbamate  $\nu(\text{C}-\text{N})$  mode. This region of the infrared is shown in Figure 23 for the free ligand, (42) and the palladium complex. In the palladium compound the "thioureide" vibration is found at  $1550\text{ cm}^{-1}$ . This shift to higher frequencies can be correlated with an increase in the double bond character of the carbamate C-N bond (structure B in Scheme 11).



Scheme 11

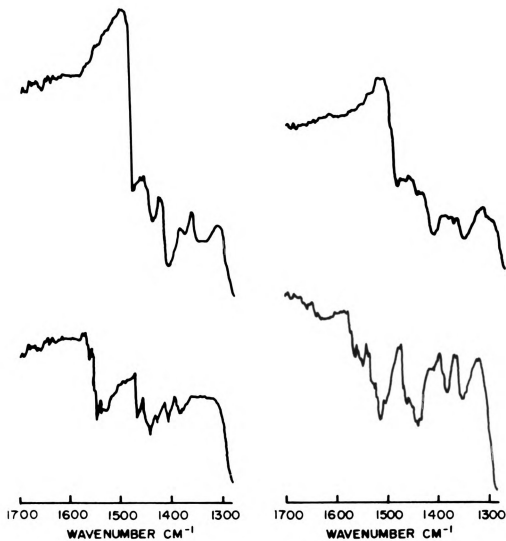


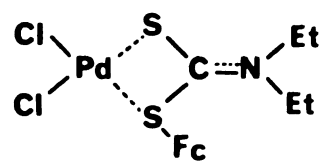
Figure 23. Infrared Spectra of (A)  $\text{Fe}(\text{C}_5\text{H}_5)(\text{C}_5\text{H}_4\text{SCSNET}_2)$  and (B) Pd complex; (C)  $\text{Fe}(\text{C}_5\text{H}_4\text{SCSNET}_2)_2$  and (D) Pd complex.



The second infrared region, between 950 and 1050  $\text{cm}^{-1}$ , is associated with the  $\nu(\text{CSS})$  vibrations and has been used to differentiate between monodentate and bidentate dithiocarbamate ligands. The compound,  $\text{Fe}(\text{C}_5\text{H}_5)(\text{C}_5\text{H}_4\text{SCSNEt}_2)$ , exhibits two bands at 1005  $\text{cm}^{-1}$  and 980  $\text{cm}^{-1}$  in this region. On the basis of Bonati and Ugo's work<sup>100</sup> the strong band at 980  $\text{cm}^{-1}$  can be assigned to an uncomplexed C=S stretch. In the palladium complex the presence of only one band at 1000  $\text{cm}^{-1}$  in this region suggests that palladium coordinates to the thiocarbonyl group. Caution must be observed as absorption from the ferrocene moiety is found in this region around 1000  $\text{cm}^{-1}$ . Many studies have supported the use of the bands in the 950 to 1050  $\text{cm}^{-1}$  region to ascertain if the dithiocarbamate ligand is monodentate or bidentate<sup>101,102</sup>. (See Figures 24 and 25 for corresponding infrared spectra.)

The third diagnostic region, between 300 and 400  $\text{cm}^{-1}$ , is associated with M-S vibrations. A broad absorption at 367  $\text{cm}^{-1}$  could be assigned to the Pd-S stretch whereas the two strong absorptions at 323 and 300  $\text{cm}^{-1}$  are probably associated with a Pd-Cl stretch.

On the basis of the infrared analysis a tentative structure for the palladium complex is shown below in Scheme 12. A crystallographic study is required before the coordination mode of  $\text{Fe}(\text{C}_5\text{H}_5)(\text{C}_5\text{H}_4\text{SCSNEt}_2)$  is definitely known.



Scheme 12.

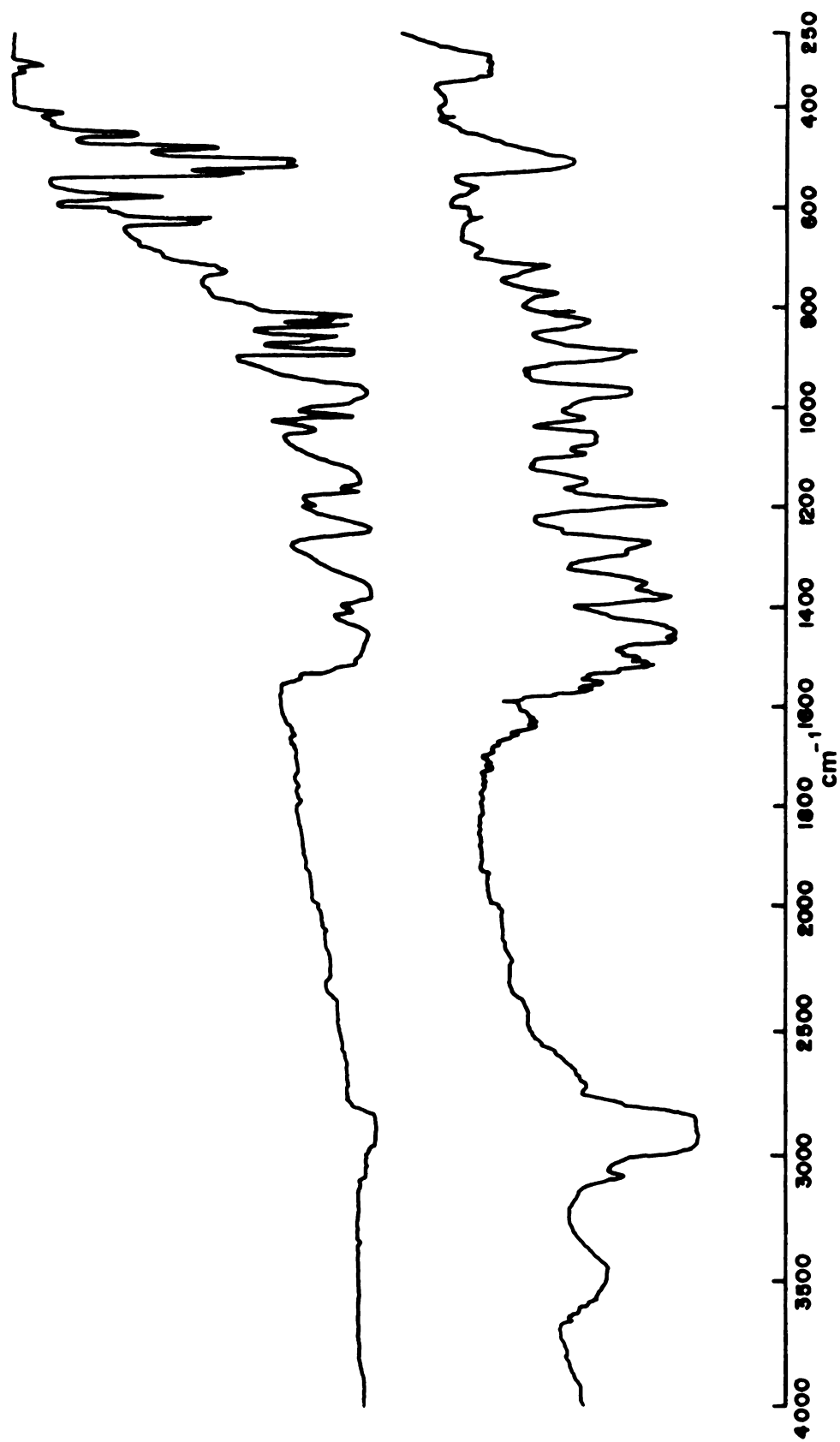


Figure 24. Infrared Spectra of  $\text{Fe}(\text{C}_5\text{H}_4\text{SCSNET}_2)_2$  (above) and  $\text{Fe}(\text{C}_5\text{H}_4\text{SCSNET}_2)_2\text{PdCl}_2$  (below).

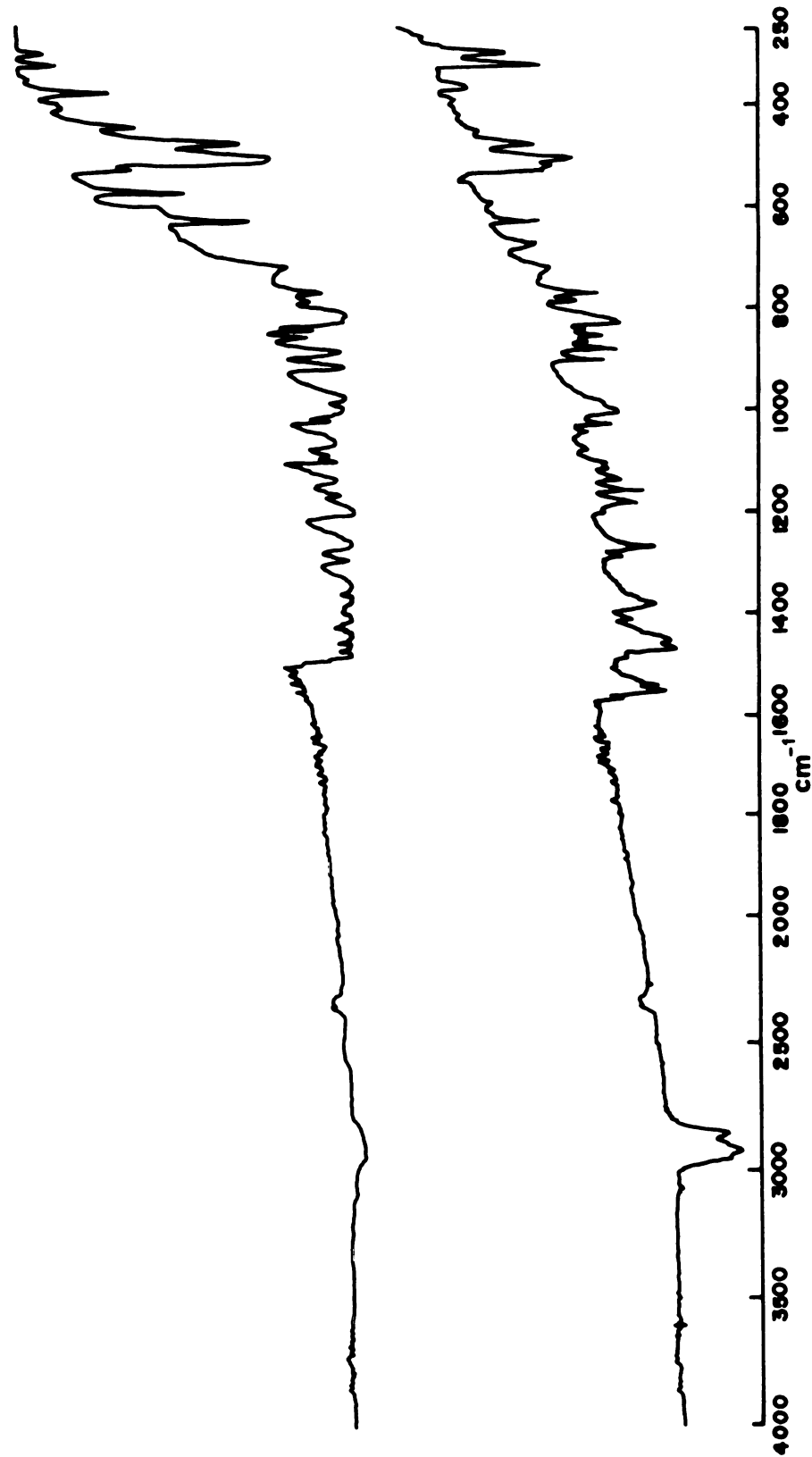


Figure 25. Infrared Spectra of Fe(C<sub>5</sub>H<sub>5</sub>)(C<sub>5</sub>H<sub>4</sub>SCSNET<sub>2</sub>) (above) and Fe(C<sub>5</sub>H<sub>5</sub>)(C<sub>5</sub>H<sub>4</sub>SCSNET<sub>2</sub>)-PdCl<sub>2</sub> (below).

PART B

TRIS(CYCLOPENTADIENYL)ZIRCONIUM DERIVATIVES

## I. INTRODUCTION

Atwood recently reported the crystal structure of tetra-(cyclopentadienyl)hafnium<sup>103</sup> and indicated that the structure of  $\text{Cp}_4\text{Hf}$  contrasted sharply with the zirconium analog,  $\text{Cp}_4\text{Zr}$ <sup>104</sup>. The hafnium complex has two  $\sigma$ -bonded and two  $\pi$ -bonded cyclopentadienyl rings whereas the zirconium species has one  $\sigma$  and three  $\pi$ -bonded cyclopentadienyl rings. This difference in structure prompted the investigation of tris-(cyclopentadienyl)zirconium derivatives. Despite the interest in bis(cyclopentadienyl)zirconium derivatives<sup>105</sup> complexes of tris(cyclopentadienyl)zirconium are relatively unknown. Russian workers<sup>106</sup> have briefly mentioned  $(\text{C}_5\text{H}_4\text{CH}_3)_3\text{ZrCl}$  and Samuel<sup>107</sup> has reported that reaction of  $\text{Cp}_2\text{ZrCl}_2$  with  $\text{NaCp}$  gave rise to  $(\text{Cp}_2\text{ZrCl})_2\text{O}$ . This product was due to the reaction conditions employed and the extreme hydrolytic instability of the tris(cyclopentadienyl)zirconium species.

Recently Russian workers<sup>108</sup> reported a vibrational analysis of  $\text{Cp}_3\text{MH}$ , where  $\text{M} = \text{Zr}, \text{Hf}$ , and concluded that the three cyclopentadienyl rings are identically  $\pi$ -bonded. The hydride,  $\text{Cp}_3\text{ZrH}$ , was prepared by reduction of the tetra-substituted species,  $\text{Cp}_4\text{Zr}$ , with lithium aluminum hydride.

An interesting aspect of zirconium chemistry is its application to Ziegler-Natta catalysis. Kaminsky and Sinn

have developed a new class of Ziegler-Natta catalysts that have a high level of catalytic activity and are extremely stable in solution and the solid state<sup>109</sup>. The catalyst consists of a bis(cyclopentadienyl)zirconium derivative complexed with an aluminoxane. The aluminoxanes are cyclic oligomers that are obtained by the addition of water to a trialkylaluminum species. Sinn and Kaminsky also report that tris(cyclopentadienyl)zirconium compounds are active polymerization catalysts for ethylene. Kopf<sup>110</sup> recently reported the crystal structure of the unusual tris(cyclopentadienyl)zirconium complex,  $\text{Cp}_3\text{ZrH}\cdot\text{AlEt}_3$ , which was obtained as a side product from the polymerization studies.

## II. EXPERIMENTAL

### General Techniques

All operations were performed under prepurified nitrogen or argon by using standard Schlenck techniques. Purified grade nitrogen and argon, obtained from Matheson, were further deoxygenated by passing them through columns of activated BASF catalyst R 3-11 and Aquasorb (Mallinckrodt). Reagent grade solvents were used. Benzene, toluene and tetrahydrofuran were distilled from sodium/benzophenone under nitrogen. Hexane and n-pentane were refluxed over calcium hydride and were freshly distilled prior to use. Diethyl ether was distilled from lithium aluminum hydride.

Electron spin resonance spectra were obtained by use of a Varian E-4 spectrometer. A Hanovia medium pressure 450 W mercury lamp with a quartz well was used as a UV light source for bench-top reactions. The glassware used for photolysis reactions was Pyrex, so the UV wavelength range was greater than 300 nm.

### Tris(cyclopentadienyl)zirconiumchloride (48)

Sodium cyclopentadienide (3.3 g, 38 mmol) was rapidly added to a solution of zirconocenedichloride (10 g, 34 mmol)



in 300 mL THF. The solution was refluxed for 3 h and then stirred for an additional hour. The reaction may be monitored by  $^1\text{H}$  NMR. (Caution must be employed as  $\text{Cp}_3\text{ZrCl}$  disproportionates to  $\text{Cp}_2\text{ZrCl}_2$  and  $\text{Cp}_4\text{Zr}$  if refluxing is prolonged.) The yellow solution was filtered and the filtrate was reduced in volume to yield 40%  $\text{Cp}_3\text{ZrCl}$  which was collected, dried and stored in a dry box. The product may be sublimed at  $90^\circ\text{C}/10^{-1}$  mm.  $^1\text{H}$  NMR: ( $\text{CDCl}_3$ ),  $\delta 6.0$  (s); ( $\text{C}_6\text{D}_6$ ), 5.67 (s); Mass spec: (rel intensity), 320 (3,  $\text{M}^+$ ), 285 (2,  $\text{M}^+ - \text{Cl}$ ), 255 (100,  $\text{M}^+ - (\text{C}_5\text{H}_5)$ ), 190 (20,  $\text{M}^+ - 2(\text{C}_5\text{H}_5)$ ), 66 (13).

Attempted Preparation of Tris(cyclopentadienyl)zirconium-  
butyl (49)

Butyllithium (0.22 mL, 0.3 mmol) was slowly added via syringe to a solution of tris(cyclopentadienyl)zirconium-chloride (100 mg, 0.3 mmol) in 50 mL of THF which had been cooled to  $-78^\circ\text{C}$ . The yellow solution was stirred at  $-78^\circ\text{C}$  for 4 h and then was gradually allowed to reach room temperature. Upon reaching room temperature the solution turned black. The solvent was removed in vacuo leaving a purple black residue.  $^1\text{H}$  NMR: ( $\text{C}_6\text{D}_6$ ),  $\delta 6.0$  (broad peak), 5.77 (s), 5.3 (s), 1.0 (broad peak).

Tris(cyclopentadienyl)zirconiumbutyl (49)

Butyllithium (0.22 mL, 0.35 mmol) was slowly added via syringe to a solution of tris(cyclopentadienyl)zirconium-chloride (100 mg, 0.3 mmol) in 100 mL of toluene which had been cooled to  $-78^{\circ}\text{C}$ . After being stirred for 4 h the yellow solution was allowed to reach room temperature. The solvent was removed in vacuo and the residue was extracted with hexane. The hexane solution was reduced in volume and cooled to  $-30^{\circ}\text{C}$ . The yellow crystals were filtered to give 65% yield of (49).  $^1\text{H NMR}$ : ( $\text{C}_7\text{D}_8$ ),  $\delta$ 5.35 (s, Cp), 1.6 (m), 1.2 (m), 1.0 (m);  $^{13}\text{C NMR}$ : ( $\text{C}_7\text{D}_8$ ),  $\delta$ 110.6 (d, Cp), 39.7 (t), 33.47 (t), 30.67 (t), 14.4 (q); Mass spec: (rel intensity), 285 (100,  $\text{Cp}_3\text{Zr}$ ), 220 (18,  $\text{Cp}_2\text{Zr}$ ), 66 (21).

Tris(cyclopentadienyl)zirconiummethyl (50)

Methyllithium (0.28 mL, 0.34 mmol) was added slowly via syringe to a solution of tris(cyclopentadienyl)zirconium-chloride (100 mg, 0.31 mmol) in 50 mL of diethyl ether which was cooled to  $-78^{\circ}\text{C}$ . After being stirred for 3 h the solution was allowed to reach room temperature. The solvent was removed in vacuo and the yellow residue was extracted with pentane. The pentane solution was concentrated and cooled to  $-30^{\circ}\text{C}$ . The yellow solid was collected and stored in the dry box, 60% yield of  $(\text{C}_5\text{H}_5)_3\text{ZrCH}_3$ .  $^1\text{H NMR}$ : ( $\text{C}_6\text{D}_6$ ),  $\delta$ 5.34 (s), 0.5 (s).

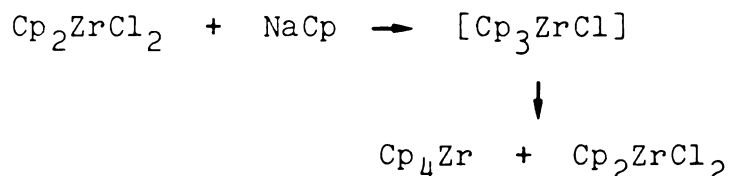
Photolysis of Tris(cyclopentadienyl)zirconiummethyl under  
CO Atmosphere

An NMR tube was filled with a toluene- $d_8$  solution of tris(cyclopentadienyl)zirconiummethyl in the dry box. The NMR tube was removed from the dry box and was evacuated and filled with CO three times on a vacuum line. This solution was photolyzed for 6 h in a water bath which was maintained at 25°C and the reaction was monitored by  $^1\text{H}$  NMR spectroscopy. There was no change in the chemical shift of the methyl signal after irradiating for 6 h.

### III. RESULTS AND DISCUSSION

#### 1. Cp<sub>3</sub>ZrCl

Tris(cyclopentadienyl)zirconiumchloride is produced by reaction of bis(cyclopentadienyl)zirconiumdichloride with sodium cyclopentadienide in refluxing tetrahydrofuran. An interesting feature of this preparation is that upon prolonged heating (more than three hours) the Cp<sub>3</sub>ZrCl species appears to disproportionate to Cp<sub>2</sub>ZrCl<sub>2</sub> and Cp<sub>4</sub>Zr as shown in Scheme 13.



Scheme 13

This disproportionation reaction suggests that the tris-(cyclopentadienyl)zirconiumchloride complex has limited thermal stability.

Tris(cyclopentadienyl)zirconiumchloride is extremely moisture sensitive and hydrolyzes rapidly to (μ-oxo)bis-(chlorozirconocene), (Cp<sub>2</sub>ZrCl)<sub>2</sub>O. The μ-oxo dimer is readily characterized by the Zr-O-Zr stretch located at

750 to 780  $\text{cm}^{-1}$  in the infrared.

Table 21 shows the solvent dependence of the chemical shifts of the cyclopentadienylzirconium complexes. The chemical shift of the cyclopentadienyl ring protons moves upfield from  $\text{Cp}_2\text{ZrCl}_2$  to  $(\text{Cp}_2\text{ZrCl})_2\text{O}$  to  $\text{Cp}_3\text{ZrCl}$  to  $\text{Cp}_3\text{ZrR}$  where  $\text{R} = \text{alkyl}$ . This trend is consistent with the subsequent removal of a deshielding chlorine atom.

Table 21.  $^1\text{H}$  NMR Data for Cyclopentadienylzirconium Complexes.

	$\text{CDCl}_3$	$\text{C}_6\text{D}_6$	$\text{C}_7\text{D}_8$
$\text{Cp}_2\text{ZrCl}_2$	6.5	6.02	
$(\text{Cp}_2\text{ZrCl})_2\text{O}$	6.3	5.74	6.00
$\text{Cp}_3\text{ZrCl}$	6.0	5.67	
$\text{Cp}_3\text{ZrCH}_2\text{CH}_2\text{CH}_2\text{CH}_3$		5.35 1.67m 1.20m 1.00m	
$\text{Cp}_3\text{ZrCH}_3$		5.34 0.50	

The  $^1\text{H}$  NMR spectrum of  $\text{Cp}_3\text{ZrCl}$  consists of a singlet at 6.0 ppm in  $\text{CDCl}_3$  which suggests that the rings exhibit rapid fluxional behavior that is too fast to be detected on the NMR time scale. This is not surprising in view of the singlet which is observed at  $-150^\circ\text{C}$  in the  $^1\text{H}$  NMR

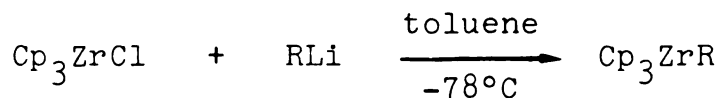
for  $\text{Cp}_4\text{Zr}^{111}$ .

The tris(cyclopentadienyl)lanthanide and actinide derivatives have three  $\pi$ -bonded cyclopentadienyl rings. If  $\text{Cp}_3\text{ZrCl}$  has three  $\pi$ -bonded cyclopentadienyl rings it is formally a twenty electron system. Hoffmann has examined the molecular orbital scheme for the hypothetical  $\text{Cp}_3\text{Ti}^+$  fragment and concluded from symmetry constraints that the three cyclopentadienyl rings donate sixteen electrons to the metal, leaving one orbital on the metal fragment empty and available for a sigma bond<sup>112</sup>. In lanthanide and actinide chemistry the presence of f orbitals invalidate the usual electron counting rules.

## 2. $\text{Cp}_3\text{ZrR}$ ( $\text{R} = \text{nBu}, \text{Me}$ )

The compound  $\text{Cp}_3\text{ZrCl}$  appears to have remarkable structural similarity to  $\text{Cp}_3\text{UCl}$  and  $\text{Cp}_3\text{ThCl}$ . The alkyls of these actinide complexes exhibit surprising thermal stability which has been attributed<sup>113</sup> to the crowded coordination sphere blocking the beta-elimination decomposition pathway. In the light of these results preparation of the analogous zirconium complexes was investigated.

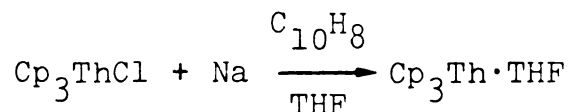
The alkyl complexes  $\text{Cp}_3\text{ZrR}$ , where  $\text{R} = \text{nBu}, \text{Me}$ , were isolated in good yield from reaction of  $\text{Cp}_3\text{ZrCl}$  and the appropriate alkyllithium reagent at low temperature.



Addition of small amounts of methanol to quench any unreacted alkyllithium led to decomposition of the zirconium alkyl. The tris(cyclopentadienyl)zirconiumalkyl complexes are extremely sensitive to protic reagents such as water and methanol.

When THF was used as the reaction solvent the solution turned black upon reaching room temperature. The  $^1\text{H}$  NMR spectrum ( $\text{C}_6\text{D}_6$ ) of the black purple solid contained very broad peaks around 6 and 1 ppm which suggests the presence of a paramagnetic species. The ESR spectrum, which is shown in Figure 26, is complex and suggests the presence of two species. A possible explanation is that THF coordinates to the metal to give the species,  $\text{Cp}_3\text{Zr}\cdot\text{THF}$ . When a noncoordinating solvent such as toluene is used no color change is observed and the zirconium alkyl is isolated in good yield.

There is precedence for a trivalent complex of this kind in actinide chemistry. Kanellakopulos<sup>114</sup> has prepared an analogous thorium complex by reduction of  $\text{Cp}_3\text{ThCl}$  with sodium naphthalide in the presence of tetrahydrofuran.



Alternatively the black purple paramagnetic zirconium species could be an anionic zirconium III complex,  $\text{Cp}_3\text{ZrR}^-$ .

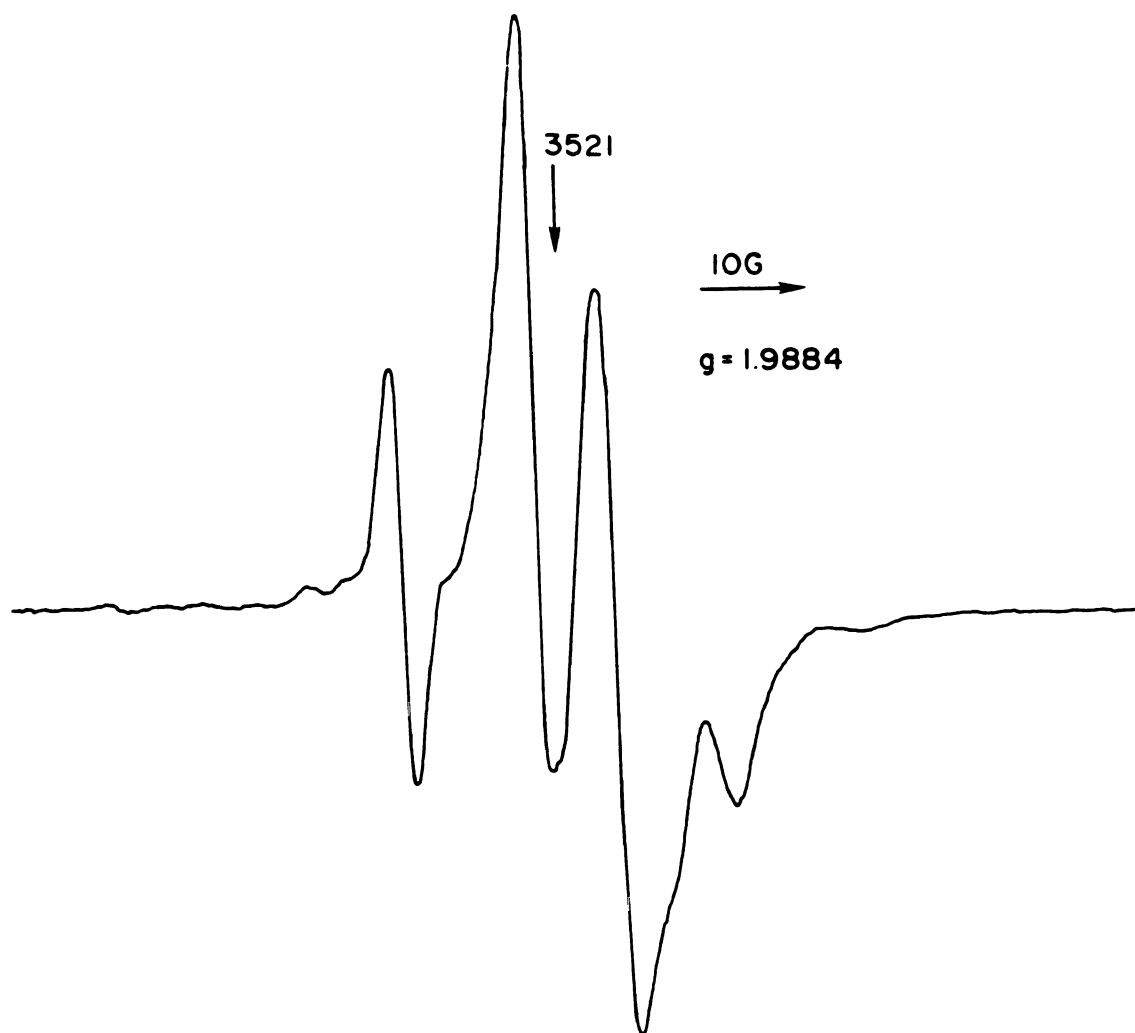


Figure 26. ESR Spectrum Obtained from Reaction of  $\text{Cp}_3\text{ZrCl}$  with  $\text{BuLi}$  in THF Solution.



Lappert<sup>115</sup> reduced a zirconocene dialkyl complex with sodium dihydronaphthylide and obtained an ESR active species. Initially he postulated that the ESR active species was  $[\text{ZrCp}_2(\text{CH}_2\text{CMe}_3)_2]^-$  but later on the basis of cyclic voltammetry data he concluded that the anionic dialkyl was unstable and the  $d^1$  complex was  $[\text{ZrCp}(\text{CH}_2\text{CMe}_3)_2]$ . The zirconium dialkyls undergo irreversible one-electron reductions at a platinum electrode at scan rates up to  $1.0 \text{ V s}^{-1}$ .

Recently Fischer<sup>116</sup> reported that exposure of  $\text{Cp}_3\text{UR}$ , where  $\text{R} = \text{Me}$ ,  $i\text{Pr}$ ,  $i\text{Bu}$  and  $n\text{Bu}$ , to excess alkyllithium in THF yields saturated hydrocarbons,  $\text{RH}$ , and a solvated species  $[\text{Li}(\text{thf})_x][\text{Cp}_3\text{U}^{\text{III}}\text{R}]$ . Both Fischer and Lappert found that THF was necessary for formation of these anionic alkyl species.

Stable transition metal alkyls are generally limited to complexes where the alkyl lacks a beta-hydrogen due to the facile beta elimination decomposition pathway<sup>117</sup>. With few exceptions, complexes of early transition metal alkyls that contain beta hydrogens are accessible only at low temperatures. For example,  $\text{Cp}_2\text{TiR}_2$ , where  $\text{R} = n\text{Bu}$  or  $n\text{Pr}$ <sup>118</sup>, is unstable above  $-40^\circ\text{C}$ . The complex  $\text{Cp}_3\text{Zr}(n\text{Bu})$  is one of the few examples of a thermally stable early transition metal alkyl containing beta hydrogen atoms. This stability is due to the presence of three  $\pi$ -bonded cyclopentadienyl rings which sterically congest the

coordination sphere around zirconium and thus block the beta elimination decomposition pathway.

The  $^{13}\text{C}$  NMR spectrum of  $\text{Cp}_3\text{Zr}(\text{nBu})$  was examined at low temperature in the hope of freezing out the fluxional cyclopentadienyl rings. A sharp singlet was observed for the cyclopentadienyl rings at  $-60^\circ\text{C}$ . In  $\text{Cp}_3\text{U}(\text{iPr})$ , Marks<sup>119</sup> observed restricted rotation of the cyclopentadienyl rings with the slow exchange limit at  $-109^\circ\text{C}$ . In the analogous zirconium complex,  $\text{Cp}_3\text{Zr}(\text{iPr})$ , restricted rotation of the cyclopentadienyl rings may be evident.

### 3. Reaction of $\text{Cp}_3\text{ZrMe}$ with CO

Many groups<sup>120</sup> have observed a facile reaction of zirconium alkyls with carbon monoxide where CO inserts into the metal alkyl bond to give an acyl species. Reaction of  $\text{Cp}_3\text{ZrMe}$  with CO was examined at ambient temperature and under photolytic conditions.

The complex,  $\text{Cp}_3\text{ZrMe}$ , in a toluene- $\text{d}_8$  solution was sealed in an NMR tube under an atmosphere of CO and the NMR tube was protected from light. The  $^1\text{H}$  NMR spectrum was monitored periodically but no change was observed in the spectrum after a few days. If an acyl species had formed the chemical shift of the methyl group would have moved downfield.

Reaction of  $\text{Cp}_3\text{ZrMe}$  with CO, however, may only be photo-induced as the sterically crowded coordination sphere

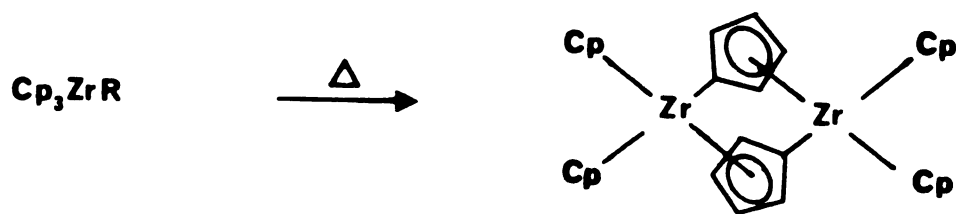
of zirconium would prevent prior coordination of CO. Photolysis could induce an excited cyclopentadienyl ring ( $\eta^3$  type) as Marks has proposed for the photo-induced beta elimination of  $\text{Cp}_3\text{Th}$  alkyls<sup>113</sup>.

An NMR tube containing a toluene- $\text{d}_8$  solution of  $\text{Cp}_3\text{ZrMe}$  under an atmosphere of CO was photolyzed for at least six hours. No change was however observed in the  $^1\text{H}$  NMR spectrum.

Even though forcing conditions (high CO pressure) have not been employed, reaction of  $\text{Cp}_3\text{ZrMe}$  with CO does not seem feasible. These results are consistent with the crowded coordination sphere of zirconium which would prevent prior coordination of the CO ligand.

#### 4. Conclusions

An interesting aspect of  $\text{Cp}_3\text{ZrR}$  chemistry could be their thermal and photolytic decomposition. The sterically crowded coordination of  $\text{Cp}_3\text{ZrR}$  could prevent beta elimination as a thermal decomposition pathway and the alkyl group would rather abstract hydrogen from a cyclopentadienyl ring to give a binuclear species, shown in Scheme 14. Beta elimination, however, may be photo-induced where a cyclopentadienyl ring may be photoactivated to  $\eta^3$  coordination. Marks<sup>121</sup> has obtained similar results in the  $\text{Cp}_3\text{ThR}$  system where beta elimination is thermally inaccessible but rather photo-induced.



Scheme 14

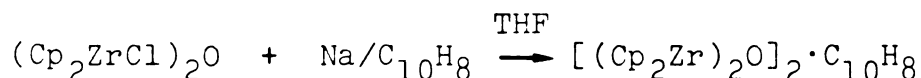
The preparation of the zirconium alkyls,  $\text{Cp}_3\text{ZrR}$ , has opened up a new area of zirconium chemistry. The apparent ease of reduction, where a paramagnetic species is obtained from the reaction of  $\text{Cp}_3\text{ZrCl}$  with butyllithium in THF, is of special interest as, in contrast to titanium, very few low valent zirconium species are known. In addition the thermal decomposition of  $\text{Cp}_3\text{ZrR}$  could lead to novel binuclear zirconium complexes as shown in Scheme 14.

## APPENDIX A

## PHOTOLYSIS OF ( $\mu$ -OXO)BIS(CHLOROZIRCONOCENE)

### Introduction

In contrast to titanium, very few low valent zirconium complexes are known<sup>122,123</sup>. Wailes<sup>124</sup> has reported that reduction of the  $\mu$ -oxo compound,  $(\text{Cp}_2\text{ZrCl})_2\text{O}$ , with sodium/naphthalene gave rise to a  $\mu$ -oxozirconium(III) species as a dark brown solid.



As naphthalene could not be removed from the complex by heating at 110°C under vacuum the complex was not further characterized. Floriani<sup>125</sup> recently reported a cyclic trimer,  $(\text{Cp}_2\text{ZrO})_3$  which was prepared by reaction of  $\text{Cp}_2\text{Zr}(\text{CO})_2$  with  $\text{CO}_2$ .

Low valent transition metal complexes have been generated by photolysis<sup>126</sup>. The photolysis of ( $\mu$ -oxo)bis-(chlorozirconocene) was investigated.

### Experimental

#### Photolysis of ( $\mu$ -oxo)bis(chlorozirconocene).

The compound,  $(\text{Cp}_2\text{ZrCl})_2\text{O}$ , was prepared according to

Wailles' procedure<sup>127</sup> and was recrystallized from  $\text{CH}_2\text{Cl}_2$ . An NMR tube containing  $(\text{Cp}_2\text{ZrCl})_2\text{O}$  in toluene- $\text{d}_8$  was sealed under vacuum and was photolyzed for over 12 h at  $25^\circ\text{C}$ . The photolysis reaction was monitored by  $^1\text{H}$  NMR and after 75 min the appearance of broad peaks in the NMR spectrum suggested the presence of a paramagnetic species. An ESR signal of the sample consists of a singlet with  $g = 1.9792$  and satellites due to  $^{91}\text{Zr}$  ( $I = 5/2$ , 11.23% natural abundance).

### Results and Discussion

A toluene solution of  $(\text{Cp}_2\text{ZrCl})_2\text{O}$  was photolyzed at room temperature for twelve hours. After irradiation for seventy-five minutes a broad peak, which increased in intensity as irradiation progressed, was observed in the  $^1\text{H}$  NMR spectra.  $^1\text{H}$  NMR spectra which were recorded at various time intervals during the photolysis reaction are shown in Figure A1. An ESR signal of the sample, shown in Figure A2, consists of a singlet with  $g = 1.9792$  and satellites due to  $^{91}\text{Zr}$  ( $I = 5/2$ ).

The above data is consistent with a zirconium(III) species which could be similar to the dimer,  $[(\text{Cp}_2\text{Zr})_2\text{O}]_2$ , reported by Wailles<sup>124</sup>. Further characterization is necessary before the nature of the zirconium(III) species is fully ascertained.

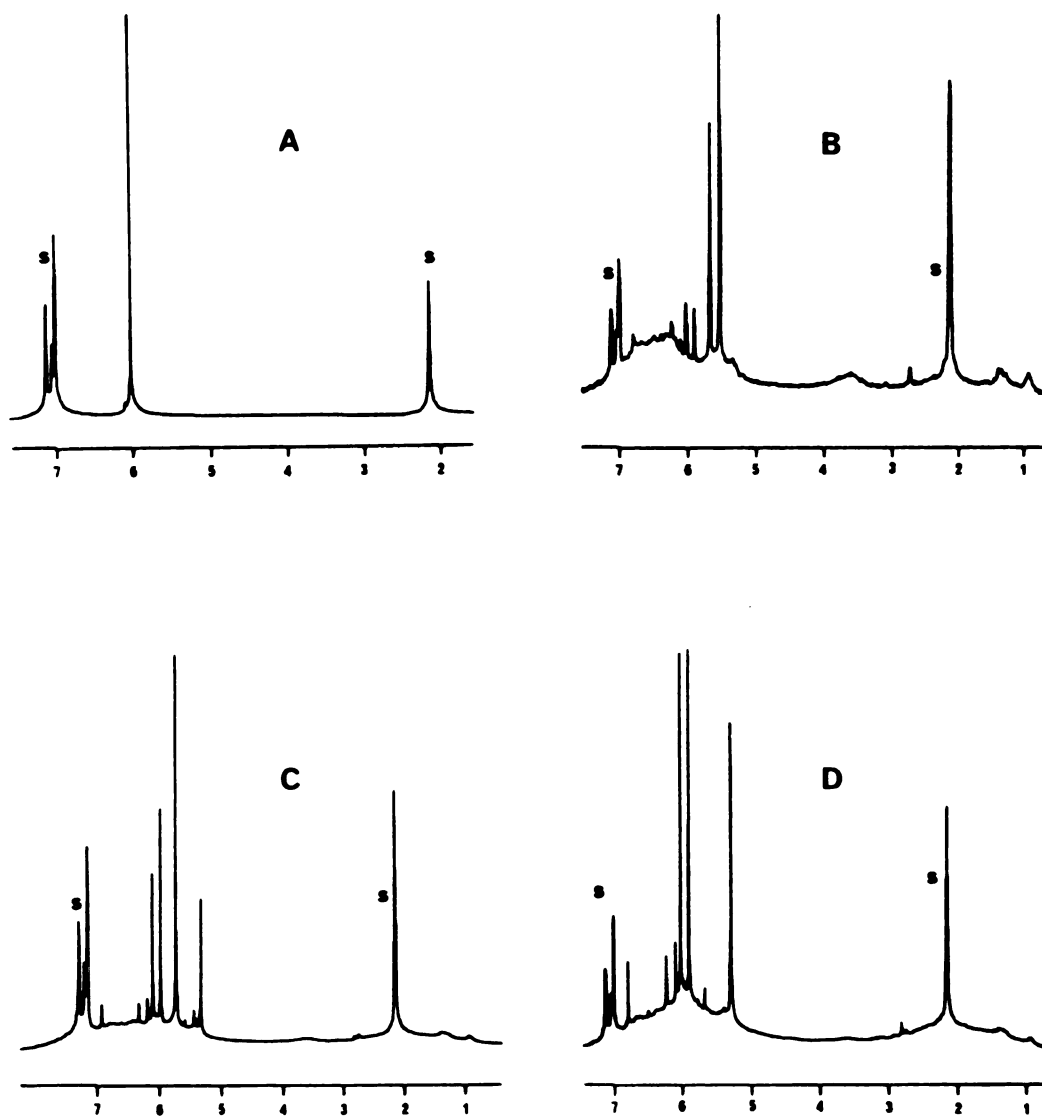


Figure A1.  $^1\text{H}$  NMR Spectra of  $(\text{Cp}_2\text{ZrCl})_2\text{O}$  during photolysis at (A)  $t = 0$ , (B)  $t = 75$  min, (C)  $t = 6$  h 35 min and (D)  $t = 16$  h.



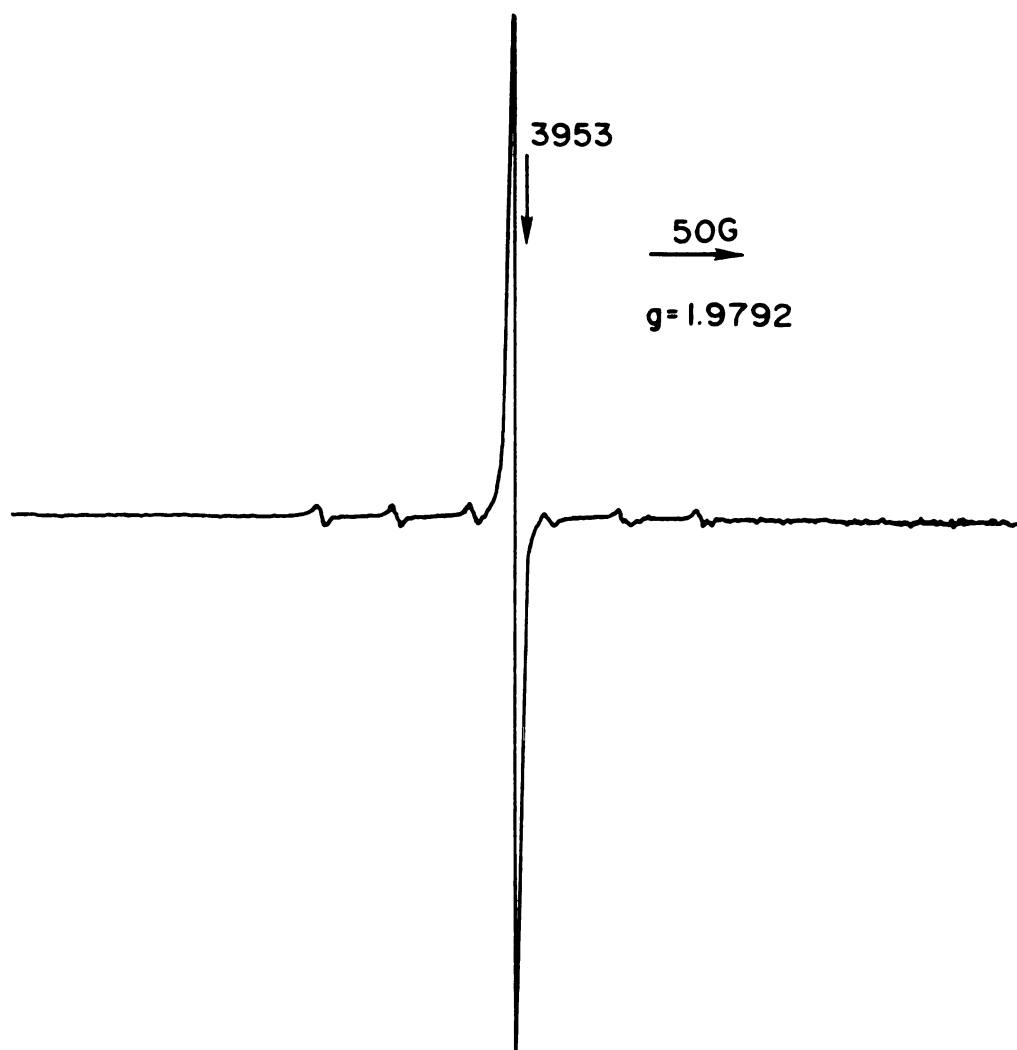


Figure A2. ESR Signal obtained from photolysis of  $(\text{Cp}_2\text{ZrCl})_2\text{O}$ .

## APPENDIX B

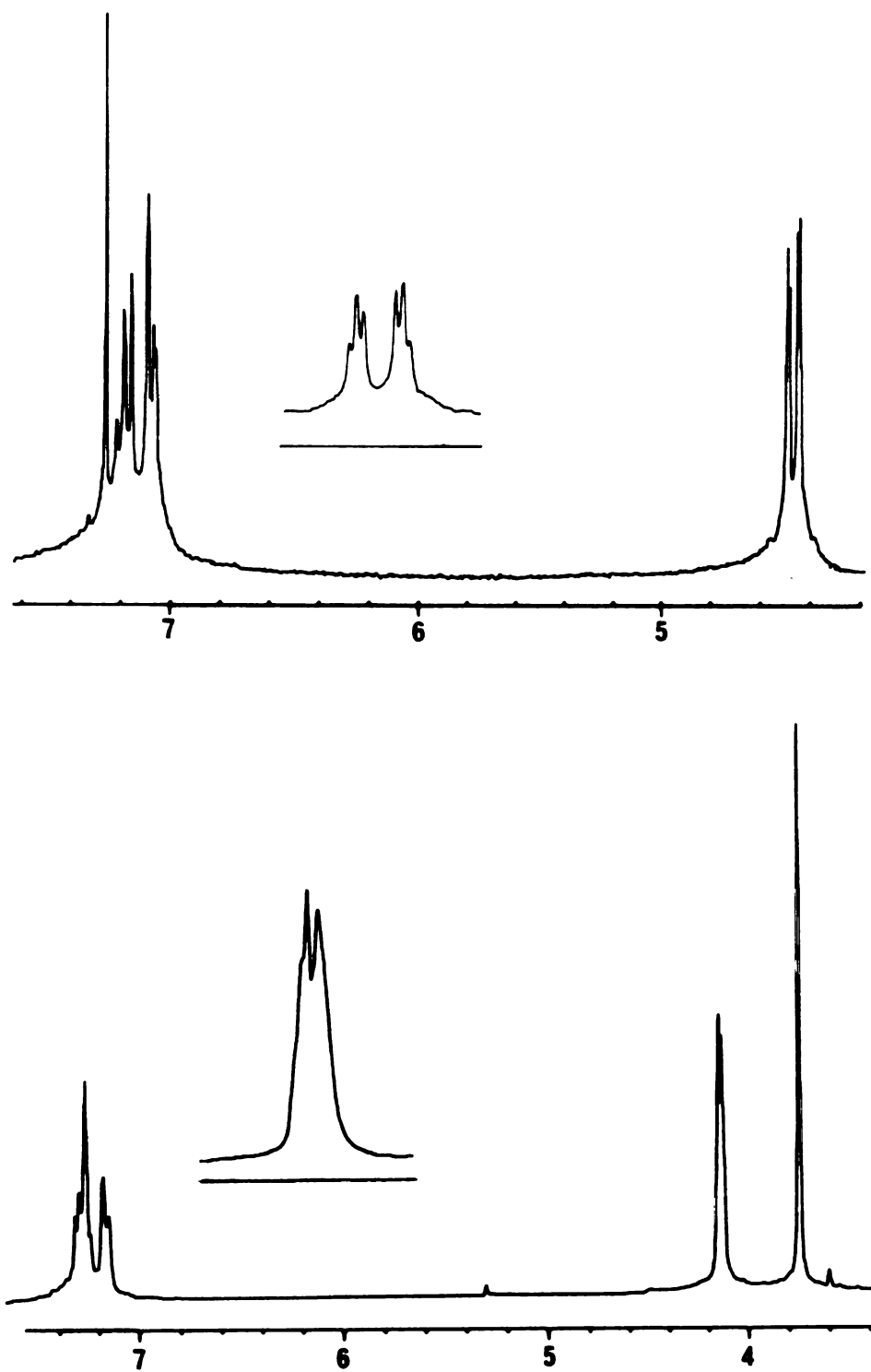


Figure B1.  $^1\text{H}$  NMR Spectra of  $\text{Fe}(\text{C}_5\text{H}_4\text{SPh})_2$  (above) and  $\text{Fe}(\text{C}_5\text{H}_4\text{SCH}_2\text{Ph})$  (below). Inset cyclopentadienyl proton region.

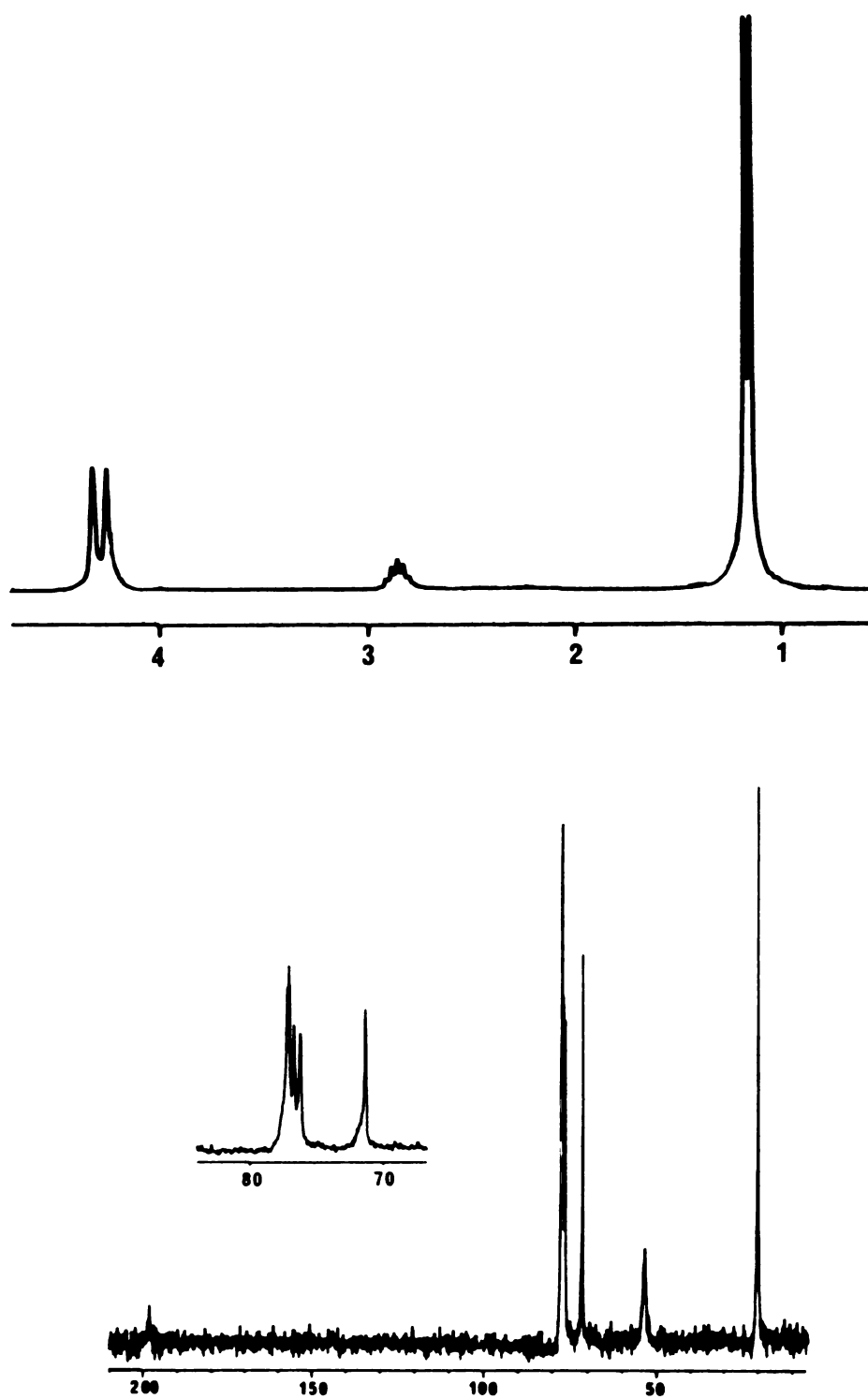


Figure B2.  $^1\text{H}$  NMR Spectrum of  $\text{Fe}(\text{C}_5\text{H}_4\text{S}-i\text{Pr})_2$  (above) and  $^{13}\text{C}$  NMR spectrum of  $\text{Fe}(\text{C}_5\text{H}_4\text{SCSNiPr}_2)_2$  in  $\text{CDCl}_3$  at  $57^\circ\text{C}$  (below).

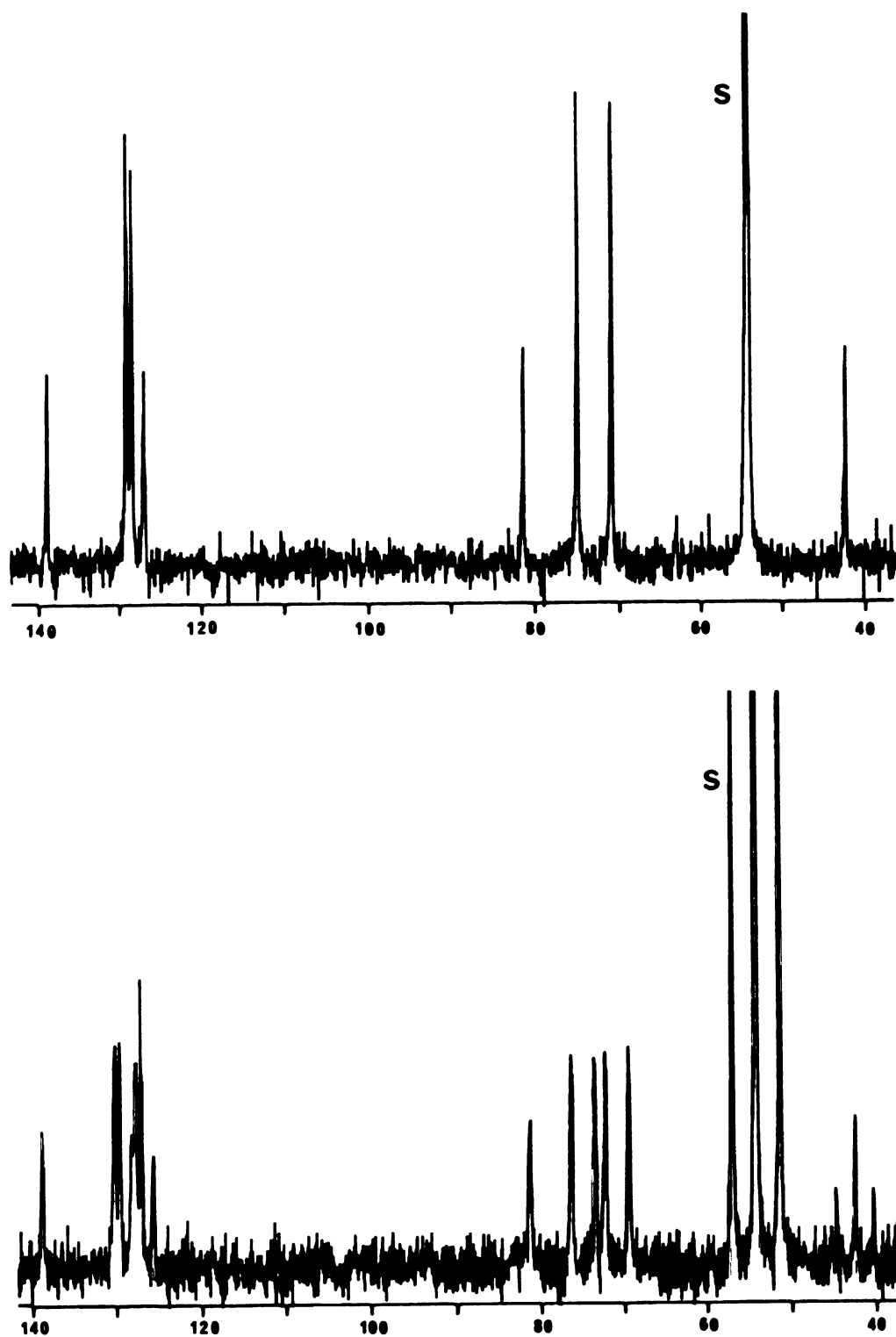


Figure B3.  $^{13}\text{C}$  NMR Spectra of  $\text{Fe}(\text{C}_5\text{H}_4\text{SCH}_2\text{Ph})_2$  proton decoupled (above) and gated decoupled (below).

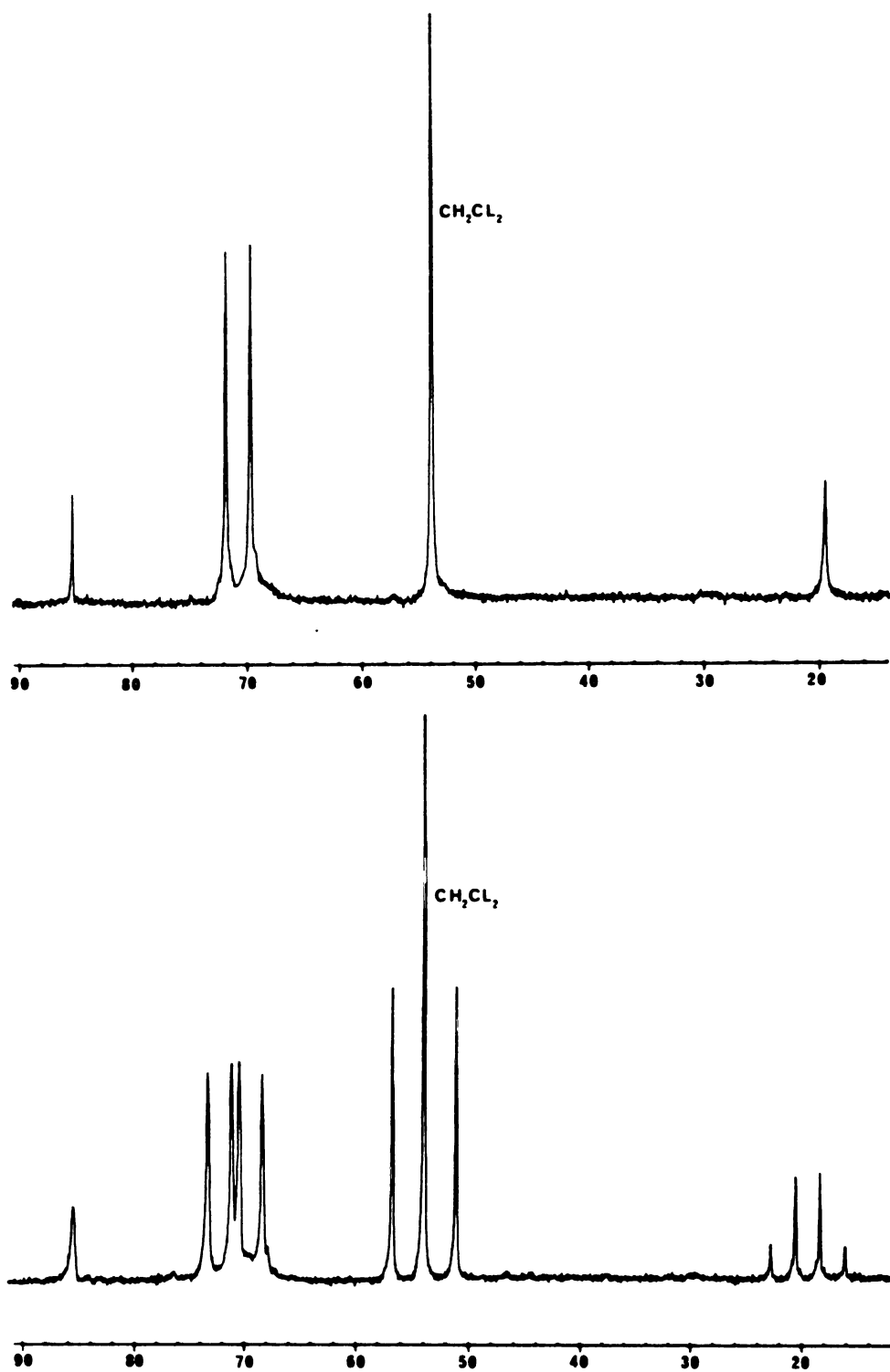


Figure B4.  $^{13}\text{C}$  NMR Spectra of  $\text{Fe}(\text{C}_5\text{H}_4\text{SMe})_2$  proton decoupled (above) and gated decoupled (below).

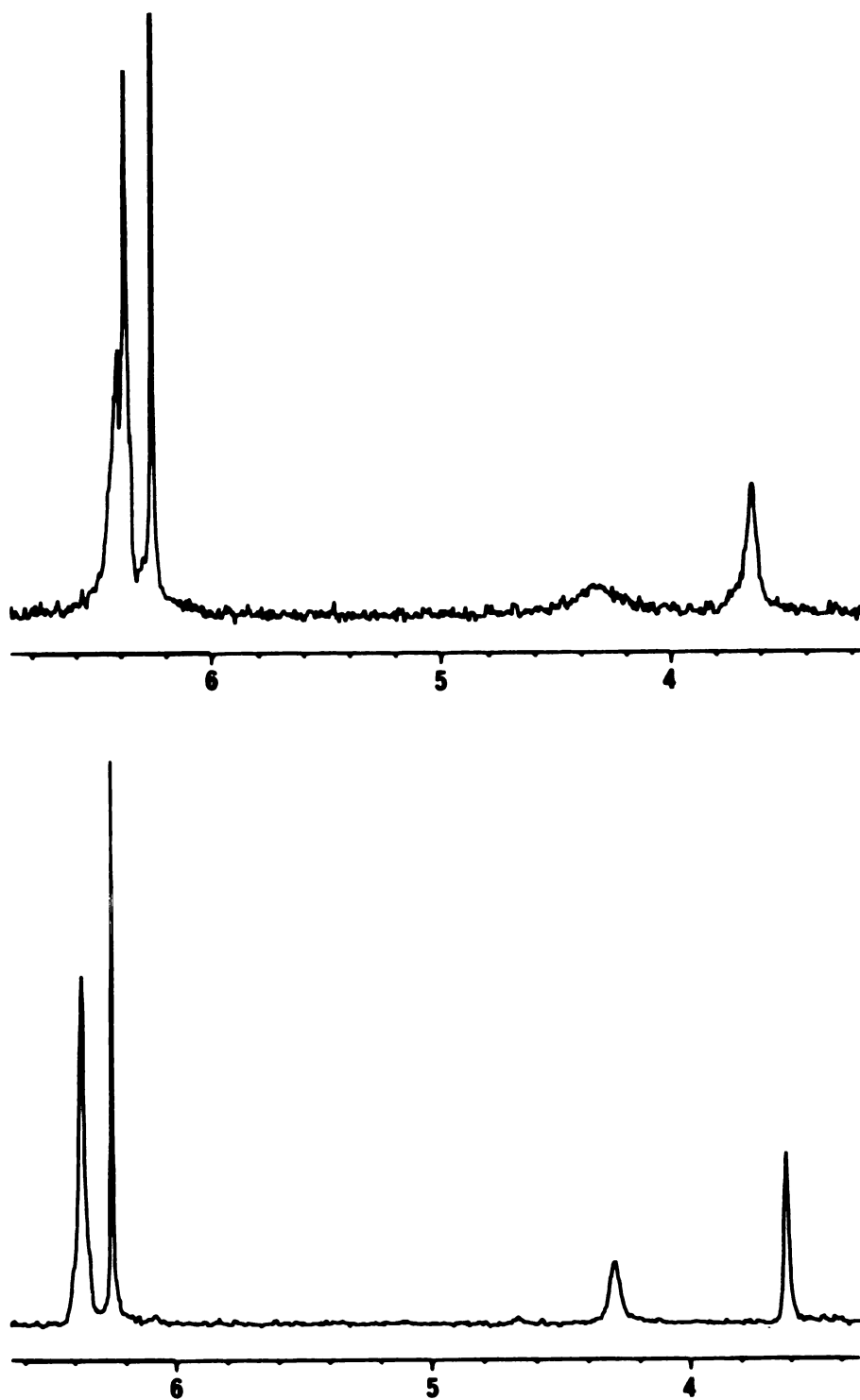


Figure B5.  $^1\text{H}$  NMR Spectra of  $\text{Fe}(\text{C}_5\text{H}_4\text{SPh})_2\text{PtCl}_2$  (above) and  $\text{Fe}(\text{C}_5\text{H}_4\text{SPh})_2\text{PtBr}_2$  at  $50^\circ\text{C}$  (below).

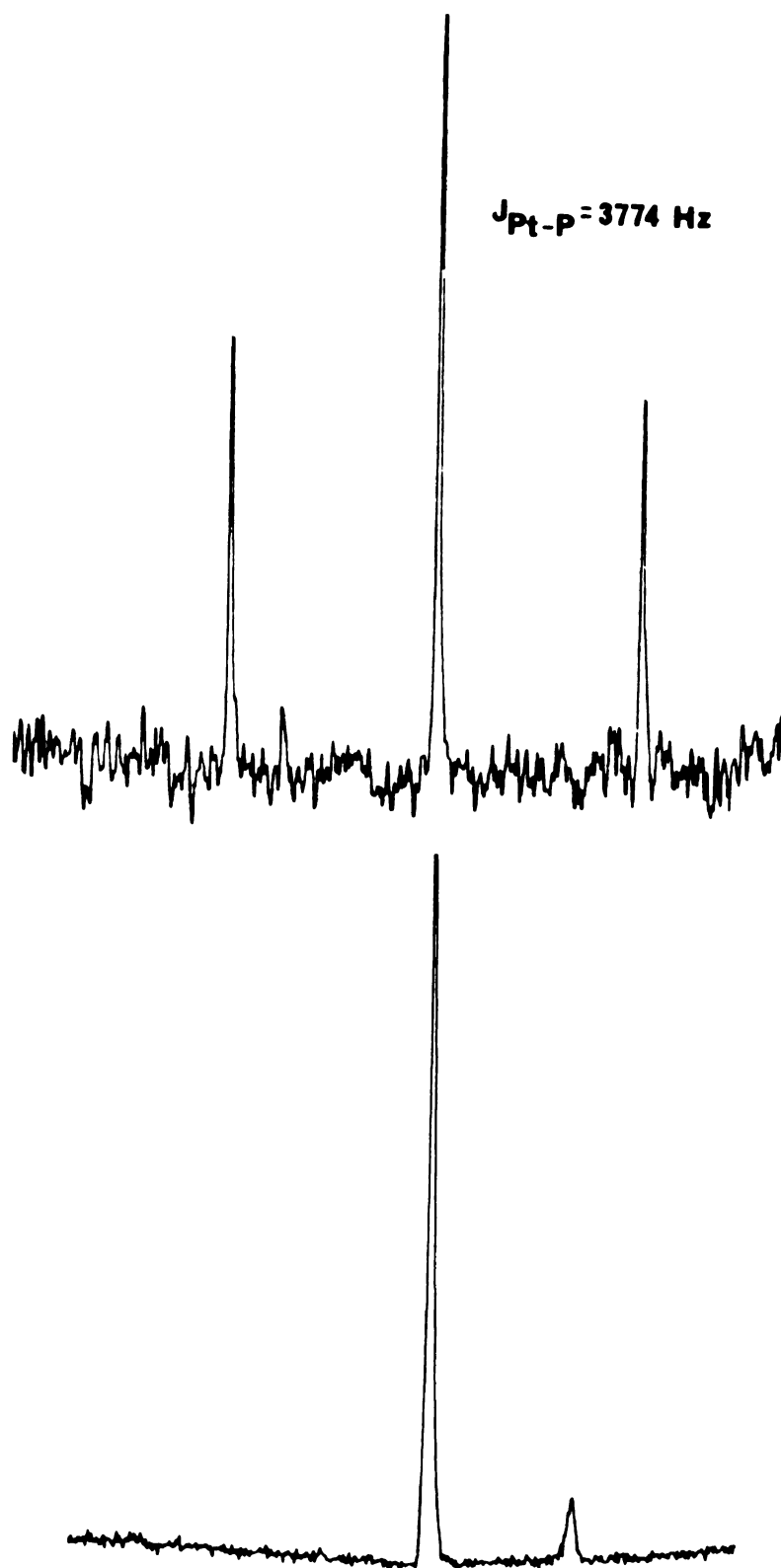


Figure B6.  $^{195}\text{Pt}$  NMR Spectra of  $\text{Fe}(\text{C}_5\text{H}_4\text{PPh}_2)_2\text{PtCl}_2$  (above) and  $\text{Fe}(\text{C}_5\text{H}_4\text{S-iBu})_2\text{PtCl}_2$  (below).



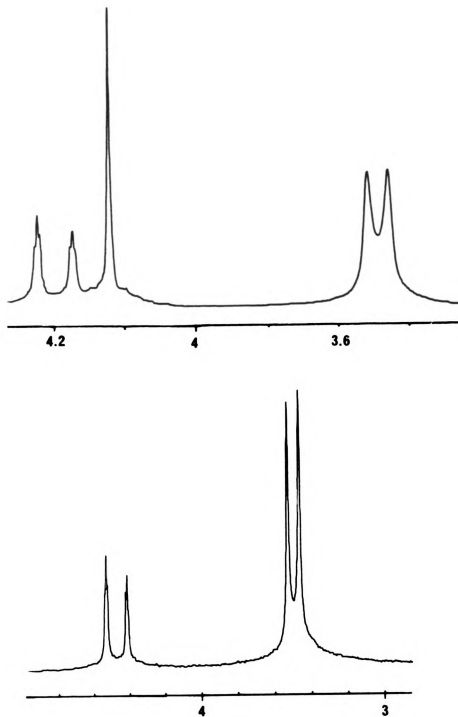


Figure B7.  $^1\text{H}$  NMR Spectra of  $\text{Fe}(\text{C}_5\text{H}_5)(\text{C}_5\text{H}_4\text{SCSNMe}_2)$  (above) and  $\text{Fe}(\text{C}_5\text{H}_4\text{SCSNMe}_2)_2$  (below).

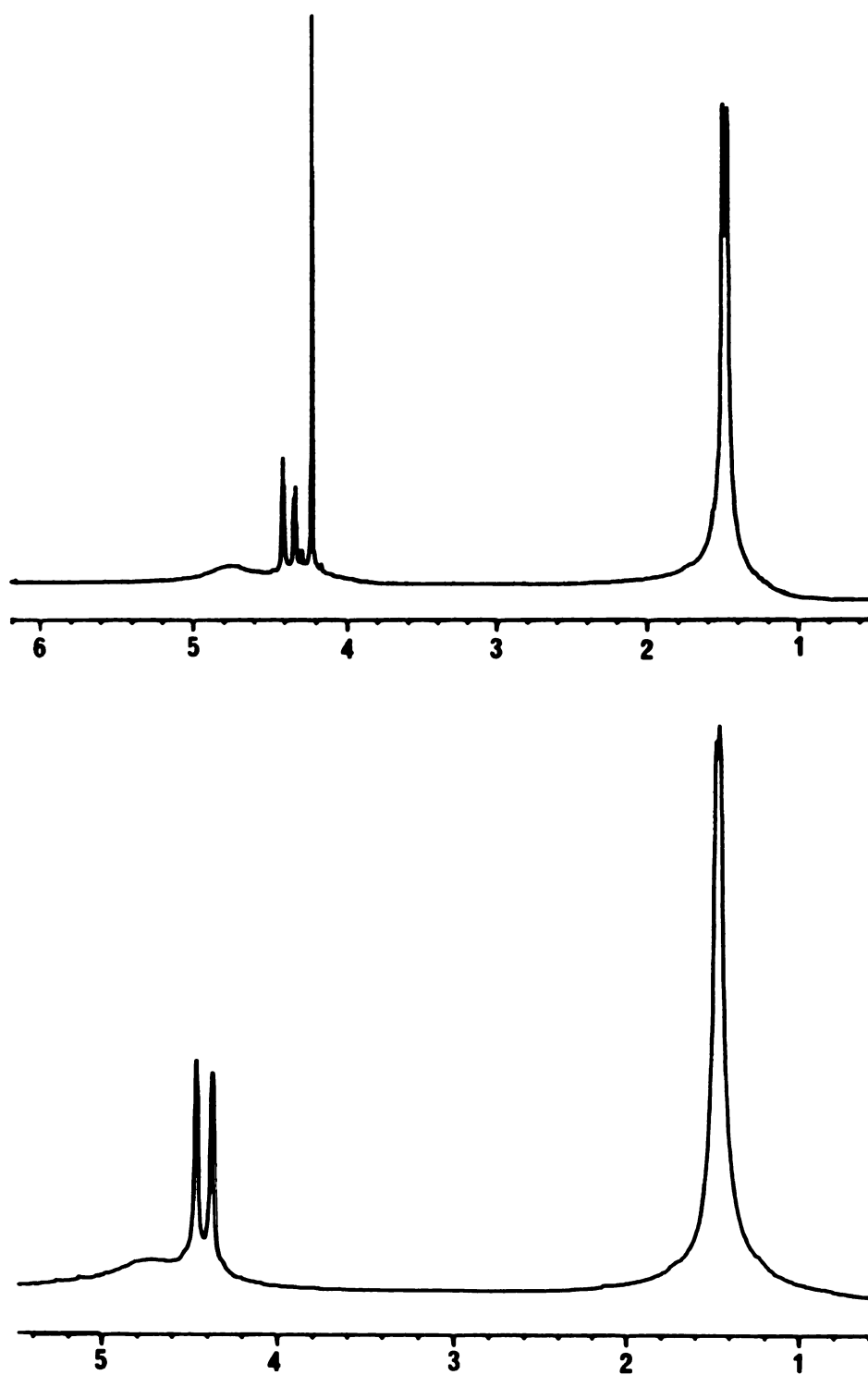


Figure B8.  $^1\text{H}$  NMR Spectra of  $\text{Fe}(\text{C}_5\text{H}_5)(\text{C}_5\text{H}_4\text{SCS}\text{NiPr}_2)$  (above) and  $\text{Fe}(\text{C}_5\text{H}_4\text{SCS}\text{NiPr}_2)_2$  (below).

## REFERENCES

## REFERENCES

1. Rosenblum, M. "Chemistry of the Iron Group Metallocenes". Part I., Wiley, New York, 1965. "Comprehensive Organometallic Chemistry" Ed., Wilkinson, G.; Stone, F.G.A. and Abel, E.W., Pergamon Press, New York, 1982. Watts, W. E. 8, 1013-1071; Deeming, A.J. 4, 377-512.
2. Slocum, D.W.; Engelmann, T. R.; Ernest, C.; Jennings, C. A.; Jones, W.; Koonsvitsky, B.; Lewis, J. and Shenkin, P., J. Chem. Ed., 1969, 46, 144-150.
3. Rausch, M. D. and Ciappenelli, D. J., J. Organomet. Chem., 1967, 10, 127-136.
4. Hedberg, F. L. and Rosenberg, H., Tetrahedron Lett., 1969, 46, 4011-4012.
5. Seyferth, D.; Hofmann, H. P.; Burton, R. and Helling, J. F., Inorg. Chem., 1962, 1, 227-231.
6. Fish, R. W. and Rosenblum, M., J. Org. Chem., 1965, 30, 1253-1254.
7. Cullen, W. R. and Woollins, D. J., Coordination Chem. Rev., 1981, 39, 1-30.
8. Bishop, J. J.; Davison, A.; Katcher, M. L.; Lichtenberg, D. W.; Merrill, R. E. and Smart, J. C., J. Organomet. Chem., 1971, 27, 241-249.
9. Osborne, A. G.; Hollands, R. E., Howard, J. A. K. and Bryan, R. F., J. Organometal. Chem., 1981, 205, 395-406.
10. Seyferth, D. and Withers, H. P., J. Organometal. Chem., 1980, 185, C1-C5; Organometallics, 1983, 2, 1275-1282.
11. Butler, I. R.; Cullen, W. R.; Einstein, F. W. B.; Rettig, S. J. and Willis, A. J., Organometallics, 1983, 2, 128-135.
12. Osborne, A. G. and Whitely, R. H., J. Organometal. Chem., 1975, 101, C27; Osborne, A. G.; Whitely, R. H. and Meads, R. E., ibid., 1980, 193, 345-357;

12. Stoekli-Evans, H., Osborne, A. G. and Whiteley, R. H., ibid., 1980, 194, 91-101.
13. Fischer, A. B.; Kinney, J. B.; Staley, R. H. and Wrighton, M. S., J. Am. Chem. Soc., 1979, 101, 6501-6506.
14. Rudie, A.W.; Lichtenberg, D.W.; Katcher, M.L. and Davison, A., Inorg. Chem., 1978, 17, 2859-2863.
15. Bishop, J. J. and Davison, A., Inorg. Chem., 1971, 10, 826-831.
16. Bishop, J. J. and Davison, A., Inorg. Chem., 1971, 10, 832-837.
17. Hayashi, T.; Konishi, M. and Kumada, M., Tetrahedron Lett. 1979, 21, 1871-1874; J. Organometal. Chem., 1980, 186, C1.
18. Hughes, O. H. and Unruh, J. D., J. Mol. Catal., 1981, 12, 71-83; Unruh, J. D. and Christenson, J. R., J. Mol. Catal. 1982, 14, 19-34.
19. Unruh, J. D., CA 90 203, 487v. U.S. Patent No. 2,834,742.
20. Mann, K. R.; Morrison, W. H. and Hendrickson, D. N., Inorg. Chem., 1974, 13, 1180-1185.
21. Whitesides, G. M.; Gaasch, J. F. and Stedronsky, E. R., J. Am. Chem. Soc., 1972, 94, 5258-5270.
22. Mague, J. T. and Nutt, M. O., Inorg. Chem., 1977, 16, 1259-1268.
23. Fellmann, J. D.; Garrou, P. E.; Withers, H. P.; Seyferth, D. and Traficante, D. D., Organometallics, 1983, 2, 818-825.
24. Hayashi, T. and Kumada, M., Acc. Chem. Res., 1982, 15, 395-401 and references therein.
25. Cullen, W. R. and Woollins, J. D., Can. J. Chem., 1982, 60, 1793-1799.
26. Levi, A.; Modena, G. and Scorrano, G., J.C.S. Chem. Comm., 1975, 6-7.
27. Hayashi, T.; Mise, T.; Fukushima, M.; Kagotani, M.; Nagashima, N.; Hamada, Y.; Matsumoto, A.; Kawakami, S.; Konishi, M.; Yamamoto, K. and Kumada, M., Bull. Chem. Soc. Jpn., 1980, 53, 1138-1151.

28. Schmidt, M. and Hoffmann, G. G., Phosphorous and Sul-  
fur., 1978, 4, 239-247; Murray, S. C. and Hartley,  
F. R., Chem. Rev., 1981, 81, 365-414.
29. Mitchell, P. C. H., Catalysis, 1981, 4, 175-209.
30. Vahrenkamp, H., Angew. Chem. Internat. Ed., 1975,  
14, 322-329.
31. Kalck, P.; Frances, J-M.; Pfister, P. M.; Southern,  
T. G. and Thorez, A., J.C.S. Chem. Commun., 1983,  
510-511.
32. Boydanovic, B.; Gottsch, P. and Rubach, M., J. Mol.  
Cat., 1981, 11, 135-141.
33. Rakowski-DuBoise, M.; Haltiwanger, R. C.; Miller,  
D. J. and Glatzmaier, G., J. Am. Chem. Soc., 1979,  
101, 5245-5252; Rakowski-DuBois, M.; McKenna, M.;  
Rajan, O. and Wright, L., Abstract 223 from 186 th  
ACS Meeting, Washington, D.C., Aug. 28-Sept. 2, 1983.
34. James, B. R. and Ng, F. T. T., J. Chem. Soc. Dalton  
Trans., 1972, 355-359: ibid. 1972, 1321-1324.
35. James, B. R. and McMillan, R. S., Can. J. Chem.,  
1977, 55, 3927-3932.
36. Knox, G. R. and Pauson, P. L., J. Chem. Soc., 1958,  
692-696. Knox, G. R., Morrison, I. G. and Pauson,  
P. L., ibid., 1967, 1842-1847.
37. Nefedov, V. A. and Nefedova, M. N., Zh. Obs. Khimii.,  
1966, 36, 122-126. English version p. 127-130.
38. Ratajczak, A. and Misterkiewicz, B., J. Organometal.  
Chem., 1979, 179, 181-185.
39. Burdorf, H. and Elschenbroich, C., Z. Naturforsch.,  
1981, 36b, 94-101.
40. Davison, A. and Smart, J. C., J. Organometal. Chem.,  
1979, 174, 321-334.
41. Seyferth, D. and Henderson, R. S., J. Am. Chem. Soc.,  
1979, 101, 508.
42. Seyferth, D.; Hames, B. W.; Rucker, T. G.; Cowle,  
M. and Dickson, R. S., Organometallics, 1983, 2,  
472-474.

43. Seyferth, D. and Hames, B. W., Inorg. Chim. Acta., 1983, 77, L1-L2.
44. Rausch, M. D. and Siegel, A., J. Organometal. Chem., 1969, 17, 117-125.
45. Hartley, F. R., "The Chemistry of Palladium and Platinum" Wiley, New York, 1973, p. 462.
46. Wei, K-T. and Ward, D. L., Acta Crystall., 1976, B32, 2768-2773.
47. Zalkin, A., 1974. Private Communication.
48. Main, P., (1978). "MULTAN78. A System of Computer Programs for the Automatic Solution of Crystal Structures from X-ray Diffraction Data." Univ. York, England.
49. Gokel, G. W. and Ugi, I. K., J. Chem. Ed., 1972, 49, 294-296.
50. Gunther, H., "NMR Spectroscopy" Wiley, New York, 1980 p. 184.
51. Koridze, A. A.; Petrovskii, P. V.; Mokhov, A. I. and Lutsenko, A. I., J. Organometal Chem., 1977, 136, 57-63.
52. Slocum, D. W. and Ernst, C. R., Organomet. Chem. Rev. A., 1970, 6, 337-353; Adv. Organomet. Chem., 1972, 10, 79-114.
53. Nesmeyanov, A. N.; Petrovskii, P. V.; Fedorov, L. A.; Robas, V. I. and Fedin, E. I., J. Structural Chem., 1973, 14, 49-57.
54. Rosenblum, M. "Chemistry of the Iron Group Metallocenes" Part I. Wiley, New York, 1965, p. 37-40.
55. Bailey, R. T. and Lippincott, E. R., Spectrochim. Acta., 1965, 21, 389-398.
56. Silverstein, R. M.; Bassler, G. C. and Morrill, T. C., "Spectrometric Identification of Organic Compounds" Wiley, New York, 1974. Third Edition, p. 89-113.
57. Marquarding, D.; Klusacek, H.; Gokel, G.; Hoffmann, P. and Ugi, I., J. Am. Chem. Soc., 1970, 92, 5389-5393.
58. Cullen, W. R.; Einstein, F. W. B.; Huang, C-H.; Willis, A.C. and Yeh, E-S., J. Am. Chem. Soc., 1980, 102, 988-993.

59. Rinehart, K. L.; Frerichs, A. K.; Kittle, P. A.; Westman, L. F.; Gustafson, D. H.; Pruett, R. L. and McMahon, J. E., J. Am. Chem. Soc., 1960, 82, 4111-4112.
60. Ismail, I. M.; Kerrison, J. S. and Sadler, P. J., Polyhedron., 1982, 1, 57-59.
61. Allkins, J. R. and Hendra, P. J., J. Chem. Soc., A., 1967, 1325-1329.
62. Plusec, J. and Westland, A. D., J. Chem. Soc., 1965, 5371-5376.
63. Coates, G. E. and Parkin, C., J. Chem. Soc., 1963, 421-429.
64. Hartley, F. R., "The Chemistry of Platinum and Palladium" Wiley, New York, 1973, p. 241-243.
65. Sohn, Y. S., Hendrickson, D. N. and Gray, H. B., J. Am. Chem. Soc., 1971, 93, 3603-3612.
66. Wheatly, P. J., "Perspectives in Structural Chemistry" Wiley, New York, 1967, pl-40; Haaland, A., Acc. Chem. Res., 1979, 12, 415-422.
67. Pauling, L., "The Nature of the Chemical Bond", Cornell University Press, 3rd Ed., 1960.
68. Reference #64, p. 177.
69. Davis, B. R. and Bernal, I., J. Cryst. Mol. Struct., 1972, 2, 107-114.
70. Pierpont, C. G. and Eisenberg, R., Inorg. Chem., 1972, 11, 828-832.
71. Cullen, W. R.; Kim, T-J.; Einstein, F. W. B. and Jones, T., Organometallics, 1983, 2, 714-719.
72. Sutherland, I. O., Ann. Reports NMR Spectroscopy, 1971, 4, 109.
73. Abel, E. W.; Booth, M. and Orrell, F. G., J. Organomet. Chem., 1981, 208, 213-224; Abel, E. W.; Booth, M.; Brown, C. A.; Orrell, K. G. and Woodford, R. L., ibid., 1981, 214, 93-105.
74. (a) Abel, E. W.; Farrow, G. W.; Orrell, K. G. and Sik, V., J. Chem. Soc. Dalton., 1977, 42-46.



74. (b) Abel, E. W.; Shamsuddin Ahmed, A. K.; Farrow, G. W.; Orrell, K. G. and Sik, V., ibid., 1977, 47-52.  
 (c) Abel, E. W.; Khan, A. R.; Kite, K.; Orrell, K.G. and Sik, V., Ibid., 1980, 1175-1181.  
 (d) Abel, E. W.; Booth, M. and Orrell, K. G., ibid, 1980, 1582-1592.
75. (a) Haake, P. and Turley, P. C., J. Am. Chem. Soc., 1967, 89, 4611-4616.  
 (b) Cross, R. J.; Green, T. H. and Keat, R., J. Chem. Soc. Dalton., 1976, 1150-1152.  
 (c) Cross, R. J.; Dalglish, I. G.; Smith, C. J. and Wardle, R., ibid., 1972, 992-996.
76. Abel, E. W.; Bhargava, S. K.; Kite, K.; Orrell, K.G.; Sik, V. and Williams, B. L., Polyhedron., 1982, 1, 289-298.
77. Jennings, W. B., Chem. Rev., 1975, 75, 307-322.
78. Collaborative studies with Dr. Keith Orrell, Univ. of Exeter, Exeter, England.
79. Pregosin, P. S., Coordination Chem. Rev., 1982, 44, 247-291.
80. Goggin, P. L.; Goodfellow, R. J.; Haddock, B. F.; Taylor, B. F. and Marshall, F. R. H., J. Chem. Soc. Dalton., 1976, 459-467.
81. Pregosin, P. S.; Sze, S. N.; Salvadori, P. and Lazzaroni, R., Helv. Chim. Acta., 1977, 60, 2514-2521.
82. Lloyd, M. K.; McCleverty, J. A.; Orchard, D. G.; Connor, J. A.; Hall, M. B.; Hillier, I. H.; Jones, E. M. and McEwen, C. K., J. Chem. Soc. Dalton., 1973, 1743-1747.
83. Kotz, J. C.; Nivert, C. L. and Lieber, J. M., J. Organometal. Chem., 1975, 91, 87-95.
84. Bond, A. M. "Modern Polarographic Methods in Analytical Chemistry." Marcel Dekker, New York, 1980, p. 192.
85. McCleverty, J. A., Prog. Inorg. Chem., 1969, 10, 49-221.

86. Mugnier, Y.; Moise, C.; Tirouflet, J. and Laviron, E., J. Organomet. Chem., 1980, 186, C49-C52, Ito, N.; Saji, T. and Aoyagui, S., J. Organomet. Chem., 1983, 247, 301-305; El Murr, N.; Chaloyard, A. and Laviron, E., Nov. J. Chim., 1977, 2, 15-17.
87. Thorn, G. D. and Ludwig, R. A., "The Dithiocarbamates and Related Compounds" Elsevier, New York, 1962.
88. Coucouvanis, D., Prog. Inorg. Chem., 1970, 11, 234-371; ibid., 1979, 26, 302-469; Burns, R. P.; McCullough, F. P. and McAuliffe, C. A., Adv. Inorg. Chem. and Radiochem., 1980, 23, 211-280.
89. Grunwell, J. R., J. Org. Chem., 1970, 35, 1500-1501.
90. Jen, K-Y., and Cava, M. P., Tetrahedron Lett., 1982, 23, 2001-2004.
91. Siddall, T. H. and Stewart, W. E., J. Org. Chem., 1970, 35, 1019-1022 and references therein.
92. Janssen, M. J., Rec. Trav. Chim., 1960, 79, 454-463. Shankaranarayana, M. L. and Patel, C. C., Acta. Chem. Scand., 1965, 19, 1113-1119.
93. Gunther, H. "NMR Spectroscopy - An Introduction". Wiley, New York, 1980; Sutherland, I. O., Ann. Reports NMR Spectr. 1971, 4, 71-225.
94. Hollaway, C. E. and Gitlitz, M. H., Can. J. Chem., 1967, 45, 2659-2663; see also Sandström, J., J. Phys. Chem., 1967, 71, 2318-2325.
95. Tanaka, T. and Watanabe, N., Org. Magn. Reson., 1974, 6, 165-169.
96. Liden, A.; Roussel, C.; Liljefors, T.; Chanon, M.; Carter, R. E.; Metzger, J. and Sandström, J., J. Am. Chem. Soc., 1976, 98, 2853-2860; Liljefors, T. and Sandström, J., Org. Magn. Reson., 1977, 9, 276-280.
97. Lindmark, A. F. and Fay, R. C., Inorg. Chem., 1983, 22, 2000-2006.
98. Takeda, Y. and Tanaka, T., Org. Mag. Reson., 1975, 7, 107-108.
99. Van Gaal, H. L. M.; Diesveld, J. W.; Pijpers, F. W. and Van der Linden, J. G. M., Inorg. Chem., 1979, 18, 3251-3260.

100. Bonati, F. and Ugo, R., J. Organomet. Chem., 1967, 10, 257-268.
101. Brown, D. A.; Glass, W. K. and Burke, M. A., Spectrochim. Acta., 1976, 32A, 137-143.
102. Coucouvanis, D., Prog. Inorg. Chem., 1979, 26, p425 and references therein.
103. Rogers, R. D.; Van Bynum, R. and Atwood, J. L., J. Am. Chem. Soc., 1981, 103, 692-693.
104. Rogers, R. D.; Van Bynum, R. and Atwood, J. L., J. Am. Chem. Soc., 1978, 100, 5238-5239.
105. Cardin, D. J.; Lappert, M. F.; Raston, C. L. and Riley, P. I., "Comprehensive Organometallic Chemistry" Pergamon Press, New York, 1982, 3, 559-634.
106. Brainina, E. M.; Mortikova, E. I.; Petrashkevich, L. A. and Freidlina, R. Kh., Dokl. Akad. Nauk. SSSR., 1966, 169, 335-338. English Version p. 681-683.
107. Samuel, E., Bull. Soc. Chim. Fr., 1968, 11, 3548-3564.
108. Lokshin, B. V.; Klemenkova, Z. S.; Ezernitskaya, M.C.; Strunkina, L. I. and Brainina, E. M., J. Organomet. Chem., 1982, 235, 69-75.
109. Sinn, H. and Kaminsky, W., Adv. Organomet. Chem., 1980, 18, 99-149: "Chemical and Engineering News", American Chemical Society, 1983, July 4, 29-30.
110. Kopf, J.; Vollmer, H-J. and Kaminsky, W., Cryst. Struct. Comm., 1980, 9, 271-276; 985-990.
111. Calderon, J. L.; Cotton, F. A.; De Boer, B. G. and Takats, J., J. Am. Chem. Soc., 1970, 92, 3801-3802. See Reference 9, Cotton, F. A. and Takats, J. unpublished results.
112. Lauher, J. W. and Hoffmann, R., J. Am. Chem. Soc., 1976, 98, 1729-1742.
113. General reference to Mark's work: Marks, T. J., "Organometallics of the f-Elements", D. Reidel, Boston, 1979, p. 121-147; Marks, T. J., Prog. Inorg. Chem., 1979, 25, 222-333.
114. Kanallakopulos, B.; Dornberger, E. and Baumgartner, H., Inorg. Nucl. Chem. Lett., 1974, 10, 155.

115. Lappert, M. F.; Riley, R. J. and Yarrow, P. I. W., J.C.S. Chem. Commun., 1979, 305-306; J. Chem. Soc. Dalton., 1981, 805-813.
116. Arnaudet, L.; Folcher, G.; Marquet-Ellis, H.; Klahne, E.; Yuulu, K. and Fischer, R. D., Organometallics, 1983, 2, 344-346.
117. Good review articles: Schrock, R. R. and Parshall, G. W., Chem. Rev., 1976, 76, 243-268; Davidson, P. J.; Lappert, M. F. and Pearce, R., Chem. Rev., 1976, 76, 219-242.
118. Chang, B-H., Ph.D. Dissertation., Michigan State Univ., 1979.
119. Marks, T. J.; Seyam, A. M. and Kolb, J. R., J. Am. Chem. Soc., 1973, 95, 5529.
120. Bercaw, J. E. and Wolcazanski, P., Acc. Chem. Res., 1980, 13, 121-127; Bristow, G. S.; Hitchcock, P. B. and Lappert, M. F., J. Chem. Soc. Chem. Commun., 1982, 462-464; Fanchinetti, G.; Fochi, G. and Floriani, C., J. Chem. Soc. Dalton., 1977, 1946.
121. Marks, T. J. and Wachter, W., J. Am. Chem. Soc., 1976, 98, 703-710.
122. Reference 105, page 606.
123. Wailes, P. C.; Coutts, R. S. P. and Weigold, H., "Organometallic Chemistry of Titanium, Zirconium and Hafnium", Academic Press, New York, 1974, p. 226.
124. Wailes, P. C. and Weigold, H., J. Organometal Chem., 1971, 28, 91-95.
125. Fachinetti, A., Floriani, C., Chiesi-Villa, A. and Guastini, C., J. Am. Chem. Soc., 1979, 101, 1767-1775.
126. Peng, M. and Brubaker, C. H., Inorg. Chim. Acta., 1978, 26, 231-235; Rausch, M. D.; Boon, W. H. and Mintz, E. A., J. Organometal Chem., 1978, 160, 81-92 and references therein.
127. Wailes, P. C. and Weigold, H., J. Organometal. Chem., 1970, 24, 405-411.

MICHIGAN STATE UNIVERSITY LIBRARIES



3 1293 03145 3701